P-161

NASA

SMALL ENGINE COMPONENT TECHNOLOGY (SECT) STUDY
FINAL REPORT

by

E. Almodovar, T. Exley, H. Kaehler and W. Schneider

Avco Lycoming Textron

Date for general Release ___March 31, 1991___

prepared for

NATIONAL AERONAUTICS AND SPACE ADMINISTRATION
Lewis Research Center

and

U.S. ARMY AVIATION RESEARCH AND TECHNOLOGY ACTIVITY
Propulsion Directorate

NASA Lewis Research Center
NAS3-24545

PG0032-2

1. Report No. NASA CR- 175077 AVSCOM TR- 86-C-12	2. Government Accession No.	3. Recipient's Catalog No.
4. Title and Subtitle Small Engine Component Technology (SECT) Study Program Final Report		5. Report Date March, 1986
		6. Performing Organization Code
7. Author(s) E. Almodovar, T. Exley, H. Kaehler and W. Schneider		8. Performing Organization Report No. LYC - 86-11
		10. Work Unit No.
9. Performing Organization Name and Address AVCO Lycoming Division 550 South Main Street Stratford, CT 06497		11. Contract or Grant No. NAS 3 - 24545
		13. Type of Report and Period Covered Contractor Report
12. Sponsoring Agency Name and Address NASA Lewis Research Center and U.S. Army Aviation Research and Technology Activity, Propulsion Directorate, Cleveland, Ohio 44135		14. Sponsoring Agency Code 535-05-01 1L161101 AH45

15. Supplementary Notes

Project Manager, Michael R. Vanco
NASA Lewis Research Center
Cleveland, OH 44135

16. Abstract

The study was conducted to identify high payoff technologies for year 2000 small gas turbine applications and to provide a technology plan for guiding future research and technology efforts.

A regenerative cycle turboprop engine was selected for a 19 passenger commuter aircraft application. A series of engines incorporating eight levels of advanced technologies were studied and their impact on aircraft performance was evaluated. The study indicated a potential reduction in fuel burn of 38.3%. At $1.00 per gallon fuel price, a potential DOC benefit of 12.5% would be achieved. At $2.00 per gallon, the potential DOC benefit would increase to 17.0%.

Four advanced technologies are recommended and appropriate research and technology programs were established to reach the year 2000 goals.

17. Key Words (Suggested by Author(s)) Commuter aircraft, Aircraft engines, Turboprop, Recuperators, Engine component technologies	18. Distribution Statement		
19. Security Classif. (of this report) Unclassified	20. Security Classif. (of this page) Unclassified	21. No. of pages 157	22. Price*

NASA

SMALL ENGINE COMPONENT TECHNOLOGY (SECT) STUDY
FINAL REPORT

by

E. Almodovar, T. Exley, H. Kaehler and W. Schneider

Avco Lycoming Textron

Date for general Release _____ March 31, 1991 _____

prepared for

NATIONAL AERONAUTICS AND SPACE ADMINISTRATION
Lewis Research Center

and

U.S. ARMY AVIATION RESEARCH AND TECHNOLOGY ACTIVITY
Propulsion Directorate

NASA Lewis Research Center
NAS3-24545

PG0032-2

TABLE OF CONTENTS

TABLE OF CONTENTS (Continued)

LIST OF TABLES

LIST OF ILLUSTRATIONS

LIST OF ILLUSTRATIONS   (Continued)

SECTION 1.0
SUMMARY

The objectives of this study were to identify high payoff technologies for year 2000 small gas turbine applications and to provide a technology plan for guiding future research and technology efforts.

A regenerative cycle turboprop engine was selected for a 19-passenger fixed-wing commuter aircraft application.

The first task was to select the evaluation procedures and assumptions for the study. The aircraft selected was based on the NASA/Beech ATDA aircraft, having a full payload design range of 600 n mi (1111 km). A Lycoming current technology engine was selected as the Reference Engine, scaled to 960 hp (716 kW) to accomplish the mission. Systems analysis was performed using the NASA-GASP computer program, which resulted in a Reference Aircraft of 12,930 lb (5870 kg) max take-off gross weight, costing $2.44M, in 1985 dollars.

Fuel prices of $1 and $2 per gallon were established, and direct operating cost, DOC, was selected for the cost trade-off procedure based on an economic mission having an average stage length of 100 n mi (185 km) and 65 percent payload. For 2800 hours utilization per year, the direct operating costs were $216 and $263 per trip for $1 and $2 fuel prices, respectively.

Noise and pollution constraints were also defined and a trade factor matrix procedure was established to relate the engine technology advancements to the resulting aircraft system performance. The engine parameters which were selected included specific fuel consumption, frontal area, weight and acquisition and maintenance costs.

The next phase of the study was to select and evaluate the advanced engine technologies. The technologies evaluated were:

Level 1:   Reference Technology + Recuperator

Level 2:   + Advanced Aerodynamics

Level 3:   + Advanced Cooling

Level 4:   + Advanced Blade Materials

Level 5:   + Advanced Aerodynamics and Gas Generator Ceramics

Level 6:   + Axi-Centrifugal Compressor

Level 7:   + Ceramic Recuperator Core

Level 8:   + Ceramic Power Turbine and Graphite Composite Case

A cycle analysis and size, weight and cost study was conducted for each of the advanced technologies for recuperator effectiveness ranging from 70 to 90 percent, and their impacts on aircraft performance were determined. Using DOC as the primary criterion, an optimum cycle was established and a

1

preliminary engine design was carried out. Based on the final advanced technology configuration, Level 8, the optimum cycle had a recuperator effectiveness of 80 percent, a turbine inlet temperature at take-off of 2640°F (1450°C) and a pressure ratio of 8.93.

The advanced recuperative engine was used with the Reference Aircraft and mission to determine the benefits of the engine advanced technologies. Mission fuel burn reduction was 38.3 percent, or 75,000 gallons savings per year per aircraft based on 2800 hours utilization. The DOC reduction at $1 per gallon was 12.5 percent, which translates to $120,000 savings per year per aircraft. At $2 per gallon fuel price, the DOC reduction rose to 17 percent, or $199,000 savings per year per aircraft.

The final phase was to identify the required advanced technologies, identify the potential benefits and rank the technologies, and provide technology plans for guiding future NASA and Army in-house and contractor efforts. The four technologies which were identified, and their potential benefits based on DOC reduction are:

	Percent DOC Reduction	
	$1 Per Gallon	$2 Per Gallon
Ceramic Combustor and Turbines	4.8	5.7
Advanced Aerodynamics	3.6	4.3
400°F (222°C) Higher Turbine Inlet Temperature	3.3	3.6
Ceramic Recuperator	0.8	3.4
Total	12.5	17.0

The technology plans to reach the year 2000 goals and objectives were established.

It is recommended that NASA pursue the advanced technologies identified in this study through sponsorship and support of the applicable technology programs. The technologies resulting from such programs will also be applicable to civil and military rotorcraft and turbofan derivatives, providing comparable economies of operation.

SECTION 2.0
INTRODUCTION

The transfer of technology advancements from large gas turbine engines to smaller (under 1,000 shp (746 kW)) engines is often not directly applicable. Limitations of scaling effects and constraints of component size, have made the large engine performance gains unattainable in the smaller powerplants. As a result, specific fuel consumption differences are as high as 15 percent to 20 percent. Pooling of foreign engine manufacturers into consortiums and joint ventures have accelerated the exchange of technology among our international market competitors such that U.S. turbine engine market share continues to decline. The Small Engine Component Technology (SECT) program will provide the advanced technology necessary to bring the performance of small engines significantly closer to that of large engines. As a result, U.S. manufacturers' worldwide market share of small turbine engine sales would then be appreciably improved by the strengthened U.S. competitive position.

A present program under the joint sponsorship of NASA and the Department of Energy for studying advanced gas turbine technology for automotive applications has emphasized the significant contributions of ceramic material technology and regenerative cycles to fuel efficient performance of engines in the 100 shp (75 kW) class. NASA and U.S. Army Aviation Research and Technology Activity - Propulsion Directorate, in recognition of the potential impact of these technologies upon aircraft propulsion systems, sponsored this SECT study to identify the high payoff technologies for year 2000 engines and to establish technology plans for future research. Application of advanced material and recuperator technology to aircraft engines along with significant improvement in component performance could permit year 2000 small gas turbine engines to achieve fuel savings approaching 40 percent with commensurate reductions in aircraft operating cost.

The study was directed at a year 2000 technology recuperative turboprop engine for a 19-passenger commuter aircraft application.

The SECT study was a 6-month effort divided into four major tasks:

- Selection of Evaluation Procedures and Assumptions

- Engine Configuration and Cycle Evaluation

- System Performance Evaluation

- Small Engine Component Technology (SECT) Plan

This report presents the results of this study. The first task is presented in Section 3.0. The second is described in Sections 4.0 through 7.0. The third task is contained in Section 8.0. The fourth is discussed in Sections 9.0 and 10.0. Conclusions and Recommendations are given in Section 11.0.

SECTION 3.0
SELECTION OF EVALUATION PROCEDURES AND GROUND RULES

The procedures and ground rules selected for evaluating the aircraft and propulsion systems are described in this section. The following six elements were addressed:

- Definition of the Reference Aircraft

- Definition of the Reference Engine

- Establishment of the projected fuel price

- Selection of the cost trade-off procedure

- Definition of current and future environmental constraints

- Establishment of trade factors

3.1   Definition of the Reference Aircraft

A 19-passenger commuter aircraft powered by twin 960 hp (716 kW) turboprop engines was selected as the Reference Aircraft for this study. As shown in Figure 1, it is a low wing, T-tail design with a maximum take-off gross weight of 12,930 lb (5870 kg), and a maximum zero-fuel weight of 11,138 lb (5057kg). Modelling and analysis of the aircraft was performed using the General Aviation Synthesis Program, (GASP), developed at NASA-Ames Research Center, Reference 1.

The SECT Reference Aircraft is essentially the advanced technology aircraft of the NASA Advanced Technology Derivative Aircraft (ATDA) study conducted by Beech, Reference 2. Installation of Lycoming Reference Engines resulted in a slight resizing of the wing and empennage, but the fuselage dimensions were not modified. A drawing (from Reference 2) showing the general arrangement of the interior is given in Figure 2. Cockpit and passenger cabin details are listed in Table 1.

The sizing mission selected for the study closely followed that of the NASA/ATDA study. It consists of a one-leg mission of 600 nautical miles (1111 km), at full payload, with a maximum rate of climb to 10,000 feet (3048 m) altitude, cruise at 238 kts and descent, with 45 minutes reserve fuel at max endurance speed. The sizing mission profile is shown in Figure 3.

A similar one-leg mission, but with a 65 percent passenger load factor, was selected for the economic evaluations of this study. Current passenger load factors are approximately 50 percent at 100 nautical miles (185 km) stage length, increase to 60 percent at 300 nautical miles (555 km) and remain essentially level at 63 percent beyond 400 nautical miles (740 km). As the commuter industry matures, significant gains in load factor at 100 n mi (185 km) are expected so that 65 percent is believed likely by the year 2000. Operating economics were therefore evaluated based on a 65 percent load factor with the full sizing mission reserve fuel load on board. A cargo load, additional to the passenger plus baggage payload, was not considered.

4

A 100 n mi (185 km) stage length was selected for the direct operating cost evaluations since this closely approximates the current, and expected, average stage distance for 19-passenger commuter aircraft.

A GASP model of the SECT Reference Aircraft was developed using the ATDA aircraft as a base, and used to resize the aircraft and engine to conform with the specified sizing mission. Sizing was accomplished by changing the wing and empennage areas while holding the specified wing loading and aspect ratio fixed. The fuselage and propeller parameters were also held fixed. GASP output of the aircraft dimensions and group weights is presented in Figures 4 and 5. These results essentially match the ATDA results except for engine and fuel-related weights which are lower due to the use of the newer, more fuel-efficient SECT Reference Engines.

The GASP output of the aerodynamic data is presented in Figure 6 and again, closely matches the ATDA aircraft data. Output for the Take-off phase is presented in Figure 7, for the Accelerate and Climb phase in Figure 8, and for the Accelerate to Cruise phase in Figure 9. The Cruise Summary is given in Figure 10. The average lift-to-drag ratio, L/D, during cruise is 8.26. The Descent phase is given in Figure 11.

The performance of the aircraft for the economic mission was very similar to the design sizing mission. The results are summarized and compared in Table 2.

It should be noted that the above aircraft performance results reflect two changes that have been made to the Lycoming version of GASP. First, the taxi fuel burn is based on the power required to just overcome the rolling resistance of the aircraft at take-off gross weight. The corresponding fuel flow rate is then determined directly from the engine tables.

Second, the nacelle sizing routine, and therefore the nacelle weight and drag predictions, were modified to accommodate engine size changes while holding fixed the space requirements of the wheels, accessories, etc. of a typical commuter installation.

3.2   Definition of the Reference Engine

The Reference Engine is based on a current technology engine modified to a turboprop configuration and scaled to a max rated power of 957.5 hp (714.0 kW), uninstalled, sea level static, on a standard day (Figure 12).

The gas generator consists of a two-stage axial plus centrifugal compressor with variable inlet guide vanes, driven by a cooled two-stage gas generator turbine. The combustor is a reverse flow, annular, atomizing type. The uncooled single-stage free-power turbine transmits output power to a front-mounted reduction gearbox via a through-shaft concentrically mounted within the compressor rotor shaft. The engine includes an integral oil system. Control is a full-authority, digital, electronic type.

The engine employs a modular design concept resulting in a total of three easily maintained and serviced components: The Accessory/Reduction Gearbox, the Gas Generator, and the Combustor/Power Turbine Assembly. A materials list is given in Table 3. The engine weight is 359 lb (163 kg) (which includes a 121 lb (55 kg) reduction gearbox) and cost is $178,000, based on

the preliminary design size, weight and cost estimating relationships used for this study.

Tables 4 and 5 list the uninstalled and installed performance of the Reference Engine. Installation losses include customer bleed air of 10 lb/min (4.5 kg/min) per engine, constant at all power levels, in conformance with the 19-passenger Small Transport Aircraft Technology (STAT) specifications reported in Reference 3. Power extraction of 12 hp (9 kW) per engine was accounted for as part of the GASP input. Flat-rating was not considered.

The ATDA propeller aerodynamic data was used unchanged throughout, namely a 3-blade, 9.17 ft (2.80 m) diameter design running at 1700 rpm, with an activity factor of 110 per blade and an integrated lift coefficient of 0.5. Since the GASP program was used, the calculated propeller efficiencies reflect a current technology aerodynamic design. A propeller weight of 82 lb (37.2 kg) was used, however, to match the weight reduction of the advanced technology propeller prescribed for the ATDA aircraft.

3.3   Establishment of the Projected Fuel Price

The current fuel price of approximately $1.00 per gallon is considerably less than was forecast during the 1979-1980 time frame when prices approaching $1.75 per gallon were predicted for 1985. (Reference 4)

Current projections of yearly fuel price increases for 1984 through 1995 were obtained from the industry cost index forecasts of Reference 5. The forecast projections established cost escalation multipliers for 1990 and 1995 of 1.372 and 2.089 respectively based on a 1983/1984 fuel price of $0.89 per gallon. The expected fuel prices, in 1985 dollars, are then $1.22 per gallon for 1990, and $1.86 per gallon for 1995. A fuel price of approximately $2.00 per gallon, in 1985 dollars, is therefore indicated for the year 2000.

The current fuel price of $1.00 per gallon was therefore selected as the projected fuel price for the operating costs comparisons, in constant 1985 dollars, based on the premise that fuel costs will essentially follow the annual average inflation rate for the foreseeable future. An alternate fuel price of $2.00 per gallon was also selected in order to gauge the effect of fuel cost escalation over and above the annual average inflation rate.

3.4   Selection of the Cost Trade-Off Procedure

The use of direct operating cost (DOC) was selected as the basis for evaluating the advanced technologies. In particular, the DOC methodology employed in the GASP computer program, which follows the standard Airline Transportation Association method, was used.

The Ground Rules selected are given in Table 6. All cost-related data sources shown were adjusted to 1985 dollars. This was accomplished using a cost adjustor derived from statistical information for the aerospace industry compiled by the U.S. Department of Commerce and U.S. Department of Labor and reported in Reference 6. From this study, an annual average inflation rate of 7.8 percent was derived, conforming to the eight year period 1977 through 1984. This cost adjustor was also used to determine the selected crew cost and maintenance labor rate shown in the table.

6

The engine cost shown in the table is based on dollars per maximum uninstalled horsepower at sea level static, standard day conditions. A Lycoming parametric cost estimating relationship established the Reference Engine base cost, adjusted for an assumed total production quantity of 1500 engines. Engine maintenance costs were determined for labor and materials using the cost estimating relationships in GASP based on max installed power and mission flight time, adjusted to conform with Lycoming 1985 maintenance costs projections.

The propeller cost was based on the commuter aircraft studies of References 7 and 8, brought forward to 1985 dollars using our cost adjustor value of 7.8 percent. The cost shown in the table includes a 25 percent cost complexity increment to conform with the cost projections for the lightweight ATDA propeller design.

The airframe acquisition cost was determined based on the 1985 cost adjustor applied to the 1978 airframe cost correlations embedded within GASP. A 20 percent cost complexity increment was added to conform with the costs projected by the ATDA airframe study. Airframe maintenance costs were determined for labor and materials using the cost estimating relationship in GASP based on airframe weight and mission block time, and brought forward to 1985 dollars using our cost adjustor value.

A maintenance burden of 80 percent was added to the airframe and engine maintenance labor costs.

The remaining Ground Rules conform to the standard values prescribed for the NASA/STAT studies referenced previously.

The economic evaluations were based on the 65 percent payload mission and 100 nautical mile (185 km) stage length described in Section 3.1. The GASP Short-Haul costing output for this mission is presented in Figure 13 for both fuel price selections. Total DOC is $216 per trip at $1.00 per gallon, increasing to $263 per trip at $2.00 per gallon. On a cents per available seat statute mile basis (c/assm), the cost increases from 9.90 cents to 12.01 cents.

The DOC breakdown is shown in Figure 14. At $1.00 per gallon, the operating costs are almost evenly distributed between the five major costing elements, i.e., fuel, crew, airframe maintenance plus its share of the burden, engine maintenance plus its share of the burden and financial (depreciation plus insurance). At $2.00 per gallon, the percentage required for fuel increases from 21 to 35 percent.

If the stage length were increased to 200 n mi (370 km), the DOC's would drop approximately 13 percent, from 9.90 to 8.60 c/assm for $1.00 per gallon, and from 12.01 to 10.50 c/assm for $2.00 per gallon.

There is little change for the 100 percent payload missions. The DOC's for the 100 n mi (185 km) trip are 9.99 and 12.17 c/assm for the two fuel prices. For the 200 n mi (370 km) trip, the DOC's are 8.66 and 10.62 c/assm for the two fuel prices.

7

3.5 Definition of Current and Future Environmental Constraints

Present FAA Aircraft Noise Standards (FAR Part 36) constrain the noise levels of turboprop aircraft over 12,500 lbs (5675 kg) to 89 EPNdB for take-off flyover, 94 EPNdB for take-off sideline and 98 EPNdB for approach flyover. Aircraft of less than 12,500 lbs (5675 kg) are constrained to 80dBA for level flyover only.

The noise levels of the SECT Reference Aircraft were analyzed using both the NASA/GASP routine and Avco Lycoming in-house gas turbine noise prediction programs. Noise levels predicted by GASP for the sizing mission are given in Table 7. The Lycoming programs predicted 6EPNdB lower noise levels than GASP for the take-off and flyover conditions.

The Reference Aircraft noise signature is dominated by the propeller for the take-off flyover and sideline conditions. Some engine contribution could be present in the approach condition for this aircraft. The noise levels of the Reference Aircraft are graphically presented on Figures 15, 16 and 17 for the take-off, sideline and approach conditions for comparison with the FAR Part 36 noise limits. In addition, the SECT aircraft A-weighted sound levels are compared with other turboprop aircraft in Figure 18.

This design used current propeller aerodynamic technology and is adequate to meet the existing aircraft certification noise limits. However, new propeller technology that results in lower noise levels is available for the aircraft designer. As the SECT Reference Aircraft noise levels are controlled by the propeller, the additions of this technology could result in a quieter aircraft should the certification noise limits be reduced in the future. There appears to be sufficient margin with respect to the engine contributed noise to achieve at least an additional 5 EPNdB noise reduction.

With respect to smoke and air pollution constraints on the environment, existing rules limit only the smoke emissions of turboprop (and turbofan) engines. Turboshaft engines used for rotorcraft are not regulated for any emissions. Smoke limits have been established such that particulate emissions are invisible and there are currently no plans to make these rules more stringent or to introduce new requirements for any small aircraft gas turbine. The smoke visibility limit can be related either to the engine exhaust plume diameter (military requirement, AV-E-8593D), or the power output, (EPS, 40 CFR, Part 87). As shown in Figure 19, the SECT Reference Engine is well below the visibility requirement.

Because smoke production is inhibited by high combustor inlet temperatures characteristic of regenerated and high pressure ratio engines, advanced engines should have extremely low smoke levels, as well as a high tolerance to low quality high aromatic fuels.

Even if more stringent rules were imposed, the high combustor inlet temperatures of these advanced engines tend to suppress emissions of unburned hydrocarbons (UHC) and carbon monoxide (CO) as well as smoke. Idle combustion efficiencies (as measured by CO and UHC) above 98 percent are achievable, as shown in Figure 20, with efficiencies above 99 percent achievable at higher power levels. On the other hand, emissions of nitric oxides (NO_x) are adversely affected by high combustor inlet temperatures. There may be some future rules to limit NO_x when the contribution of NO_x to acid rain becomes

better understood. Stationary power sources above 1200 hp (900 kW) are currently limited to 150 ppm NO_x. Since NO_x missions of advanced technology aircraft engines can exceed 200 ppm at maximum power, reduction of NO_x emissions may be required should the same limits be imposed on aircraft engines. A trade-off could then be made between combustion efficiency (UHC plus CO) and NO_x, or the dry NO_x control technique currently used for stationary power sources could be extended to aircraft engines.

3.6   Establishment of Trade Factors

A trade factor matrix was developed to evaluate the benefits and penalties to the aircraft resulting from changes in the engine characteristics. The sensitivity of aircraft characteristics to specified changes in engine characteristics were determined by the use of the GASP program. The selected aircraft characteristics included aircraft fuel burn (WF), take-off gross weight (TOGW), take-off shaft power (SP), aircraft acquisition cost (CA_{acq}), and direct operating cost (DOC). The selected engine-related characteristics included specific fuel consumption (SFC), propulsion system weight (WPS), frontal area (APS), acquisition cost (CPS_{acq}), and maintenance cost (CPS_m). The impacts of changes in engine-related characteristics were determined through the use of trade factors, TF_{ij}, represented by the following sensitivity matrix equation.

$$
\begin{Bmatrix} \Delta WF \\ \Delta TOGW \\ \Delta SP \\ \Delta CA_{acq} \\ \Delta DOC \end{Bmatrix}
=
\begin{bmatrix} MATRIX \\ OF \\ TRADE \\ FACTORS \end{bmatrix}
\times
\begin{Bmatrix} \Delta SFC \\ \Delta WPS \\ \Delta APS \\ \Delta CPS_{acq} \\ \Delta CPS_m \end{Bmatrix}
$$

To determine the trade factors, the Reference Aircraft characteristics and mission profile were held constant while each of the selected engine parameters were changed individually. With this method, the aircraft is resized as required to ensure that all the effects of each parameter change are taken into account. For example, for a specified percentage change in SFC and with the remaining engine parameters held constant, the GASP program determined the changed aircraft parameters, and therefore, the associated column of trade factors. Each column of trade factors were determined in this way corresponding to changes in each selected engine parameter.

Changes in aircraft fuel consumption, take-off gross weight, take-off power, acquisition cost and direct operating costs were plotted against engine specific fuel consumption, propulsion system weight, frontal area, acquisition cost and maintenance cost. For ease in application, the parameters were normalized with respect to the Reference Aircraft. The resulting trade factor matrices for both fuel prices are shown in Table 8. The values shown were established based on data points nearest the engine reference point, typically within +20 percent. Due to non-linearities in some of the plots, the values used during the engine design phase were adjusted as required.

Bar graphs of these results are presented in Figures 21 through 26 to illustrate the effect on aircraft parameters of a 10 percent change in engine parameters. Note that by far, the strongest influences on aircraft fuel burn

9

is engine SFC. In the case of aircraft DOC, engine SFC is again the strongest driver, but the cost of propulsion system maintenance also has a substantial influence.

During the engine design phase described in the following section, the overall changes to the aircraft resulting from each of the advanced technology engine changes were determined directly from the trade factor matrices.

SECTION 4.0
ADVANCED TECHNOLOGY SELECTION AND CYCLE EVALUATION

This section describes the advanced technologies which were selected for evaluation. The assumptions and ground rules affecting the thermodynamic cycle are also presented. The improvement in cruise SFC was first determined as a function of recuperator effectiveness for each advanced technology. Then, for each value of effectiveness and advanced technology an optimum engine cycle was established. The corresponding sea level static, uninstalled take-off performance was also obtained in order to determine the engine size, weight and costs, as described in Section 5.0.

4.1   Selection of Advanced Technologies

The first advanced technology selected for evaluation was recuperation of a reference technology engine. Accordingly, a recuperative engine was designed having the same aerodynamic efficiency, cooling and materials technology as used in the non-recuperative SECT Reference Engine. This Reference Technology + Recuperator engine provides the first level of comparison with the SECT Reference Engine. Using this as a base, additional levels of advanced technologies were introduced as follows:

Level 1:	Reference Technology + Recuperator
Level 2:	+ Advanced Aerodynamics
Level 3:	+ Advanced Cooling
Level 4:	+ Advanced Blade Materials
Level 5:	+ Advanced Aerodynamics and Gas Generator Ceramics
Level 6:	+ Axi-Centrifugal Compressor
Level 7:	+ Ceramic Recuperator Core
Level 8:	+ Ceramic Power Turbine and Graphite Composite Case

Technology Level 2 includes improved turbomachinery efficiencies brought about by advanced aerodynamics. Both Levels 1 and 2 have reference technology cooling and materials, so the cycles were evaluated for the same turbine inlet temperature as the Reference Engine, i.e., 2100°F (1150°C).

The next two technology levels, (Levels 3 and 4), include advanced cooling and advanced metallic blade materials to permit a turbine inlet temperature of 2500°F (1370°C) at cruise. The Level 4 configuration represents the highest potential which can be achieved by cooled metallic turbine designs consistent with a year 2000 small turboprop. For Technology Levels 5 through 8, ceramic gas generator blading materials were selected for operation at 2500°F (1370°C) with no cooling.

A single-stage centrifugal compressor was assumed for Technology Levels 1 through 5 and an axi-centrifugal compressor was selected for Technology Levels 6 through 8.

11

Technology Level 7 consists of the Level 6 configuration with a ceramic recuperator core to reduce weight and cost. Level 8 also includes ceramic power turbines and a graphite composite gearbox casing and compressor inlet.

Note that Levels 1 through 6 impact the cycle selection and performance as well as engine size, weight and costs because these advanced technologies provide improved efficiencies, lower cooling requirements and higher temperatures. The effect of additional material substitutions, Levels 7 and 8, were studied to determine their further impact on engine weight and costs. Since technology Levels 7 and 8 do not affect engine thermodynamics, the cycles established for Level 6 were used.

4.1.1   Level 1: Reference Technology + Recuperator

Figure 27 shows the efficiency curves used for reference technology compressors, expressed as functions of pressure ratio and air flow rate. For a single centrifugal stage an efficiency characteristic was established as a function of pressure ratio for optimum specific speed and extended to a function of airflow by scaling losses to the 1/6th power of Reynold's number. The axi-centrifugal curves were generated from test data combined with the centrifugal characteristics.

Figures 28 and 29 show the adiabatic efficiency curves used for a reference technology cooled single-stage gas generator turbine, and for a two-stage power turbine, operating at a cruise temperature of 2100°F (1150°C). The turbomachinery components of the SECT Reference Engine conform to these curves.

The cooling requirements for reference technology turbines were generated from the cooling performance characteristic shown in Figure 30. A Lycoming computer analysis which relates representative chord lengths, solidities, gas Mach numbers, stator pattern factors and gas and metal temperatures to this curve was used to develop the cooling schedules shown in Figures 31 and 32 for the nozzle vanes and rotor blades. The turbines of the SECT Reference Engine conform to these cooling schedules.

The advanced technology curves shown in Figures 27 - 32 are described in the appropriate sections.

The recuperator designs are based on the Lycoming wave-plate configuration developed for our AGT1500 engine. As shown in Figure 33, the exhaust gas enters at the center of the recuperator core and passes radially outward between alternate wave-plates. The air from the compressor is fed to the core through the triangular passages and enters each wave-plate near the outer diameter. The air is turned radially inboard, flowing counter to the exhaust, and, at the inner diameter is fed to the oval passages and out to the combustor. Lycoming computer programs were used in predicting recuperator performance, size, weight and costs which were necessary for conducting the trade-off study.

For the cycle analysis, a total pressure loss, (air side plus gas side), of 7 percent was specified in all cases, since previous studies at Lycoming have shown this parameter to have only a weak, second-order effect on recuperator size, weight and costs. The results of a typical recuperator sizing analysis is shown in Figure 34. For a specified inner diameter, as determined by the

gas flow rate and Mach number, the analysis shows the variation in effectiveness and total pressure loss as a function of core length and outer diameter. A line of constant core weight passing through a pressure loss of 7 percent and 80 percent effectiveness is also shown.

Two types of recuperator cores, shown in Figure 35 were investigated. The first is the standard single-pass design, while the second is a two-pass design having half the radial passage length per plate, but twice the number of plates. The latter configuration reduces recuperator frontal area, hence aircraft drag, without changing the core surface area, weight or cost. Throughout the study recuperator effectiveness was varied between 70 and 90 percent for both the single and two-pass configurations and their impacts on engine and aircraft performance and costs were established to determine the optimum effectiveness for each technology level.

The cycle study was conducted for the Reference Aircraft cruise condition of 620 shp (462 kW), 10,000 ft (3048 m) altitude and 238 kts flight speed. Installation losses included ½ percent inlet pressure loss and 10 lb/min (4.5 kg/min) customer bleed. Compressor and turbine efficiencies and cooling flow rates were varied with airflow, pressure ratio, temperature and technology level in accordance with the curves described above.

The results of the design point cycle analysis are shown in Figures 36, 37 and 38 for recuperator effectiveness of 70, 80 and 90 percent, respectively. Specific fuel consumption (SFC) is plotted against specific power for turbine inlet temperatures ranging from 1900°F (1038°C) to 2700°F (1482°C). Solid curves represent centrifugal compressor configurations and dashed curves represent axi-centrifugal compressor configurations. The optimum cruise cycle was established at the minimum SFC point as indicated by the symbols on the 2100°F (1150°C) temperature curve. Note that over the temperature range shown, the optimum SFC decreases 5 percent for 70 percent recuperative effectiveness, while at 90 percent effectiveness the optimum SFC does not decrease with increasing turbine inlet temperature above 2300°F (1260°C). The reason for the lack of improvement in SFC is that turbine cooling air is bled from the cycle before the recuperator, and therefore it is not available to absorb heat from the gas. In a non-recuperative cycle, increasing cycle temperature increases the useful power output faster than the losses incurred to produce the power, and therefore, a continuing improvement in SFC is obtained. However, in a recuperative cycle, the air absorbs more heat with high effectiveness than with low, so that it becomes more costly to remove it from the cycle. At high effectiveness, therefore, turbine cooling requirements offset the improvements which usually comes with higher temperatures. SFC improvements at higher temperature are restored by raising the allowable metal temperatures to reduce cooling needs, or by introducing ceramics to eliminate turbine cooling.

Figure 39 shows the SFC reduction at 2100°F (1150°C) cruise cycle temperature for several values of effectiveness. For minimum fuel consumption the following optimum cycles were established:

Effectiveness, percent		70	80	90
SFC	, lb/hr/hp, (kg/hr/kW)	0.396 (0.241)	0.371 (0.226)	0.341 (0.207)
HP/W_a	, hp.sec/lb, (kW.sec/kg)	141 (232)	138 (227)	131 (215)
W_a	, lb/sec, (kg/sec)	4.38 (1.99)	4.50 (2.04)	4.74 (2.15)
PR		6.81	6.02	4.99
T4	, °F, (°C)	2100 (1150)	2100 (1150)	2100 (1150)

Level 1, Reference Technology + Recuperator, shows 15.6, 20.9 and 27.2 percent SFC reductions from the non-recuperative SECT Reference Engine for 70, 80 and 90 percent recuperator effectiveness, respectively. This represents the SFC improvement resulting from recuperation.

4.1.2   Level 2: Advanced Aerodynamics

This technology level is identical to the Reference Technology except for improved component efficiencies. The cycle temperature, 2100°F (1150°C), is the same as for the Reference Engine because the cooling technology was not changed.

The compressor efficiency characteristics used to represent advanced aerodynamic technologies are shown in Figure 27. A 1.5-point efficiency gain over the Reference Technology compressor has already been demonstrated, so that a 5-point efficiency improvement was postulated for the year 2000 aerodynamic technology. This assumes advanced 3D viscous codes are developed and applied to the flowpath and blading designs. Improved tip clearances control and blade finish are also assumed.

Figure 28 shows the improved efficiency used for the gas generator turbine brought about by advanced aerodynamic technology. A 2-point efficiency improvement was assumed achievable with year 2000 technology. Here again, it was assumed that 3D viscous codes would be developed and applied to the design of the flowpath and blading, and that improved tip clearance control and blade finish would also be available. Note that the efficiency characteristics account for the disruption of the working gas due to injection of stator and rotor cooling air. For convenience in performing the cycle analysis, the efficiency values were set by the rotor cooling flows as shown.

The power turbine advanced aerodynamic efficiency characteristic shown in Figure 29 was increased 1.6-points over the Reference Technology. Slightly less improvement was predicted than for the gas generator turbines because the power turbine blades are longer so that the impact of improved tip clearance control will not be as significant.

The SFC versus specific power performance curves are shown in Figure 40 for 2100°F (1150°C) cruise cycle temperature and 70, 80, and 90 percent effectiveness. For the minimum fuel consumption point, the following optimum cruise cycles were established:

Effectiveness, percent		70	80	90
SFC	, lb/hr/hp (kg/hr/kW)	0.362 (0.220)	0.343 (0.209)	0.318 (0.193)
HP/W$_a$	, hp.sec/lb (kW.sec/kg)	159 (261)	155 (255)	148 (243)
W$_a$	, lb/sec (kg/sec)	3.89 (1.77)	3.99 (1.81)	4.18 (1.90)
PR		7.70	6.56	5.47
T4	, °F (°C)	2100 (1150)	2100 (1150)	2100 (1150)

Level 2, which includes Advanced Aero, shows an additional 7.2, 6.1 and 5.1 percent reduction in SFC from the Level 1 engine at 70, 80 and 90 percent effectiveness due to improved component efficiencies. Note that advanced aero components have less impact at high recuperator effectiveness.

4.1.3 Level 3: + Advanced Cooling

Over the next fifteen years, film cooling techniques will become more advanced and their application to small gas turbine engines will permit higher gas operating temperatures with current blade metal temperatures. Turbine inlet temperatures approaching 2500°F (1370°C) in cruise are expected by year 2000. Technology Level 3 includes the effects of higher temperatures and advanced cooling along with advanced aerodynamics.

The higher cooling effectiveness characteristic shown previously in Figure 30 was used to represent the advanced cooling technology available by year 2000. External film cooling was assumed, in conjunction with internal convection to reach this level of performance. The stator and rotor cooling schedules shown in Figures 31 and 32 were developed from this characteristic. The same metal temperatures were assumed as for the Reference Technology blading.

The resulting SFC versus specific power performance curves are shown in Figure 41 for a cruise turbine inlet temperature of 2500°F (1370°C). The optimum cycles for the Advanced Cooling Technology engines are:

Effectiveness, percent		70	80	90
SFC	, lb/hr/hp (kg/hr/kW)	0.346 (0.210)	0.328 (0.200)	0.306 (0.186)
HP/W$_a$	, hp.sec/lb (kW.sec/kg)	204 (335)	201 (330)	192 (316)
W$_a$	, lb/sec (kg/sec)	3.03 (1.38)	3.09 (1.40)	3.23 (1.47)
PR		9.11	8.01	6.44
T4	, °F (°C)	2500 (1370)	2500 (1370)	2500 (1370)

Level 3, Advanced Aero + Advanced Cooling, shows an additional 3.5, 3.2 and 2.5 percent SFC reduction from the Level 2 engine at 70, 80 and 90 percent effectiveness due to more efficient cooling and to the 400°F (222°C) increase in turbine inlet temperature. A 35 percent specific power increase

is obtained due to higher temperature. Note that even though advanced
cooling technology is introduced, the cooling flow increased because of the
higher cycle temperature. Since the thermal energy absorbed by the com-
pressed air in the recuperator increases with increasing effectiveness, it
becomes more costly to the cycle to bleed air for turbine cooling. As a
result the improvements in SFC are reduced with increasing effectiveness.

4.1.4   Level 4:   + Advanced Blade Materials

With advanced metallic materials and thermal barrier coatings, it is expected
that turbine blades will operate at 200°F (111°C) higher surface temperatures
by the year 2000. The higher surface temperature results in a lower heat
flux and cooling air requirement. Technology Level 4 includes advanced aero,
advanced cooling and advanced blade materials. The turbine inlet temperature
is maintained at 2500°F (1370°C) for a direct comparison with advanced
cooling and reference technology materials.

Using the advanced cooling technology blade effectiveness characteristic and
by assuming a 200°F (111°C) increase in metal temperature, cooling schedules
were established as shown previously in Figures 31 and 32 for the stator and
rotor, respectively.

The resulting SFC versus specific power curves are shown in Figure 42 for a
cruise turbine inlet temperature of 2500°F (1370°C). The optimum cycles for
minimum SFC are:

Effectiveness, percent		70	80	90
SFC	, lb/hr/hp (kg/hr/kW)	0.339 (0.206)	0.320 (0.195)	0.297 (0.181)
HP/W_a	, hp.sec/lb (kW.sec/kg)	211 (347)	207 (340)	195 (321)
W_a	, lb/sec (kg/sec)	2.93 (1.33)	3.00 (1.36)	3.18 (1.44)
PR		9.08	7.85	6.24
T4	, °F (°C)	2500 (1370)	2500 (1370)	2500 (1370)

Level 4, Advanced Aero + Advanced Cooling + Blade Materials, shows an addi-
tional 1.4, 1.6 and 2.0 percent SFC reduction from the Level 3 engine
at 70, 80 and 90 percent effectiveness. Here, the 200°F (111°C) increase in
allowable metal temperature reduces the cooling requirement, and the relative
cycle improvements now increase with increasing recuperator effectiveness.

4.1.5   Level 5:   Advanced Aero + Gas Generator Ceramics

Introducing ceramics into the gas generator allows for the elimination of
stator and rotor blade cooling which results in improved specific fuel
consumption and specific power. Ceramic parts are lighter, and in produc-
tion, will be less expensive than the intricately cooled metallic parts which
they replace. The higher specific power also results in smaller, lighter and
less expensive engine components.

The cruise cycle temperature was established at 2500°F (1370°C) as for the advanced cooling technologies, Levels 3 and 4. To achieve this with uncooled components, a material operating capability of 2850°F (1566°C) is required, with a combustor pattern factor of 0.15. A combustor pattern factor of 0.15 also appears achievable for year 2000 technology level since by using an uncooled ceramic combustor liner, more air becomes available to tailor the combustor flow pattern.

For this technology level, the advanced aero compressor and power turbine efficiencies of Figures 27 and 29 are used. The uncooled gas generator turbine efficiencies are shown in Figure 28. Here a ½-point efficiency improvement over the highest cooled design characteristic was assumed since uncooled airfoils can be designed for optimum thickness/chord ratios and minimum trailing edge thicknesses.

Although no cooling air was used for stator or rotor blade cooling, one percent compressor bleed air was used before and after the turbine rotor to pressurize seals and bearing cavities and to cool the rotor disk.

The results of the design point cycle analysis are shown in Figures 43, 44, and 45 for recuperator effectiveness of 70, 80 and 90 percent respectively. Note that now, contrary to the cooled turbine results, the uncooled designs show a continual reduction in SFC with increasing turbine inlet temperature, even for a 90 percent recuperator effectiveness.

The comparison of SFC versus specific power for 70, 80, and 90 percent effectiveness is shown in Figure 46 for constant turbine inlet temperature (2500°F) (1370°C). The optimum ceramic cycles are:

Effectiveness, percent		70	80	90
SFC	, lb/hr/hp (kg/hr/kW)	0.326 (0.198)	0.305 (0.186)	0.279 (0.170)
HP/W_a	, hp.sec/lb (kW.sec/kg)	225 (370)	219 (360)	203 (334)
W_a	, lb/sec (kg/sec)	2.75 (1.25)	2.83 (1.28)	3.06 (1.39)
PR		9.05	7.58	5.78
T4	, °F (°C)	2500 (1370)	2500 (1370)	2500 (1370)

Level 5, Advanced Aero + Gas Generator Ceramics, shows an additional 2.9, 3.2 and 3.7 percent SFC reduction from the Level 4 engine at 70, 80 and 90 percent effectiveness. Here, the turbine blade cooling requirement is eliminated entirely, so the relative cycle improvements continually increase with increasing recuperator effectiveness.

4.1.6   Level 6:   + Axi-Centrifugal Compressor

An axial centrifugal compressor was selected for this technology level in order to achieve the highest efficiency potential. Accordingly, the advanced aero axi-centrifugal compressor, ceramic gas generator turbine and advanced power turbine characteristics of Figures 27, 28, and 29 were used to establish component performance.

In addition, one percent compressor bleed air was used before and after the turbine rotor to pressurize seals and bearing cavities and to cool the rotor disk.

The SFC versus specific power characteristics for Level 6 are shown by the dashed curves in Figure 46. The optimum cycles for the Level 6 technology engines are:

Effectiveness, percent		70	80	90
SFC	, lb/hr/hp (kg/hr/Kw)	0.321 (0.195)	0.302 (0.184)	0.278 (0.169)
HP/W_a	, hp.sec/lb (kW.sec/kg)	232 (381)	224 (368)	207 (340)
W_a	, lb/sec (kg/sec)	2.68 (1.22)	2.77 (1.26)	3.00 (1.36)
PR		9.82	7.97	5.95
T4	, °F (°C)	2500 (1370)	2500 (1370)	2500 (1370)

As noted previously, the Technology Level 6 cycles apply to the Level 7 and 8 configurations, since they include material substitutions only, and do not affect engine thermodynamics.

Level 6, Advanced Aero + Gas Generator Ceramics + Axi-Centrifugal Compressor, shows an additional 0.9, 0.6 and 0.1 percent SFC reduction from the Level 5 engine for 70, 80 and 90 percent recuperator effectiveness. As effectiveness increases toward 90 percent, the optimum cycle pressure ratio approaches 6 where the efficiency of the axi-centrifugals are nearly the same as single stage centrifugal compressors. Although the SFC improvements are not significant, there are design benefits to the axi-centrifugal compressors which are taken into account in the preliminary design phase described in Section 7.

4.2   Cruise Performance Summary

The engine performance gains attributed to each technology level are compared in Figure 47, 48, and 49 for recuperator effectiveness of 70, 80 and 90 percent respectively. The SFC improvements from the non-recuperative SECT Reference Engine to the advanced technology optimum cycles are indicated in percent ΔSFC. An objective of the cycle analysis was to determine the delta SFC of the advanced technologies from the SECT Reference Engine. This is the first engine parameter required for the right hand vector of the trade factor matrix to couple the engine optimization study to the performance of the aircraft. A summary of cruise specific fuel consumption versus effectiveness is shown in Figure 50 where the various technology levels are compared to the non-recuperative SECT Reference Engine.

The optimum cruise cycle pressure ratio which produces minimum specific fuel consumption is shown in Figure 51. The pressure ratio decreases 25 percent from 70 to 90 percent effectiveness. This trend results in higher component efficiencies because of favorable size effects. With improved technology, the optimum cruise pressure ratio must be increased nearly 30 percent from Level 1, Reference Technology + Recuperator, to Level 5, Advanced Aero + Gas

18

Generator Ceramics. The optimum pressure ratio is still well below that of the non-recuperative Reference Engine however.

The rotor cooling flow rates are presented in Figure 52. The stator cooling flow rates were of similar magnitudes. Levels 1 and 2, Reference Technology + Recuperator and Advanced Aero, have the same cooling requirements as the Reference Engine since all have the same turbine inlet temperature and cooling technology. For Level 3, which includes Advanced Cooling, the turbine inlet temperature was increased to 2500°F (1370°C) and as a result, the cooling requirement increased 25 percent; however, by introducing advanced blade materials, Level 4, the cooling rate was reduced essentially to the reference level. The ceramic blades and vanes of Levels 5 and 6 were uncooled except for the 1 percent shown for pressurization of the seals and bearing cavities.

4.3   Sea Level Static, Uninstalled, Take-off Performance

In order to estimate propulsion system size, weight and costs, as described in Section 5 below, it is first necessary to determine engine power, cycle pressure ratio and airflow at the sea level, uninstalled take-off condition. This information was obtained from the design point results by creating a computer match point simulation for each optimum cycle. The resultant take-off performance data is summarized in Figures 53 through 57 for shaft horsepower, cycle pressure ratio, airflow, SFC and specific power.

All engines were sized to produce 620 installed horsepower (462 kW) at cruise; however due to the installed/uninstalled lapse rate effect of customer bleed the sea level static uninstalled take-off power varied as shown in Figure 53. The impact of customer bleed on lapse rate is a function of engine pressure ratio and airflow. As the technology level improves, the cycle pressure ratio increases (Figure 54) and the engine airflow decreases (Figure 55), both causing the customer bleed to have a greater impact on lapse rate. This required the advanced technology engines to be sized 4 percent larger at sea level static uninstalled take-off than the reference technology engines.

4.4   Summary

In summary, the recuperator has the greatest impact on SFC reduction, approximately 20 percent, but also has the disadvantage of increased size, weight and costs. Advanced aerodynamic components have a 6 percent impact on SFC reduction. Higher cycle temperature with gas generator ceramics (Level 5) shows an 8 percent SFC reduction as compared to 4.8 percent for the combined Advanced Cooling + Advanced Materials of Level 4. The impact of the axi-centrifugal compressor is less than 1 percent; however, it can be optimized for a higher rotational speed than a single stage centrifugal, and this will have a beneficial impact on the gas generator turbine's performance.

SECTION 5.0
PROPULSION SYSTEM SIZE, WEIGHT AND COST ANALYSIS

In this section, the propulsion system sensitivity to size, weight and acquisition and maintenance costs are determined as a function of the engine advanced technologies defined in Section 4.0. In addition, two further levels of advancement, incorporating advanced material substitutions, are defined.

- Level 7: Level 6 + Ceramic Recuperator. This level substitutes advanced ceramic core plates for the reference metallic plates used in the Level 6 recuperator.

- Level 8: Level 7 + Advanced Materials (PT/Case). This level also substitutes advanced ceramics for the reference metallic power turbine and advanced graphite composites for the gearbox casing and engine inlet.

5.1 Parametric Estimating Relationships

Parametric analysis has proven to be a powerful and flexible approach to engine size, weight and cost estimation. Past independent research activities and contracted studies have resulted in computerized procedures allowing comparison of alternative engine systems on the basis of their different characteristics, including their impact on system direct operating cost (References 9 and 10).

The parametric estimating relationships are modular in order to allow individual components to be combined with any basic engine configuration. The relationships are primarily functions of engine cycle parameters, but include modifiers to account for advanced design technologies, such as improved aerodynamics and improved cooling capabilities. Modifiers are also included to account for substitutions of current materials with advanced materials. Costs which are considered include maintenance labor costs and maintenance materials cost, as well as total engine acquisition cost. Cost adjustments based on production quantities and current year dollars are also made.

The primary driving factors which characterize the core engine size, weight and costs are air flow rate, compressor pressure ratio and turbine inlet temperature, all defined at uninstalled take-off power. The gearbox was defined by maximum input power and overall speed reduction ratio. The recuperator was defined by the engine air flow rate, effectiveness and total pressure loss (air side plus gas side).

5.2 Advanced Material Substitutions

The materials selected for determining their impact on size, weight and costs were:

- Ceramics; in monolithic or composite form, applied to the engine hot end components and to the recuperator plates.

- Graphite composites; fiber re-inforced polymides, applied to the engine inlet and reduction gearbox casing.

Relative weight and acquisition cost values for the advanced materials technologies were determined from industry trends and Lycoming projections (Reference 11). Advanced material weight and cost reductions used for the study are shown in Table 9. These ratios, when combined with the respective weight and cost fractions of each component, determine the material substituion influence at both the component, and overall engine levels.

The impact of material substitutions on engine maintenance costs were determined using a Lycoming direct maintenance cost (DMC) model. The DMC analysis accounts for parts costs and parts repairability variances as well as reduced wear-out or erosion levels, Figure 58. The overall change to maintenance costs are expressed as a modifying term dependent on the proportion of substitution of each material type.

5.3 Propulsion System Size

Propulsion system size was characterized by its frontal area installed in the nacelle. The effective installation diameter was taken from the larger of the engine diameter plus clearance for the mounting structure, or the recuperator diameter plus clearance for insulation.

The results of the parametric area estimating analysis is shown in Figure 59 for the engine designs with a single-pass recuperator. Although air flow rate reductions approaching 40 percent were achieved at constant power with consequent reductions in engine and recuperator diameters, a 200 to 300 percent increase in frontal area can still result for the higher effectiveness designs, leading to marked increases in aircraft size, drag and power and fuel requirements.

The engine designs incorporating two-pass recuperators (Figure 60), are able to maintain a diameter similar to the core engine, resulting in an overall reduction in frontal area, except at the higher effectiveness levels. Because of the clear benefit of the advanced two-pass configuration over the single-pass, only the results of the two-pass recuperated designs will be discussed in the remainder of the report.

5.4 Propulsion System Weight

The propulsion system weight includes the reduction gearbox, engine and accessories, recuperator and the 82 lb (32.7 kg) propeller. As shown in Figure 61, at any given technology level, higher recuperator effectiveness causes a significant increases in weight, driven primarily by the increased heat transfer area requirements of the recuperator plates. Advances in technology, on the other hand, reduce engine air flow requirements, leading to smaller, lighter components for any given effectiveness.

Substitution of advanced materials reduces the weight further. Most of the weight reduction from Level 2 to Level 5 is due to the smaller components resulting from increased specific power, but part is due to the lighter weight of the ceramic hot section of the gas generator. The weight reduction from Level 6 to 7 is due entirely to the lighter weight ceramic plates in the recuperator since the cycle did not change. Introducing the ceramic plates results in an effective propulsion system weight reduction of 7.9 percent for the Level 7 design, at 80 percent effectiveness, where the recuperator accounts for 42 percent of the propulsion system weight.

5.5   Propulsion System Acquisition Cost

Engine costs are primarily a function of weight, and as noted above, weight is sensitive to advanced technologies and cycle selection. Figure 62 shows that the addition of a recuperator in the Level 1 Reference Technology + Recuperator engine results initially in increased propulsion system cost, (18.2 percent at 80 percent effectiveness). With technology advancements which result in higher specific power, component and engine weights decrease and as a consequence, engine acquisition costs are reduced. The largest reductions are due to improved aerodynamics (Level 2), and increased cycle temperature achieved either with improved cooling (Level 3) or with no cooling made possible by gas generator ceramics (Level 5).

With all technologies incorporated (Level 8), cost reductions are forecast at 36 percent of the SECT Reference Engine acquisition cost, at 80 percent effectiveness.

5.6   Propulsion System Maintenance Cost

Since maintenance costs are dependent upon combinations of the number of parts contributing to maintenance actions, their frequency of occurrence and the cost of component repair or replacement, the addition of the recuperator module to the reference technology engine results initially in increased maintenance costs, as shown in Figure 63.

Introduction of advanced technologies, leading to reduced size, weights and acquisition costs, also results in reduced maintenance costs.

It is not until the introduction of advanced materials, however, that the maintenance costs are reduced below those of the non-recuperative SECT Reference Engine. The smaller, less costly components affect replacement costs, and the anticipated gains in material durability and erosion resistance combine to reduce the frequency of maintenance actions.

It is expected that, at 80 percent effectiveness, maintenance costs can be reduced by 12 percent with a Level 8 advanced technology engine.

SECTION 6.0
IMPACT OF ADVANCED TECHNOLOGIES ON REFERENCE AIRCRAFT

In this section, advanced engine technologies were evaluated on the basis of overall Reference Aircraft performance improvement to establish the requisite engine cycle and technologies for the best economic performance.

The aircraft system trade-off evaluations were calculated from the trade factor matrices for all eight levels of technologies, for recuperator effectiveness ranging from 70 to 90 percent, and for fuel prices of $1.00 and $2.00 per gallon.

The resultant changes in system fuel burn, maximum take-off gross weight, maximum take-off power, aircraft acquisition cost and direct operating costs are shown in Figures 64 thru 69, and are discussed in the following sections.

6.1 Aircraft Fuel Burn

Fuel burn reduction for the 65 percent payload, 100 n mi (185 km) stage length flight is shown in Figure 64. Significant reductions are evident, beginning with the initial introduction of a recuperator module in technology Level 1, and further augmented by each successive technology. Fuel consumption in actual system operation is principally influenced by SFC and secondarily by system size and weight. Each of the key contributors have benefitted from the technology levels considered. The combined effects of primary and secondary influences results in a maximum reduction in fuel burn of 42 percent for the Level 8 design at a recuperator effectiveness of 84 percent. At 80 percent effectiveness, the Level 8 design can achieve a fuel savings of 40.7 percent. This translates to 18 gallons per flight or 80,000 gallons per year per aircraft, based on 2800 hrs utilization.

6.2 Maximum Take-off Gross Weight

As shown in Figure 65, the maximum take-off gross weights are generally greater for recuperated engines, especially for the initial technology levels. This is because the propulsion system's increased weight and size at high effectiveness more than cancel out the gains made by improved SFC. It is seen that technology Level 8 requires a recuperator effectiveness below 83 percent to achieve an overall aircraft weight reduction. At 80 percent effectiveness a Level 8 design indicates a weight reduction of 2.5 percent.

6.3 Maximum Take-off Power

Maximum take-off power, as shown in Figure 66, follows the same trend as the maximum take-off gross weight. To maintain the Reference Aircraft take-off power level, a technology Level 8 design must be constrained to an effectiveness below 86 percent. At 80 percent effectiveness a 3.4 percent reduction in take-off power is indicated.

6.4 Aircraft Acquisition Cost

Acquisition cost changes also follow the maximum take-off gross weight trends as shown in Figure 67. Here, the reductions in propulsion system cost with increasing technology level, coupled with reduced aircraft weight

23

corresponding to lower SFC and fuel weight, provide cost savings for effectiveness up to approximately 85 percent. For technology Level 8, at 80 percent effectiveness, an aircraft acquisition cost reduction of 7.2 percent, or $176,000 is achievable.

6.5   Direct Operating Costs

Direct operating cost was selected as the primary indicator to measure and monitor the aircraft/propulsion system design efficiency. DOC combines influences of engine-related characteristics, aircraft characteristics, current industry costs and mission operational usage into a single parameter representative of initial and recurring costs. As shown in Figure 68, at $1.00 per gallon fuel price, the application of advanced technologies results in a DOC reduction of 13.4 percent compared to the Reference Aircraft for a Level 8 design with a recuperator effectiveness of 80 percent. Figure 69, shows that for $2 per gallon fuel, DOC reductions of 18.6 percent are achievable for the Level 8 design with 80 percent effectiveness.

SECTION 7.0
COMPONENT SELECTION AND PRELIMINARY ENGINE DESIGN

The impact of the selected technologies on aircraft performance, fuel burn and direct operating cost was established in the previous section. Cycles were optimized to determine the recuperator effectiveness which produced the minimum aircraft DOC. Technology Level 8 showed the most benefit in terms of DOC improvement and therefore it was selected for preliminary design analysis. The advanced technologies included in the recommended advanced recuperative turboprop engine are: advanced aerodynamic components; ceramic combustor, turbines and recuperator core; and graphite composites for the gearbox casing and engine inlet.

In this section, cycle and performance data were generated for the advanced recuperative engine design. Based on this cycle, components were selected and a preliminary engine layout was made to establish size and feasibility. Estimates of the advanced engine weight and cost are also presented in this section.

7.1   Cycle Selection

The aircraft performance characteristics indicate that minimum DOC is achieved for recuperator effectiveness ranging between 70 and 80 percent. The engine cycle for the preliminary design was optimized for 80 percent effectiveness for two reasons. First, it is believed that advances in packaging and aircraft integration can be made to minimize the negatives associated with larger recuperators. Second, there are other applications that are not so sensitive to size and weight, such as ground vehicles, which can benefit from this technology. Selecting the effectiveness at the upper end of the optimum range, therefore, broadens the future application base.

For this design, as was shown previously in Figure 48, the recuperator accounts for a 20.9 percent SFC improvement over the non-recuperative SECT Reference Engine, advanced aerodynamic components account for 6.1 percent and ceramics 8 percent. One third of the 8 percent is attributed to operating at 400°F (222°C) higher turbine inlet temperature than the Reference Engine.

At the uninstalled take-off condition, for a cycle temperature of 2640°F (1450°C), the compressor pressure ratio which produces minimum cruise SFC is 8.9. The corresponding output power is 949 hp (708 kW), SFC is 0.30 lb/hr/hp (0.18 kg/hr/kW) and the engine airflow is 3.76 lb/sec (1.71 kg/sec). Detailed performance and cycle data are given in Table 10 and component data are given in Table 11, for uninstalled take-off and installed take-off and cruise conditions.

7.2   Mechanical Description

The preliminary design engine with a two-pass recuperator, designated PD-2, as configured in Figure 70, is made up of three basic sections: reduction gearbox, engine and recuperator.

7.2.1   Reduction Gearbox
The reduction gearbox consists of two epicyclic gear trains, made of iron and nickel-based alloys, coupled together to produce a 25:1 speed reduction ratio

between power shaft and propeller. The graphite composite gearbox casing bolts directly to the front of the inlet which is a two-piece assembly of graphite composite and titanium. The reduction gearbox weight is 116 pounds (53 kg).

7.2.2 Engine

The single spool gas generator is comprised of a straddle mounted compressor driven by an overhung single-stage axial gas generator turbine. The compressor is a two-stage design, one axial and one centrifugal, both made of titanium. The front drive, two-stage free power turbine is straddle-mounted, providing power to the reduction gearbox.

The turbine nozzles and blades are ceramic. The stators are mechanically attached to inner and outer positioning shrouds and the blades are attached to modified IN100 disks.

The single can combustor and scroll, both made from ceramics, are contained in a nickel-based alloy housing which ducts the compressed air to the recuperator.

The graphite composite accessory gearbox casing, (not shown in the figure), is top mounted above the inlet.

The engine weight, (less reduction gearbox and recuperator) is 178 pounds (81 kg) which includes 89 pounds (40 kg) for the accessories and accessory gearbox.

7.2.3 Recuperator

The recuperator has a two-pass annular core to minimize engine frontal area. The core is made from ceramic which has a higher temperature capability than metallics and in addition, has a lower weight and cost. The housing is made from a nickel-based alloy. The weight of the recuperator section is 281 pounds (128 kg).

7.2.4 Gas Flowpath

Air enters the engine through a downward facing inlet and is delivered to the axi-centrifugal compressor. The compressed air is fed via 12 tubes to a plenum in the recuperator aft header. The air travels radially outward through the wave-plates in the aft half of the recuperator, then passes to the forward half where it flows radially inward, always in the counter-flow direction to the hot gas. After leaving the recuperator, the heated air enters the single can combustor. The hot gas then flows through the scroll to the turbines. At the power turbine exit, the exhaust gas is diffused and flows radially outward between the wave-plate of the forward section of the recuperator, turns, and then flows radially inward through the aft section of the recuperator. The exhaust gas then exits axially along the engine centerline.

7.3 Aerodynamic Components

A description of the aerodynamic component selection and technology requirements is given below.

7.3.1 Compressor

To achieve the overall 8.9 cycle pressure ratio, the axi-centrifugal compressor was sized for a 1.7/5.2 pressure ratio split at sea level static. With this pressure ratio split, the stages can be close coupled thus eliminating the necessity for a transition duct.

The rotational speed is 68,000 rpm which yields an optimum specific speed for the centrifugal stage. The axial stage inlet hub/tip ratio (0.44) was set as low as possible to provide just enough space for the front gas generator bearing and the passing of the power shaft. As a result of the inlet hub/tip ratio and rotational speed, the inlet relative tip Mach number is 1.4 which is acceptable for a 1.7 pressure ratio stage. The stator is designed to leave pre-whirl in the direction of rotation at its exit to favor the relative tip Mach number into the centrifugal inducer. Also, by leaving pre-whirl, the stator's diffusion is reduced which improves the axial stage efficiency.

The centrifugal stage runs at a specific speed of 99 and the relative tip Mach number into the inducer is 1.0. The impeller is designed to have 50° leanback with an exit tip speed of 2150 ft/sec (655 m/sec). As a result of blade-leanback, the Mach number entering the diffuser is reduced to 0.98, providing for shock-free diffusion. The impeller stress levels associated with the high leanback and tip speed require advanced high-strength materials. 3-D viscous codes must be developed and applied to compressor design to achieve the projected efficiency objectives.

A single-stage high pressure ratio (8.9) centrifugal was considered as an alternate approach. However, the rotational speed would have had to be decreased 10 percent to balance the losses resulting from the high relative tip Mach number into the inducer (1.3) with those resulting from frictional effects. Since higher risk is associated with the high pressure ratio centrifugal and since the lower rotational speed adversely affects the gas generator turbine efficiency, the axi-centrifugal design was selected for the advanced technology engine.

7.3.2 Gas Generator Turbine

A single-stage axial turbine was sized to meet the gas generator requirements. The design goals can be met since the design loading ($\Delta H/U_m^2 = 1.3$) and Mach number (under 0.9) are consistent with an efficient design. However, to achieve these goals, ceramics materials, 3-D viscous codes and tip treatments are required.

Ceramic materials for vanes and blades are necessary in order to operate the turbine uncooled. To allow for circumferential hot spots above the specified 2640°F (1450°C) turbine inlet temperature at take-off the ceramics must have an operating temperature capability of at least 2850°F (1566°C). Ceramics contribute to an efficiency improvement in two ways. First, the airfoils can be designed with optimum thickness/chord ratios and thin trailing edges because they do not have to be compromised for cooling passages. Secondly, there is no disruption of the working gas due to the ejection of cooling air from the blade surface.

3-D viscous codes are required to minimize boundary layer and secondary flow losses. With an improved representation of the flow conditions from the viscous codes plus interactive design techniques and systematic testing, turbine losses can be reduced as much as 15 percent.

To achieve high aerodynamic performance in advanced gas turbines, tip clearance losses must be held to a minimum. The conflicting requirement for adequate clearance to preclude deleterious tip rubs under all steady state and transient engine operating conditions requires comprehensive knowledge of the dynamic growth behavior of the turbine in its operational environment. By intensifying research and testing efforts in the areas of blade tip treatment and casing treatment to reduce sensitivity to tip clearance, efficiencies of small turbines will be significantly improved.

7.3.3   Power Turbine

A two-stage high speed (42,000 rpm) axial flow turbine was selected to meet the design requirements, because it offers the following benefits over a single stage design.

- Higher Efficiency

- No Interturbine Duct Loss. Since a two-stage power turbine has a smaller diameter than a single-stage, it can be close-coupled to the gas generator thus eliminating the interturbine duct loss.

- Lower Exit Diffuser Loss. A two-stage power turbine has a lower blade velocity and therefore for optimum efficiency a lower axial velocity is required. The lower axial velocity results in less diffusion and a lower pressure loss between the power turbine exit and the recuperator.

The turbine blading is entirely subsonic and has mean loading levels ($\Delta H/U_m^2$) of 1.6 and 1.2 for the first and second stage, respectively. The second stage is designed for 0.34 exit Mach number to minimize diffusion to the recuperator.

Variable power turbine nozzles were initially considered to improve partload performance, but were decided against for the following reasons:

- The turboprop primarily operates near maximum continuous power and therefore does not benefit substantially from the improved partload cycle.

- The turbine efficiency is adversely impacted due to the clearance required for the variable nozzles and this affects maximum continuous power where most of the mission fuel is consumed.

The power turbine requires the same advanced technologies as the gas generator turbine. The maximum operating temperature of the power turbine is 2200°F (1204°C). This turbine operates uncooled and therefore ceramics are also required, especially if they are more cost-effective.

7.3.4 Combustor

From a performance viewpoint, the most desirable combustor configuration should provide the required performance with minimum weight (minimum surface area and number of accessories). From an overall cost of ownership viewpoint, the combustor should be inexpensive to manufacture, have high reliability, require little maintenance and be composed of a minimum number of parts. Both viewpoints stress the need for a minimum number of components. The measurable performance requirements were chosen to be:

- Efficiency greater than 98.5 percent at idle, (higher at cruise power)

- Total pressure loss less than 4 percent

- Invisible exhaust smoke

- Maximum exit temperature variance 15 percent (Pattern Factor <0.15)

Various combustor configurations are capable of achieving the above performance requirements. However, in order to determine which has the greatest chance of meeting the overall mission goals, a study of three basic configurations was undertaken:

- A single can-scroll

- A four can-scroll

- Annular reverse flow

The four can-scroll configuration looked attractive from a packaging viewpoint. However, the biggest detraction is the need for multiple ignition sources (2 per can) or flame cross-over pipes. Since the cans would be far apart (circumferentially), the use of cross-over pipes was judged to be an unacceptable risk for reliability and durability.

The results of the study are summarized in Table 12. The combustor efficiency scaling parameter theta (θ) was held constant at 1 million for sizing at the idle condition for both can-scroll configurations. The heat release rate in the can was 10.8 million BTU/ft^3 atm (3.97 x 10^3 kJ/m^{3}Pa). The annular configuration meets the theta value easily but would have a narrow flame tube height and will require a very high heat release rate (about 50 percent higher than the can). Therefore, the annular size was increased in flame tube height to match the same heat release rate of the single can configuration. This also reduces the number of fuel injector required for the annular combustor. The results clearly show that a single can provides a minimum surface area for the combustor and a maximum for the scroll ducting to the turbine. The four-can system requires more surface in the hot combustors but decreases the overall surface slightly. The annular configuration requires the most surface area which makes it undesirable from the weight and durability aspects. In addition, fuel breakdown and plugging of fuel injectors is a major concern in this type of engine due to the operational temperature and heat soakback after shutdown. Therefore, the fuel injector passage sizes

should be maximized and the number of injectors should be minimized. The single can-scroll arrangement was selected because it permits more fuel cooling of the injector, longer life and facilitates maintenance. It also minimizes the number of parts.

The exit temperature distribution uniformity can best be achieved by non-metallic parts in the scroll that do not require film cooling. Combustor exit temperature distribution must be equal to the goal of 15 percent so that the scroll is not distressed. A combustor to achieve this goal is attainable in a single can configuration because of the minimum number of parts which helps to eliminate the need for fuel injector matching and air flow distribution tailoring.

7.3.5   Recuperator

Based on the waveplate heat transfer surface characteristics, three recuperator cores were configured and sized: single pass annular, two-pass annular and rectangular. They were sized for 80 percent effectiveness and a total pressure loss of 7 percent (2 percent airside and 5 percent gas side). The two-pass annular and rectangular configurations have the same frontal area and the final selection would depend on a detailed airframe integration study to determine which design provides the best packaging arrangement. However, for the preliminary design layout, the two-pass annular recuperator was used because it conforms to a current engine installation in a similar size commuter aircraft. The current production engine has a diameter and length of 19 in (0.48 m) and 76 in (1.93 m), respectively, compared to 20 in (0.51 m) and 60 in (1.52 m), respectively, for the PD-2 preliminary design configuration.

In the PD-2 engine configuration, the recuperator diameter extends beyond the combustor housing by 5 inches (0.13 m) and is also larger than the diameter predicted by the parametric equations. This discrepancy is due to additional duct area used to maintain acceptable Mach number and pressure loss levels. However, a 16 inch (0.41 m) diameter objective can be met with the introduction of advanced recuperator technologies which include:

- Compact core design to reduce size; area density increased 25 percent and j/f characteristics increased 25 percent, where j is the Colburn heat transfer factor and f is the Fanning friction factor.

- Ceramic core to achieve lower cost and weight, higher temperature capability and improved durability. Plate thickness should be less than 0.013 in (0.33 mm).

- Packaging and aircraft integration to minimize impact on aircraft drag.

7.4   SECT Advanced Technology Engine

For the year 2000 the advanced recuperative engine will have similar aero components and performance as the preliminary design configuration, PD-2, but with the smaller 16 in (0.41 m) diameter recuperator of technology Level 8. A comparison of weight, size and cost of this advanced configuration to the

non-recuperative SECT Reference Engine is shown in Table 13. This configuration is defined as the SECT Advanced Technology engine and will be evaluated in the system performance analysis and compared to the preliminary design engine, PD-2.

In summary, the preliminary design study showed that the engine and its components are aerodynamically and mechanically feasible with the year 2000 advanced technologies. The study confirmed that the installation of either the SECT Advanced Technology Engine or the PD-2 preliminary design engine in an aircraft is achievable.

SECTION 8.0
SYSTEM PERFORMANCE ANALYSIS

This section describes the aircraft sizing and mission analysis studies which were conducted to determine the benefits of the engine advanced technologies. Both the PD-2 engine layed-out in the previous section, and the SECT Advanced Technology engine with the Level 8 reduced diameter recuperator were considered. The GASP computer program was used for direct comparisons with the Reference Aircraft results of Section 3.0.

In addition, the trade factor analysis predictions were compared to the GASP results to gauge the accuracy of the prediction method, and to quantify the benefits of the individual technologies identified by the design study.

8.1   Trade Factor Analysis Comparisons

The trade factor analysis predictions of fuel burn benefits and DOC benefits were determined for each level of technology identified during the engine design study. The progressive reduction in fuel burn achieved by each technology advancement is shown in Figure 71. Note that the difference between the Level 8 prediction and the GASP calculations for the SECT Advanced Technology engine is a measure of the accuracy of the trade factor calculations used for the design study. The difference between the two methods is only 2.4 percent, and is attributable to the use of matrix coefficients developed for the non-recuperative Reference Engine which had slightly different off-design characteristics than the recuperative SECT Advanced Technology engine.

A similar check of the DOC predictions is shown in Figure 72. Here, the differences between the two methods are only 0.9 percent for $1.00 per gallon fuel costs and 1.6 percent for $2.00 per gallon.

The trade factor results were used with the GASP results in Section 9.0 to quantify the benefits of each of the advanced technologies.

8.2   Preliminary Design Engine PD-2

The design and off-design performance data were generated for this engine, and the aircraft was resized using GASP for the 600 n mi (1111 km) mission, as in Section 3.0. The larger O.D. recuperator on this engine resulted in increased nacelle drag and therefore slightly greater power requirements and aircraft size. The calculated fuel burn and DOC values are therefore up slightly from the Level 8 predictions.

8.3   SECT Advance Technology Engine

The design and off-design performance data were also generated for this engine, and the aircraft was again resized for the 600 n mi (1111 km) mission using GASP.

For the same wing loading and aspect ratio as the Reference Aircraft, the new aircraft shown in Figure 73 is essentially the same size as the Reference, but has a slightly reduced take-off gross weight of 2.8 percent. Max uninstalled power is reduced 1 percent, but the maximum installed power is

down 5 percent due to the impact of the 10 lb/min (4.5 kg/min) bleed requirement imposed on the much reduced airflow rate of the advanced technology engines.

A weight comparison of the two aircraft is shown in Table 14. A slight reduction in airframe weight was realized for the new aircraft, but the heavier recuperative engines resulted in an aircraft empty weight increase of 316 lb (143 kg). The reduced fuel load requirement of the advanced technology engines, however, resulted in the overall take-off gross weight reduction of 362 lb (164 kg).

Acquisition cost comparisons are shown in Table 15. Engine cost has been reduced 38 percent, due partly to the reduced turbomachinery size and partly to the use of advanced composites and ceramic materials. Total aircraft acquisition cost is down 7.6 percent.

The aircraft performance benefits provided by the SECT Advanced Technology engine are summarized in Figure 74.

Direct operating cost comparisons are shown in Table 16. Fuel burn for the 65 percent payload, 100 n mi (185 km) flight is reduced 38.3 percent. Engine maintenance costs are reduced 14 percent. Total DOC is down 12.5 percent at $1.00 per gallon fuel cost and down 17 percent at $2.00 per gallon. The DOC breakdown for the new aircraft is shown in the pie plots of Figure 75. At $1.00 per gallon, fuel now represents only 15 percent of DOC compared to 21 percent for the Reference Aircraft. At $2.00 per gallon, fuel represents 26.2 percent of DOC, compared to 35 percent for the Reference Aircraft.

SECTION 9.0
BENEFITS ANALYSIS

In this section, the advanced technologies that provided the most gain in fuel burn and direct operating cost reductions are identified, and the benefits accruing from each are determined. The technology plan, which was assembled to identify the path to achieve these gains, is described in Section 10.0.

9.1   Identification of the Required Advanced Technologies

Identification of the technology requirements for the recuperative SECT Advanced Technology engine indicated the following four major needs:

- A recuperator with a ceramic core.

- Advanced aerodynamic components.

- A 400°F (222°C) increase in turbine inlet temperature.

- Ceramic materials for the combustor and turbines.

The recuperator design requirements include an effectiveness of 80 percent, a 7 percent total pressure loss (air side plus gas side), a 1500°F (816°C) surface temperature and a compact ceramic core necessitating a j/f increase of 25 percent over reference design capabilities.

The compressor design requirements include a 5 percent efficiency improvement and an axi-centrifugal design incorporating an integral shaft configuration.

The combustor must be designed for 2640°F (1450°C) take-off temperature with a pattern factor of 0.15. A ceramic liner and scroll are required.

The gas generator turbine, operating uncooled at 2640°F (1450°C) take-off temperature, requires ceramic blades and vanes with an operating temperature capability of 2850°F (1560°C). A 3.5 percent efficiency improvement has also been identified.

The power turbines require an efficiency improvement of 1.6 percent, and ceramic blades and vanes are required with an operating temperature capability of 2200°F (1204°C) during take-off.

9.2   Benefits and Ranking of Each Required Technology

The potential benefits were identified primarily by reductions in direct operating cost, with secondary consideration given to reduced fuel burn, both calculated for the 65 percent payload, 100 n mi (185 km) stage length mission.

The benefits accruing from the recuperator were evaluated by comparison with a non-recuperative engine brought up to the same technology level as the SECT Advanced Technology engine. As shown in Table 17, the advanced technology non-recuperative engine provided a fuel burn reduction of 22.4 percent from the Reference Engine, compared to 38.3 percent reduction for the SECT Advanced Technology engine, indicating a net benefit attributable to the

34

recuperator of 15.9 percent. At $1.00 per gallon fuel price, the advanced technology non-recuperated engine provided an 11.7 percent reduction in DOC, compared to 12.5 percent for the SECT Advanced Technology engine, indicating a net benefit of 0.8 percent due to the recuperator. At $2.00 per gallon, the advanced technology non-recuperated engine provided a DOC reduction of 13.6 percent, compared to 17.0 percent for the SECT Advanced Technology engine, or a 3.4 percent benefit due to the recuperator.

Based on these results, and the trade factor and GASP results of Section 8.0, the benefits attributable to the required advanced technologies were then determined and ranked. As shown in Tables 18 and 19, the ceramic recuperator contributes most towards fuel burn reduction (15.9 percent), while the ceramic combustor and turbines contribute least (5.1 percent). For DOC reduction, their relative importance is reversed. That is, the ceramic combustor and turbines contribute most while the ceramic recuperator contributes least.

It is important to note that the fuel burn reduction of 38.3 percent saves 75,000 gallon per year per aircraft (Table 20). The reduced DOC of 12.5 percent saves an operator $120,000 per year per aircraft based on $1.00 per gallon fuel price. This increases to $199,000 per year per aircraft for $2.00 per gallon fuel price. For a fleet of 500 aircraft, 37.5M gallons of fuel would be saved per year, while the operating cost savings would amount to $60M per year at $1.00 per gallon, and $99M per year at $2.00 per gallon fuel price.

SECTION 10.0
SMALL ENGINE COMPONENT TECHNOLOGY (SECT) PLAN

In this section, specific component technology programs are recommended to obtain the small engine propulsion system technologies by the year 2000. The prime emphasis entails the integration of component programs involving component experimental rigs and engine environment testing. The technology plans are grouped via the major categories in order of benefits as established by DOC: (1) ceramic materials, (2) advanced aerodynamics and (3) recuperator technology. During all phases of the component technology programs, the development of propulsion system analytical prediction capability is crucial to the overall program.

10.1   Ceramic Materials

10.1.1   Ceramic Nozzle

The ceramic HP nozzle will be designed for silicon carbide (SiC) materials systems. Other structural ceramics, such as silicon nitride (Si_3N_4), are temperature limited, typically less than 2500°F (1370°C). The first phase mechanical design will be based upon a hybrid approach. That is the vanes and shrouds will be separately manufactured allowing design and process optimization as well as interchangeability of components. The vanes will be injection molded and sintered alpha SiC and the shrouds and supporting rings will be some form of sintered SiC, depending upon strength requirements. A parallel activity will address developing SiC/SiC (fiber/matrix) composite rings for shroud application; this will be discussed later in this section. The ceramic nozzle technology plan is presented in Figure 76.

Two design concepts are of prime interest for this application. The first concept utilizes individual net shape vanes inserted into shroud channels or pockets. A second concept utilizes multi-airfoil vane segments which would include a shroud on either the outer or inner surface. Both of these vane concepts have been successfully manufactured to near net shape. The structural arrangement will be the key criteria which will determine the selected approach.

The process evaluation activity will address two major requirements of material quality and net shape parts. Several government and industry sponsored programs have identified problems in these areas. Therefore, activities will evolve around the iteration of process and shape requirements for the individual components. It is very important that the airfoils can be made to net shape and within aerodynamic tolerances. This will not only drive down the costs of producing the parts, but will eliminate the need for flaw inducing machining operations.

Isopress (hot or cold) plus sintered SiC rings will be investigated for initial nozzle assembly evaluation. However, the primary manufacturing process for ring shaped components will be a SiC matrix reinforced with woven SiC fibers/whiskers to increase the fracture toughness. Recent research has demonstrated the feasibility of infiltrating a woven preform with a ceramic matrix, thus creating a three-dimensional ceramic structure. The approach will evaluate gas and polymer infiltration of a woven SiC preform. Density optimization, fracture toughness and strength will be prime factors affecting the final process selection.

Initial nozzle rig tests which closely simulate the engine environment will include only monolithic SiC materials to enable early and less costly evaluation of the basic nozzle concepts. A composite shroud will be tested to provide a comparison with the monolithic approach. Since the high pressure turbine nozzle experiences very severe operating conditions, it is expected that two design iterations will be required over the course of this program.

10.1.2 Ceramic Blades

Injection molded plus sintered alpha silicon carbide (SiC) was selected as the materials system for the blade based upon the 2640°F (1450°C) $T_{4.0}$ thermal environment. SiC has good strength and environmental characteristics in this temperature range. Supporting this activity will be an evaluation of several compliant materials systems to interface between the ceramic blade and metallic rotor. The third activity addresses abradable tip treatment for the airfoils. Figure 77 shows the ceramic blade technology plan.

The mechanical design will trade-off individual blades versus segmented or multiple airfoil approaches. Also, axial blade insertion will be evaluated versus circumferential clamping. The goal of the materials processing activity will be to optimize material quality and consistency while attaining a net shape part. Initial concepts will be evaluated via room temperature vacuum spin testing.

Compliant materials will be necessary for interfacing between the blade root form and the disk for several reasons. First, the net shape product of the ceramic process will not achieve grinding tolerances; therefore it would be desirable to fill the gap with another material. The compliant material would reduce any line or point contact stresses due to surface irregularities resulting from fabrication or handling. An interface material could either sacrificially crack or redistribute the stress concentration over a larger area. Also it is desirable to minimize any surface reaction between the SiC and superalloy disk material. Two approaches are of primary interest. The simple application of brush-on, low temperature curing ceramic potting compounds offers several compositions for selection. Chemical vapor deposited coatings such as zirconia provide a controlled, fine grain processing method, which is amenable to high volume application.

A tip treatment program for the ceramic blades will be coordinated as a system approach with the high pressure turbine tip seal program. Candidate methods to enhance the rub-in capability of the tip include the use of hard particles or ceramic coating systems. The inherent hardness and wear resistance of SiC may obviate the need for either system.

Cold vacuum spin testing will be used for initial structural evaluation of the various root forms and design tolerances. Warm aerodynamic rig testing will be conducted at temperatures less than 1800°F (982.°C) to evaluate the performance of the compliant materials in an oxidizing environment. The variables that will be evaluated include compliant material thickness versus assembly tolerances and composition versus oxidizing and diffusion characteristics. An iteration of this effort should be sufficient to establish the requirements of the final design which will be optimized for aerodynamic performance. Blades for the final design will be proof tested in a cold spin

rig and hot rig tested using the optimized blade tip treatment and root compliant materials.

10.1.3   High Pressure Turbine Tip Seal

The high pressure turbine tip seal project will be a materials processing intensive program. Temperature requirements dictate that the system matrix will be silicon carbide (SiC). A SiC fiber-reinforced cylinder will be established to enhance the strength and fracture toughness of the structure and to provide fiber/whisker options for the abradable seal. The ceramic matrix composite (CMC) material effort has generic benefit to the nozzle and liner projects. The tip seal plan schedule is shown in Figure 78.

The CMC approach will be to weave a two-dimensional SiC fiber/whisker preform and to subsequently infiltrate SiC matrix into the voids. Chemical vapor infiltration and polymer infiltration pyrolysis offer ways to densify SiC preforms with ceramic phase at low temperatures, thus minimizing degradation reactions. The concepts have been demonstrated to a limited extent at Avco Systems Division. Piercing of the ceramic preform in the radial direction could serve as a basis for tip seal construction.

Abradable seal systems will be based on ceramic coatings with and without whisker/fiber reinforcement. Coating deposition processes and compositions will be evaluated for environmental and spallation resistance via gas fired hot corrosion and thermal fatigue rigs, respectively. The composition and porosity of the systems will be adjusted to enhance abradability, relative to the baseline SiC turbine blade.

The mechanical design of the high pressure turbine seal will incorporate producibility features which will be a by-product of the processing trials. Evaluation of the tip seal system will require engine testing to full temperature and pressure conditions. One iteration of the full scale testing has been planned into this program.

10.1.4   Ceramic Single Can Combustor

A ceramic single can combustor will be evolved to satisfy both the structural and performance requirements of the regenerative engine, as Figure 79 shows. Silicon carbide will be evaluated since the operating temperature and oxidizing environment rules out silicon nitride and lower strength ceramics. Lycoming has a baseline production experience with the AGT 1500 can combustor. Also, the government sponsored Automotive Gas Turbine engine programs are evaluating ceramic designs.

The small, simple shape of a single can liner permits manufacture by several different materials processing techniques. Basic strength requirements will be established during the preliminary design of the combustor. Slip casting and an infiltrated SiC/SiC composites approach are the primary methods under consideration. The casting technique presents a simple, low cost way to produce the part. However, higher strength and toughness requirements may dictate a CMC part. The composites technique described for the high pressure turbine tip seal will be also used here.

Initial component testing will be performed in a combustor rig. The primary goal will be to evaluate the attachment concepts and liner wall integrity by

progressively increasing the severity of the test conditions. The test sequence will be from steady state to rapid acceleration to a series of ignition tests. Infrared photography and rig instrumentation will be used to quantify the temperature distribution (pattern factor, radial profile) from the combustor. Refinements in structural and aerothermodynamic design features will be incorporated upon selection of the materials approach. Several modifications and iterations will be necessary to satisfy both structural and performance requirements.

10.1.5   Combustor Scroll

A combustor scroll-shaped transition duct is necessary to deliver the combustion gas from the single can liner to the high pressure nozzle. Lycoming has a production base of experience (AGT 1500) with a cooled sheet metal design which is ceramic coated. The uncooled approach for this project will utilize a thicker ceramic coating, strain-isolated from the superalloy sheet metal structure. This method should present less structural complexity or risk than a monolithic ceramic approach. The technology plan is shown in Figure 80.

Strain isolation of the thermal barrier coating will be achieved by brazing fiber pads directly to sheet metal details. These parts will be formed to shape and joined prior to coating. The collector halves will then be coated with a thermal barrier coating system such as the NASA composition. This concept is currently under investigation for lower temperature application in the AGT 1500. In this case, a Brunsbond™ pad will provide compliancy.

In the beginning of the program the thermodynamic requirements for the layered structure will be assessed. Optimization of the pad and coating systems (composition, thickness, etc.) will be based on environmental stability, resistance to spallation and insulating efficiency. Initial materials screening tests will be performed in gas fired thermal fatigue and hot corrosion rigs. The best coating systems will be integrated into the manufacturing process for the combustor scroll. Testing and evaluation will be accomplished in a combustor rig at full pressure and temperature. One design-test iteration is anticipated.

10.2   Advanced Aerodynamics

10.2.1   Flow Field Prediction

Achieving higher performance levels in future gas turbine aero components presents a continuing challenge to aerodynamic designers. Truly advanced designs will result from a detailed understanding of the fluid flow field throughout the engine. Prediction capability has advanced dramatically over the last decade with the increase in computing capability. The next decade will produce dramatically increased capability made possible by expanded computing capability.

The evolution of aerodynamic modeling started with simple inviscid two-dimensional (2D) potential flow solutions. These have been enhanced to account for viscous effects (a particular concern in small turbomachinery components) by coupling separate boundary layer analyses. This has been further expanded to three-dimensional (3D) solutions to account for the major effects present in turbomachinery components. Additional effort is seen to

further refine this technique and approach the full predictive capability of this method. Effort is required to introduce computation methods that increase the computational accuracy and speed. This will lead to increased design capability and reduced design cost. The proposed plan is outlined in Figure 81.

A true viscous analysis that treats the highly three-dimensional, rotational, turbulent and unsteady effects is still in the early development stage. A major effort over the next decade will expand the present design capability and provide for geometries customized for minimum losses and extended stable operation that are required for high efficiency with fewer and more highly loaded stage components.

The rotating annular cascade problem is fundamental to the turbomachinery designer. It will initially focus on the steady flow case and add complexities of tip leakage, introduction of endwall flows such as disk cooling in the turbine, inlet turbulence and spatial and temporal entry distributions of pressure, temperature and velocity. The resulting prediction of local flow behavior, particularly adjacent to airfoil surfaces will allow the designer to customize geometries to extend and optimize performance and stability with confidence.

The unsteady flow effects resulting in preceding and succeeding cascade rows represents an area for still further performance improvements. Turbomachinery aerodynamics is inherently unsteady but the computational magnitude (and associated cost) of the solution has thus far limited serious work in this area. Compressor designers particularly will benefit from this capability by extending stable operation and blade loading. Even with larger faster computers, more efficient computational techniques must be developed to reduce cost and hasten its acceptance.

Validation of the aerodynamic computer code requires fundamental high quality experimental data and identification of areas requiring still better predictive capability. A series of controlled experiments is required where detailed non-obstructive measurements are made. Examples of benchmark experiments include large scale model testing to evaluate such phenomena as viscosity effects on the main flow, secondary flows, rotational effects on flow fields, boundary layers with and without film cooling, turbulence effects and shock boundary layer interaction. These experiments can be designed to investigate selected phenomena of interest and will allow collection of data generally not possible on full scale gas turbine components .

The culmination of the next decade's flow modelling effort will be a substantially improved and refined design capability that directly addresses the fundamental physics involved.

10.2.2   Compressor Technology

The recuperated small engine study has shown the requirement for an advanced technology 4 lb/sec (1.8 kg/sec), 9:1 pressure ratio axial-centrifugal compressor. The long range program to achieve the aggressive increase in performance relative to the reference engine requires a systematic program that incorporates advanced design methods and component test. (See Figure 82)

Overall compressor performance prediction capability must be able to forecast the combined axial centrifugal characteristics over the full range of operation. This effort combines experimental results and analytical performance predictions. Interaction effects on overall performance are of particular interest.

Axial stage technology is needed in this small size to minimize the penalties associated with non-scalable factors such as tip clearance, surface finish, manufacturing tolerances and minimum thickness. The performance potential of the first stage is high due to the predictable, fairly uniform in-flow conditions and relatively controllable endwall clearance and axial position compared with multistage axial compressors. Investigations of endwall contouring, rub-in coatings which minimize operating clearance and range-extending casing treatments are needed to maximize tip section performance. Flowpath surface treatments that have low frictional loss and control boundary layer secondary flow will be evaluated to improve performance.

Improved 3D viscous computational methods will provide a detailed understanding of the flow loss mechanisms and provide the ability to optimize designs. Endwall loss, for example, can be minimized by reducing the endwall loading and concentrating the work in the midspan region.

Since the centrifugal stage produces most of the compressor work, its performance is critical. The largest gains will result from detailed modelling and control of the flow within the compressor. Secondary flows, clearance leakage flows and surface frictional effects must be both predicted and experimentally verified. The entry flow into the diffuser and the resulting diffuser entry design is critical to centrifugal performance and requires a detailed analytical and experimental effort. The integration of the centrifugal diffuser and the combustor system is needed to improve the overall system performance through reduced pressure loss and improved combustor entry flow conditions.

A multiyear centrifugal stage research effort for this configuration is required utilizing advances in computational methods and measurement capability to reach the full performance potential.

10.2.3   Turbine Technology

The engine study shows the need for improvements in both gas producer and power turbine efficiencies to achieve the overall engine performance goals. The plan is presented in Figure 83. Elimination of cooling air provides improvements both in terms of reduced losses and initial cost with less complex hardware made possible with advances in high temperature materials technology. Additional loss reduction will result from advances in aerodynamic flowfield modeling using 3D viscous methods to refine the design process through careful attention to detail.

The present 3D design capability will be enhanced through a combination of fundamental benchmark experiments and improved analytical modeling methods to produce a more accurate description of the flowfield. This must be used in combination with testing of advanced stage designs to better define loss producing mechanisms to accurately predict performance over the full range of operation. Advanced designs will initially concentrate on reduction of

secondary flows and their associated losses through tailored geometrics made possible by advanced 3D viscous flowfield prediction capabilities. The endwall losses due to boundary layer, tip clearance and shroud wall configurations must be optimized through a combined experimental program to describe the detailed flow conditions and aerodynamic analysis leading to accurate design capability. The tip clearance sensitivity will be further reduced by optimal shroud wall geometries such as trenching, blade tips designed for reduced leakage flow and blading designs that control tip loading.

The hub wall flowpath will also benefit from detailed design analysis and improvements. Flowpath steps between stationary and rotating shrouds must be optimized to prevent hot gas ingestion into the disk cavities and to provide a minimum loss configuration for the main flow.

Controlling the tip clearance level is important for maintaining high performance with rotors of small channel height. Passive clearance control designs must be developed to vary shroud cooling air to minimize running clearance. A "smart" active system should also be studied to assess the additional benefits of further reduced clearances against the additional cost and complexity.

Rig testing in an engine operating pressure and temperature environment is important to assure a successful high temperature gas generator turbine program. With a high temperature hot section rig, both the aero/thermo aspects and the mechanical/materials issues can be effectively evaluated. This provides a relatively low cost and flexible approach with access capability for detailed diagnostic instrumentation.

Testing in the engine environment must also be performed to assess interaction effects. This is particularly important for high temperature configurations with advanced materials systems.

10.2.4   Combustor Technology

The objective of the combustor program is to evolve the design capability for a low pattern factor value within a constrained volume size required for an advanced small engine system. Durable high temperature operation of engine "hot section" components requires particular attention to the variation of temperature within and exiting the combustor. A plan to achieve the objective is shown in Figure 84.

The aerodynamics within the combustor will be modeled using three-dimensional, turbulent viscous flow solutions providing sufficient detail to represent complex flow mixing solutions. Integration of the flowfield solution with reacting chemical kinetics to predict gas species and temperature is crucial to achieving the objective. Prediction of combustor wall temperature involving radiation and cooling flows will be incorporated to obtain representative simulations. Experimental verification will be provided with component rigs to establish the validity of the analytical procedures. Experiments will measure the detailed fluid and chemical distributions within combustors using laser diagnostic measurements, and wall cooling effectiveness using liner wall segments in a rig with controlled and measured boundary conditions.

The combustor configuration will be a single can with variations of the mixing process. One potential mixing configuration may consist of a

multi-annular swirl type without downstream radial jets. Traditional wall cooling schemes using radial penetration jets will also be configured. The end result of the mixing process is to tailor the combustor exit pattern factor which is a measure of the ratio the local combustor temperature rise to the mean temperature rise. The turbine nozzle component may suffer life limiting operational restrictions when the pattern factor is excessive. Combustor performance prediction capability to control the temperature distributions becomes a prime prerequisite for a successful advanced small engine.

Fuel injection into the combustor will be accomplished using simplex-type injectors. These injectors provide improved durability and reliability required for long term, low cost commercial engine operation. The orifice size for this type injector is large which retards formation of coke deposits which would require injector replacement. The simplex design requires a pressure difference to operate. The crucial condition exists in the starting regime where low airflow through the engine results in a low pressure difference at the injector which leads to insufficient atomization for proper ignition. Combustor volume constraints result from engine size and weight considerations and the need to minimize liner surface area further aggravates the problem since ignition is related to combustor volume. Fuel injectors with enhanced atomization at low pressure differentials will result from the improved ability to model fuel droplet formation and spray behavior.

The potential to achieve proper combustor ignition may be enhanced through the use of photon energy ignition systems. Advanced research has shown significant energy can be imparted to fuel droplets via a radiation process to create a local high fuel dispersion and ignition process. This concept must be optimized and converted from a laboratory demonstration system to a compact, lightweight and durable configuration for engine use.

10.3   Recuperator

The recuperator represents the longest lead time component of the overall advanced engine plan. The technologies involved in the recuperator plan are grouped by three major categories: (1) heat transfer surface improvement, (2) ceramic material and (3) configuration or installation packing arrangement. The recuperator technology plan is shown in Figure 85.

The type of heat exchanger, as defined previously, will be a plate or plate-fin type design. The heat transfer characteristics are becoming amenable to the analytical techniques of three-dimensional viscous flow prediction. The internal flowfield passages have complex geometries to enhance the heat transfer qualities. The analytical capability will lead to understanding the details of developing optimized surface geometries. The overall performance of the recuperator depends upon the combination of multiple heat transfer surfaces operating with simultaneously varying pressure, temperature and flow conditions. Performance enhancements will be achieved upon accounting for these conditions including the transient operating characteristics of the overall engine during power excursions required for the aircraft mission.

The development of the analytical design and prediction capability will be validated via a series of experimental configurations involving detailed heat

43

transfer surface geometries, advanced section module configurations and full size recuperator cores. Specialized test rigs and engine environment testing will be required to acquire the verification data for both performance and structural design.

The operating temperature conditions of the recuperator will require a material program. Current metallic heat exchanger designs will be incapable of durable operation for the intended engine design and mission. The temperature capability of ceramic material will provide the means to achieve the desired performance. Ceramic material processing into a configuration having multiple heat transfer surfaces entails a crucial segment of the recuperator technology plan. The current most desirable ceramic material appears to be silicon nitride having the temperature capability with the greatest fracture toughness. Forming processes such as calendering or extrusion will be evaluated to determine the fabrication method.

Metallic materials will be used during initial phases of the module testing to evaluate heat transfer surfaces. For full size recuperator core experimentation, the ceramic material will be used. A minimum of two units of different heat transfer design will be evaluated. The durability of the recuperator must be verified through accelerated mission life testing.

The mechanical design of a recuperator requires several considerations. Because of the significant volume occupied by the recuperator, unique configuration concepts must be used to establish an overall integrated engine propulsion system design. The mechanical design techniques must be capable of predicting the life of the recuperator for the intended mission. The need for life prediction capability for brittle materials, such as ceramics, is not specific to this problem alone but it is a generic design technology which must support the overall small engine program. The overall engine propulsion system, in turn, must be integrated to the applicable airframe. Depending upon the trade-offs of overall airframe-to-engine integration, the configuration of the recuperator may be a prime consideration. Therefore, a program to include airframe integration will be included to arrive at a recuperator configuration.

SECTION 11.0
CONCLUSIONS AND RECOMMENDATIONS

This report summarizes the results of the Small Engine Component Technology (SECT) study. A non-recuperative turboprop engine was defined and evaluated in a 19 passenger commuter aircraft to serve as the reference system for the study.

A series of recuperated turboprop engines incorporating 8 levels of advanced technologies were studied and their impact on aircraft performance was compared with the reference.

Four advanced technologies were identified which yielded significant fuel and DOC savings. In rank order with respect to fuel burn benefits the technologies are:

	Fuel Burn Benefits
Ceramic Recuperator Core	15.9
Advanced Aerodynamics	10.8
400°F (222°C) Higher T4.0	6.5
Ceramic Combustor And Turbine	5.1
TOTAL	38.3 percent

In rank order with respect to DOC benefits the technologies are:

	DOC Benefits	
	$1.00/GAL	$2.00/GAL
Ceramic Combustor and Turbine	4.8	5.7
Advanced Aerodynamics	3.6	4.3
400°F (222°C) Higher T4.0	3.3	3.6
Ceramic Recuperator Core	0.8	3.4
Total	12.5 percent	17.0 percent

The fuel burn reduction of 38.3 percent saves 75,000 gallons per year per aircraft. The reduced DOC of 12.5 percent saves an operator $120,000 per year per aircraft based on $1.00 per gallon fuel price. This increases to $199,000 per year per aircraft for $2.00 per gallon fuel price. For a fleet of 500 aircraft, 37.5M gallons of fuel would be saved per year, while the operating cost savings would amount to $60M per year at $1.00 per gallon, and $99M per year at $2.00 per gallon fuel price.

Appropriate research and technology plans to reach year 2000 goals were established.

It is recommended that NASA pursue the advanced technologies identified in this study through sponsorship and support of the applicable technology programs. The technologies resulting from such programs will also be applicable to civilian and military rotorcraft and turbofan derivatives, providing comparable economies of operation.

SYMBOLS AND ABBREVIATIONS

Ag	Gas Flow Area
APS	Frontal Area of Propulsion System
ATDA	Advanced Technology Deviative Aircraft
atm	atmosphere
Btu	British Thermal Units
C	Celsius
Cp	Specific Heat at Constant Pressure
c/assm	cents per available seat, statute mile
CA acq	Cost of Aircraft, Acquisiiton
CMC	Ceramic Matrix Composite
CO	Carbon Monoxide
CPS acq	Cost of Propulsion System, Acquisition
CPS m	Cost of Propulsion System, Maintenance
dBA	decibels, A-weighted
dia	diameter
DMC	Direct Maintenance Cost
DOC	Direct Operating Cost
EPNdB	Effective Perceived Noise measured in decibels
f	friction factor
F	Fahrenheit
FAR	Federal Air Regulations
ft	feet
GASP	General Aviation Synthesis Program
hg	Gas Heat Transfer Coefficient
hp	horsepower
HP	high pressure
hr	hour
in	inch
j	Colburn heat transfer factor
kg	kilogram
kJ	kilojoule
km	kilometer
kPa	kilopascal
kts	knots
kW	kilowatts
L/D	Lift-Drag ratio
lbf	pound force
lbm	pound mass
m	meter
M	Mach number, Million
min	minutes
mm	millimeter
n mi	nautical mile
NO_x	Nitric Oxide
PR	Pressure Ratio
PT	Power Turbine
rpm	revolution per minute
s, sec	second
SFC	Specific Fuel Consumption
SHP	Shaft Horsepower
SiC	Silicon Carbide
Si_3N_4	Silicon Nitride

SL	Sea Level
SP	Shaft Power
STAT	Small Transport Aircraft Technology
T_c	Cooling Air Temperature
T^g	Gas Temperature
T^g_m	Metal Temperature
TOGW	Take-off Gross Weight
UHC	Unburned Hydrocarbon
Um	Meanline Blade Speed
W_c	Cooling Air Flowrate
W^c_a	Airflow Rate
WF	Fuel Burn
WPS	Weight of Propulsion System
Δ	Difference, Change
ΔH	Enthalpy Change

REFERENCES

1. Galloway, T. et al., "GASP-General Aviation Synthesis Program", NASA CR-152303, January 1978.

2. Renze, P.P. and Terry, J.E., "Application of Advanced Technologies to Derivatives of Current Small Transport Aircraft", NASA CR-166197, July 1981.

3. Kraus, E.F., et al, "Application of Advanced Technologies to Small, Short-Haul Transport Aircraft (STAT), NASA CR-152362, August 1982.

4. Sandford, J.W., "The Domain of the Turboprop Airplane", SAE Paper 801242, October 1980.

5. Cost Forecast Service (Transportation Indexes), Data Resources Inc.

6. "Aerospace Facts and Figures. 1984/85" Aerospace Industries Association of America, Inc., Washington, D.C.

7. Baerst, C.E., et al, "Study of Advanced Propulsion Systems for Small Transport Aircraft Technology (STAT), NASA CR-165610, March 1981.

8. Smith, C.E., et al, "Propulsion System Study for Small Transport Aircraft Technology" (STAT) NASA CR-165330, May 1981.

9. Nelson, J.R., Timson, F.S., "Relating Technology to Acquisition Costs: Aircraft Turbine Engines", RAND Report, R-1288-PR, March 1974.

10. Brennan, T. "Maurer Factor - The Navy's Answer to Production Engine Cost Estimation", Aircraft Engine Design and LCC Seminar, NADC, November 1975.

11. Schwaar, P., Dale, J., Banks, J., "Regenerative Engine Analysis Program", USAAVRADCOM-TR-80-D1-29, January 1981.

TABLE 1
COCKPIT AND PASSENGER CABIN DETAILS

170 lb. (77 kg) passenger weight; 200 lb (91 kg) passenger + baggage.

2-man crew, no cockpit observer jump seat.

No flight attendant (19 passengers).

Baggage Stowage Volumes and Arrangement		188 ft^3	(5.3 m^3)
Forward Nose Baggage	(Max 150 lbs/68 kg) 100 lbs (45 kg)	14 ft^3	(0.4 m^3)
Cabin Compartment Baggage	(Max 540 lbs/245 kg) 315 lbs (143 kg)	48 ft^3	(1.4 m^3)
Aft Compartment Baggage	(Max 630 lbs/286 kg) 115 lbs (52 kg)	56 ft^3	(1.6 m^3)
Nose Equipment Compartment	(Radios, etc.)	14 ft^3	(0.4 m^3)
Aisle or Cabin Height		57. in	(1.45 m)
Aisle Width (below 25 in (0.64 m) above floor)		18.3 in	(0.46 m)
(above 25 in (0.64 m) above floor)		19. in	(0.48 m)
Seat Pitch		30. in	(0.76 m)
Seat Width (no armrests)		16. in	(0.41 m)

10 in (0.25 m) garment stowage area @ 0.53 in (13. mm) width/passenger.

Underseat stowage for carry-on baggage of 13 in x 18.5 in x 6 in (0.33 m x 0.47 m x 0.15 m) per passenger

Easy Loading of preloaded baggage @ 5.47 ft^3 (0.155 m^3)/pass. interior, to 6.21 ft^3/(0.176 m^3) pass. interior + exterior.

No beverage service provision (optional)

No lavatory

Cabin pressurization - 4.8 psi. (33 kPa)

TABLE 2
SECT REFERENCE AIRCRAFT PERFORMANCE SUMMARY

		SIZING MISSION	ECONOMIC MISSION
Take-Off Gross Weight,	lb (kg)	12930. (5870.)	11600. (5266.)
Zero-Fuel Weight,	lb (kg)	11138. (5057.)	9808. (4453.)
Payload,	lb (kg)	3800. (1725.) (19 PAX)	2470. (1121.) (65% L.F.)
Fuel Weight,	lb (kg)	1792. (814.)	1792. (814.)
All Engine Dist. to 35 ft, (10.7 m)	ft (m)	2965. (904.)	2551. (778.)
Engine-Out Dist. to 35 ft, (10.7 m)	ft (m)	3501. (1067.)	2861. (872.)
Accelerate - Stop Distance,	ft (m)	4306. (1312.)	4038. (1231.)
Cruise Speed @ 10,000 ft, (3048. m)	KTAS	238.5	238.5
Cruise Average L/D		8.263	7.564
Landing Weight,	lb (kg)	11408. (5179.)	10078. (4575.)
Approach Speed,	KTAS	102.	96.
Landing Stall Speed,	KTAS	78.6	73.9
Block Fuel,	lb (kg)	1521. (691) (600 n. mi./1111. km)	1521. (691.) (615 n. mi./1138. km)
Block Time,	hr	2.727	2.788
Block Fuel,	lb (kg)	306. (139.) (100 n. mi./185. km)	295. (134.) (100 n. mi./185. km)
Block Time,	hr	0.630	0.629

TABLE 3
REFERENCE ENGINE MATERIALS LIST

COMPONENT	MATERIAL/COATING

REDUCTION GEARBOX COMPONENTS

Planet Gear	AISI 9310
Planet Gear Shaft	AISI 4340
Planet Carrier	AISI 4340
Ring Gear	Nitralloy 135 Mod
Ring Flange	Nitralloy 135 Mod
Sungear Shaft	AISI 4140
Propeller Shaft	AISI 4340
Gearbox Housing	356-T6
Inlet Housing	356-T6
I.G. Vanes	321 S.S.

COMPRESSOR COMPONENTS

Compressor Casing	6AL-4V TI (ANN)
Compressor Shrouds	6AL-4V TI (ANN)
1st. Compressor Rotor	10V-2FE-3AL TI (HT)
2nd. Compressor Rotor	Custom 450
Compressor Vanes (2)	
Variable Vane Linkage	321 S.S.
Impeller	6-2-4-6 TI (HT)
Outer Diffuser	6AL-4V TI (ANN)
Impeller Shroud	6AL-4V TI (ANN)

COMBUSTOR COMPONENTS

Combustor Liner	Hastelloy-X
Combustor Curl	Hastelloy-X
Combustor Casing	IN718
	IN713LC

GAS PRODUCER COMPONENTS

1st. Stage G.P. Nozzle	C101/701 Coated
1st. Stage G.P. Blade	C103/701 Coated
1st. Stage G.P. Disc	LC Astroloy
1st. Stage G.P. Cylinder	C101
2nd. Stage G.P. Nozzle	C101/701 Coated
2nd. Stage G.P. Blade	C103
2nd. Stage G.P. Disc	LC Astroloy
2nd. Stage G.P. Shroud	C101
Gas Producer Shaft	IN718

POWER TURBINE COMPONENTS

1st. Stage P.T. Nozzle	IN713
1st. Stage P.T. Blade	C101
1st. Stage P.T. Disc	IN718
Power Turbine Aft Frame	IN713LC
Power Turbine Shaft	
Aft Shaft	17-22 AS
Forward Shaft	AISI 9310

TABLE 4
REFERENCE ENGINE PERFORMANCE AND CYCLE DATA

PARAMETER	UNITS	UNINSTALLED	INSTALLED	
FLIGHT CONDITIONS				
Rating	-	T.O.	T.O.	Cruise
Altitude	ft (m)	0 (0)	0 (0)	10,000 (3048.)
Flight Speed	kts	0	0	238.
Amb. Temp.	F (C)	59 (15)	59 (15)	23 (-5.)
PERFORMANCE				
Power (Equiv.)	hp (kW)	957.5 (714.)	847.3 (631.8)	624.8 (465.9)
SFC	lb/hp-hr (kg/kW-hr)	0.466 (.283)	0.495 (.301)	0.469 (.285)
CYCLE CONDITIONS				
W_{AT}	lb/s (kg/s)	5.74 (2.61)	5.49 (2.49)	4.15 (1.88)
P_r	-	13.25	12.31	11.82
$T^r_{4.0}$	F (C)	2240. (1227.)	2240 (1227.)	2100. (1150.)
PRESSURE LOSSES				
Combustor	%	2.90	2.83	2.84
Interturbine Duct	%	2.0	2.0	2.0
Exhaust	%	1.0	0.88	0.96
TURBINE COOLING				
Before 1st. G.P. Stator	%	4.16	4.16	4.16
After 1st. G.P. Rotor	%	3.13	3.13	3.13
After 2nd. G.P. Stator	%	0.92	0.92	0.92
After 2nd. G.P. Rotor	%	0.92	0.92	0.92
OVERBOARD LEAKAGE				
Compressor Discharge	%	1.00	1.00	1.00
MECHANICAL EFFICIENCY				
Gas Generator Shaft	%	98.5	98.5	98.5
Power Shaft	%	98.0	98.0	98.0
CUSTOMER BLEED				
Compressor Discharge	lb/min (kg/min)	0.0 (0.0)	10.0 (4.54) (3.0%)	10.0 (4.54.) (4.0%)
POWER EXTRACTION	hp (kW)	0.0 (0.0)	0.0 (0.0)	0.0 (0.0)

TABLE 5
REFERENCE ENGINE COMPONENT DATA

PARAMETER	UNITS	UNINSTALLED	INSTALLED	
FLIGHT CONDITIONS				
Rating	-	T.O.	T.O.	Cruise
Altitude	ft (m)	SL	SL	10000. (3048)
Flight Speed	kts	0	0	238.
Amb. Temp.	F (C)	59. (15.)	59. (15.)	23. (-5.)
COMPONENT DATA				
COMPRESSOR				
$W \sqrt{\theta}/\delta$	lb/s (kg/s)	5.74 (2.61)	5.49 (2.49)	5.82 (2.64)
P_r	-	13.25	12.31	11.82
η_{Poly}	%	83.9	83.9	84.0
N	rpm	53400.	52360.	50640.
Power	hp (kW)	1420. (1059.)	1305. (973.)	921. (687.)
η_{AD}	%	77.5	77.5	77.7
$W\sqrt{\theta}/\delta$ exit	lb/s (kg/s)	0.667 (0.303)	0.682 (0.309)	0.690 (0.313)
GAS GENERATOR TURBINE (FIRST)				
$W \sqrt{\theta}/\delta$	lb/s (kg/s)	0.968 (.439)	0.969 (.440)	0.969 (.440)
P_r	-	2.03	2.02	2.03
η_{AD}	%	86.2	85.7	85.5
Power	hp (kW)	793. (591.)	728. (543.)	514. (383.)
$T_{4.0}$	F (C)	2240. 1227.)	2240. (1227.)	2100. (1150.)
GAS GENERATOR TURBINE (SECOND)				
$W \sqrt{\theta}/\delta$	lb/s (kg/s)	1.88 (0.853)	1.88 (0.853)	1.88 (0.853)
P_r	-	1.89	1.89	1.89
η_{AD}	%	87.1	86.6	86.5
Power	hp (kW)	649. (484.)	596. (444.)	421. (314.)
POWER TURBINE				
$W \sqrt{\theta}/\delta$	lb/s (kg/s)	3.45 (1.57)	3.45 (1.57)	3.45 (1.57)
P_r	-	3.13	2.92	3.07
η_{AD}	%	88.0	88.7	88.8
N	rpm	28500.	28500.	28500.
Power	hp (kW)	976.7 (728.3)	864.6 (644.7)	635.1 (473.6)
COMBUSTOR				
η_B	%	99.9	99.9	99.9
$\Delta P/P$	%	2.90	2.83	2.84

TABLE 6
DIRECT OPERATING COST GROUND RULES

CONSTANT 1985 DOLLARS

Annual Average Inflation Rate	= 7.8%
Crew Cost	= $ 64.60/Block Hour
Maintenance Labor Rate	= $ 13.50/Maint. Hour
Fuel Cost	= $ 1.00 and $ 2.00/Gal.
Engine Cost	= $186./hp ($249.4/kW)
Propeller Cost	= $ 63.10/lb ($140./kg)
Utilization	= 2800 hrs/year
Annual Insurance Rate	= 1.5% of Aircraft Price
Depreciation Period	= 12 Years
Depreciation Residual Value	= 15% of Aircraft Price
Maintenance Burden	= 80% of Labor Cost
Spares Factor	= 6% of Aircraft Price
Nonproductive Maneuvering Time	= 10 Minutes

TABLE 7
REFERENCE AIRCRAFT NOISE LEVELS
100% Payload
12390 lb (5870 kg) TOGW

Aircraft Noise Levels at FAR Part 36 Stations:

		GASP	LYCOMING
Take-Off	EPNL	89	83
Sideline	EPNL	89	
Approach	EPNL	79	
90.0 EPNL Contour Area	sq. mi. (km²)	1.1 (2.85)	

Propeller Noise for 2 Engines at Flyover:

		GASP	LYCOMING
Altitude	ft (m)	1000 (305)	
Speed	KTAS	258	
Noise Level	PNDB	92	86
	DB(A)	80	74

TABLE 8
REFERENCE AIRCRAFT TRADE FACTOR MATRIX

FUEL PRICE = $1.00/GALLON

$$
\begin{Bmatrix} \Delta\ WF \\ \Delta\ TOGW \\ \Delta\ SP \\ \Delta\ CA_{acq} \\ \Delta\ DOC \end{Bmatrix} = \begin{bmatrix} 1.3220 & 0.1175 & 0.0241 & 0.0 & 0.0 \\ 0.2110 & 0.1114 & 0.0124 & 0.0 & 0.0 \\ 0.1475 & 0.1131 & 0.0286 & 0.0 & 0.0 \\ 0.1685 & 0.1053 & 0.0289 & 0.1494 & 0.0 \\ 0.3565 & 0.0635 & 0.0166 & 0.0343 & 0.1685 \end{bmatrix} X \begin{Bmatrix} \Delta\ SFC \\ \Delta\ WPS \\ \Delta\ APS \\ \Delta\ CPS_{acq} \\ \Delta\ CPS_{m} \end{Bmatrix}
$$

FUEL PRICE = $2.00/GALLON

$$
\begin{Bmatrix} \Delta\ WF \\ \Delta\ TOGW \\ \Delta\ SP \\ \Delta\ CA_{acq} \\ \Delta\ DOC \end{Bmatrix} = \begin{bmatrix} 1.3220 & 0.1175 & 0.0241 & 0.0 & 0.0 \\ 0.2110 & 0.1114 & 0.0124 & 0.0 & 0.0 \\ 0.1475 & 0.1131 & 0.0286 & 0.0 & 0.0 \\ 0.1685 & 0.1053 & 0.0289 & 0.1494 & 0.0 \\ 0.5280 & 0.0696 & 0.0179 & 0.0281 & 0.1400 \end{bmatrix} X \begin{Bmatrix} \Delta\ SFC \\ \Delta\ WPS \\ \Delta\ APS \\ \Delta\ CPS_{acq} \\ \Delta\ CPS_{m} \end{Bmatrix}
$$

56

TABLE 9
ADVANCED MATERIAL WEIGHT AND COST REDUCTIONS

REFERENCE MATERIAL	ADVANCED MATERIAL	WEIGHT RATIO	COST RATIO
Aluminum	Graphite Composite	0.60	0.50
Alloy Steel	Metal Matrix	0.85	1.00
Nickel Base Alloy	Ceramics	0.33	0.50

TABLE 10
ADVANCED TECHNOLOGY ENGINE PERFORMANCE AND CYCLE DATA

PARAMETER	UNITS	UNINSTALLED	INSTALLED	
FLIGHT CONDITIONS				
Rating	-	T.O.	T.O.	Cruise
Altitude	ft (m)	0	0	10,000 (3048.)
Flight Speed	kts	0	0	238.
Amb. Temp.	F (C)	59 (15)	59 (15)	23 (-5)
PERFORMANCE				
Power (Equiv.)	hp (kW)	949. (708.)	833. (621.)	625. (466.)
SFC	lb/hp-hr (kg/kW-hr)	0.303 (0.184)	0.312 (0.190)	0.301 (0.183)
CYCLE CONDITIONS				
W_{AT}	lb/s (kg/s)	3.76 (1.71)	3.61 (1.64)	2.77 (1.26)
P_r^{AT}	-	8.93	8.2	8.0
$T_{4.0}^r$	F (C)	2640. (1450.)	2640 (1450.)	2500. (1370.)
PRESSURE LOSSES				
Combustor	%	4.0	4.0	4.0
Diffuser (PT Exit)	%	2.1	1.8	2.0
Recuperator				
Air Side	%	2.0	2.0	2.0
Gas Side	%	5.2	4.5	5.0
Exhaust	%	1.0	0.9	1.0
TURBINE DISC COOLING				
Before G.P. Rotor	%	1.0	1.0	1.0
After G.P. Rotor	%	1.0	1.0	1.0
OVERBOARD LEAKAGE				
Compressor Discharge	%	1.00	1.00	1.00
MECHANICAL EFFICIENCY				
Gas Generator Shaft	%	98.5	98.5	98.5
Power Shaft	%	98.0	98.0	98.0
CUSTOMER BLEED				
Compressor Discharge	lb/min (kg/s)	0.0	10.0 (4.5) (4.6%)	10.0 (4.5) (6.0%)
POWER EXTRACTION	hp (kW)	0.0 (0.0)	0.0 (0.0)	0.0 (0.0)

58

TABLE 11
ADVANCED TECHNOLOGY ENGINE COMPONENT DATA

PARAMETER	UNITS	UNINSTALLED	INSTALLED	
FLIGHT CONDITIONS				
Rating	-	T.O.	T.O.	Cruise
Altitude	ft (m)	SL	SL	10000. (3048.)
Flight Speed	kts	0	0	238.
Amb. Temp.	F (C)	59. (15.)	59. (15.)	23. (-5.)
COMPONENT DATA				
COMPRESSOR				
$W \sqrt{\theta}/\delta$	lb/s (kg/s)	3.76 (1.71)	3.63 (1.69)	3.60 (1.63)
P_r	-	8.93	8.2	8.0
η_{Poly}	%	89.6	89.6	89.4
N	rpm	68000.	66230.	64330.
Power	hp (kW)	668. (498.)	609. (454.)	440 (328.)
η_{AD}	%	86.1	86.1	86.0
$W\sqrt{\sigma}/\delta$ exit	lb/s (kg/s)	0.591 (0.269)	0.613 (0.278)	0.622 (0.282)
GAS GENERATOR TURBINE				
$W \sqrt{\theta}/\delta$	lb/s (kg/s)	1.093 (0.496)	1.093 (0.496)	1.093 (0.496)
P_r	-	2.07	2.07	2.07
η_{AD}	%	89.9	89.9	89.9
Power	hp (kW)	678. (506.)	618. (461.)	447. (333.)
$T_{4.0}$	F (C)	2640. (1450.)	2640. (1450.)	2500. (1370.)
POWER TURBINE				
$W \sqrt{\theta}/\delta$	lb/s (kg/s)	2.12 (0.962)	2.12 (0.962)	2.12 (0.962)
P_r	-	3.48	3.26	3.44
η_{AD}	%	91.7	92.0	91.9
N	rpm	42000.	42000.	42000.
Power	hp (kW)	968. (722.)	850. (634.)	633. (472.)
COMBUSTOR				
ηB	%	99.9	99.9	99.9
$\Delta P/P$	%	4.0	4.0	4.0
RECUPERATOR				
ε	%	80.0	80.0	80.0
$\Delta P/P$ Air Side	%	2.0	2.0	2.0
Gas Side	%	5.2	4.5	5.0

TABLE 12
COMBUSTOR DESIGN RESULTS

	UNITS	SINGLE CAN/SCROLL	FOUR CAN/SCROLL	ANNULAR
Volume	in^3	85/195	75/75	85/78
	(mm^3)	(1.39/3.20)	(1.23/1.23)	139/1.28)
Total	in^3	280	150	163
	(mm^3)	(4.59)	(2.46)	(2.67)
Surface	in^2	103/111	151/49	198/75
	(mm^2)	(6.65/7.16)	(9.74/3.16)	12.77/4.84)
Total	in^2	214	200	273
	(mm^2)	(13.81)	(12.90)	(17.61)
Efficiency Scaling Parameter, θ @ Idle	10^6 lb-ft-sec (10^6 N-m-sec^2)	1.0 (1.4)	1.0 (1.4)	1.5 (2.1)
Heat Release Rate,	10^6 BTU/hr-ft^3-atm (10^6 kJ/hr-m^3-Pa)	10.8 (3.96)	12.1 (4.44)	10.8 (3.96)
Number Fuel Injectors		1	4	24/10*
Number Ignitors		2	8**	2

* Horseshoe Vortex

** Alternate-Crossover Tubes

60

TABLE 13
ENGINE SIZE, WEIGHT AND COST COMPARISON

		REFERENCE ENGINE	ADVANCED TECHNOLOGY ENGINE
Length	in (m)	46.0 (1.17)	60.1 (1.53)
Diameter	in (m)	19.0 (0.483)	16.1 (0.409)
Weight	lb (kg)		
Gearbox		121. (54.9)	116. (52.7)
Engine		238. (108.)	178. (80.8)
Recuperator		- (-)	281. (128.)
TOTAL		359. (163.)	575. (261.)
Acquisition Cost	$K	178.	114.

TABLE 14
AIRCRAFT WEIGHT COMPARISON

	UNITS	REF A/C	SECT A/C
FUSELAGE	lb (kg)	1665. (756.)	1659. (753.)
WING	lb (kg)	703. (319.)	680. (309.)
HORIZONTAL TAIL	lb (kg)	106. (48.)	103. (47.)
VERTICAL TAIL	lb (kg)	90. (41.)	88. (40.)
ENGINES	lb (kg)	718. (326.)	1120. (508.) (+ 201. (91.) EA)
ENGINE INSTALLATION & SYSTEMS	lb (kg)	323. (147.)	319. (145.)
PROPELLERS	lb (kg)	166. (75.)	165. (75.)
NACELLES	lb (kg)	316. (143.)	290. (132.)
LANDING GEAR	lb (kg)	540. (245.)	525. (238.)
CONTROLS	lb (kg)	209. (95.)	203. (92.)
FIXED EQUIPMENT	lb (kg)	2162. (982.)	2162. (982.)
WEIGHT EMPTY	lb (kg)	6998. (3177.)	7314. (3321.) (+ 316. (144.))
FIXED USEFUL LOAD (CREW)	lb (kg)	340. (154.)	340. (154.)
OPERATING WEIGHT EMPTY	lb (kg)	7338. (3331.)	7654. (3475.)
PAYLOAD (19 PAX)	lb (kg)	3800. (1725.)	3800. (1725.)
FUEL (600 (1111 KM) N.MI. + RESERVES)	lb (kg)	1792. (814.)	1114. (506.) (- 678. (308.))
TAKE-OFF GROSS WEIGHT	lb (kg)	12930. (5870.)	12568. (5706.) (- 362. (164.))

TABLE 15
AIRCRAFT ACQUISITION COST COMPARISON

ACQUISITION COST	REFERENCE AIRCRAFT	ADVANCED TECHNOLOGY
AIRFRAME	$ 2,074,000.	2,026,000.
ENGINE (EACH)	$ 178,000.	110,000.
PROPELLER (EACH)	$ 5,242.	4,171.
TOTAL AIRCRAFT	$ 2,441,000.	2,255,000.

TABLE 16
DOC COMPARISON

65% PAYLOAD,
100 n.mi. (185. km) STAGE LENGTH

	REFERENCE AIRCRAFT	ADVANCED TECHNOLOGY
BLOCK FUEL (lb) (kg)	295. (134.)	182. (83.)
BLOCK TIME (hr)	0.629	0.629
CREW ($/TRIP)	40.62	40.61
FUEL AND OIL $1.00 /gal ($2.00/gal)	46.18 (92.35)	28.50 (57.00)
INSURANCE ($/TRIP)	8.22	7.59
AIRFRAME MAINTENANCE ($/TRIP)	31.74	31.48
ENGINE MAINTENANCE ($/TRIP)	29.45	25.27
MAINTENANCE BURDEN ($/TRIP)	19.00	17.88
DEPRECIATION ($/TRIP)	41.16	38.00
TOTAL D.O.C. ($/TRIP)	216.37 (262.55)	189.32 (217.82)

TABLE 17
BENEFITS OF RECUPERATOR

	PERCENT FUEL BURN REDUCTION	PERCENT DOC REDUCTION	
		($1/GAL)	($2/GAL)
REFERENCE ENGINE	-	-	-
ADVANCED NON-RECUPERATIVE ENGINE (ADV. AERO + CERAMICS)	22.4%	11.7%	13.6%
ADVANCED RECUPERATIVE ENGINE (ADV. AERO + CERAMICS)	38.3%	12.5%	17.0%
BENEFITS OF RECUPERATOR	15.9%	0.8%	3.4%

TABLE 18
ADVANCED TECHNOLOGIES RANKED FOR FUEL BURN REDUCTION

CERAMIC RECUPERATOR	15.9%
ADVANCED AERO	10.8%
400°F (222°C) HIGHER $T_{4.0}$	6.5%
CERAMIC COMBUSTOR AND TURBINES	5.1%
TOTAL	38.3%

TABLE 19
ADVANCED TECHNOLOGIES RANKED FOR DOC REDUCTION

	1 $/GAL	2 $/GAL
CERAMIC COMBUSTOR + TURBINES	4.8%	5.7%
ADVANCED AERO	3.6%	4.3%
400°F (222°C) HIGHER $T_{4.0}$	3.3%	3.6%
CERAMIC RECUPERATOR	0.8%	3.4%
TOTAL	12.5%	17.0%

TABLE 20
SUMMARY OF POTENTIAL BENEFITS

	Percent Reduction	Savings Per Aircraft
Fuel Burn	38.3%	75,000 gallons per year
DOC		
$1.00 per gallon	12.5%	$120,000 per year
$2.00 per gallon	17.0%	$199,000 per year

SECT REFERENCE AIRCRAFT

- 19 Passenger Pressurized

- Engines: Twin 960 hp(716kW) Turboprops

- Weight: 12,930 lb (5870 kg) TOGW
  11,138 lb (5057 kg) Zero-Fuel

- Wing Loading: 50.7 psf (2428 N/m²)
  9.8 Aspect Ratio

- Cruise L/D: 8.3

- Cost: $2.44M
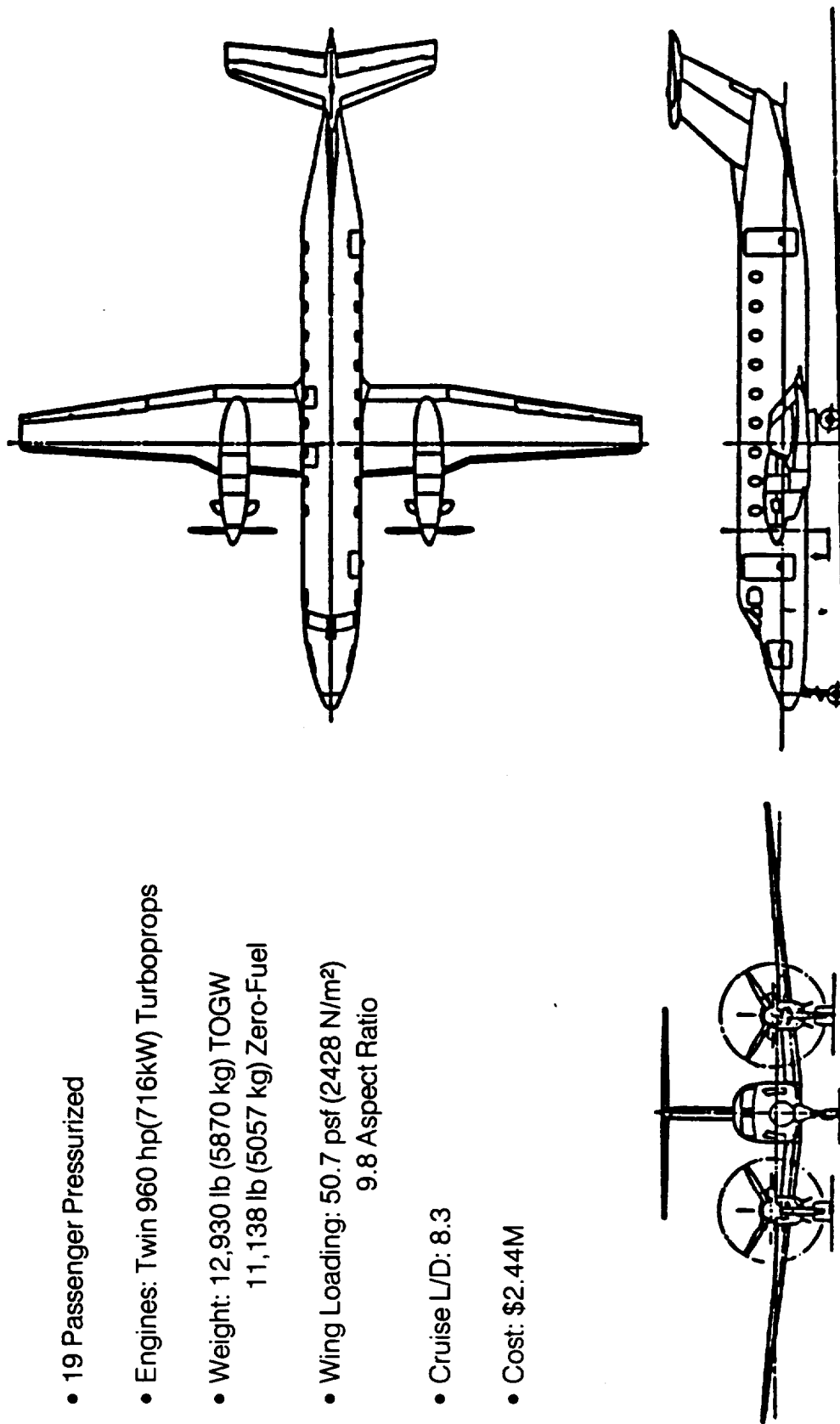
BT1141-2

Figure 1. SECT Reference Aircraft

69

SEATING ARRANGEMENT

19 PASSENGER

Aisle Width	19 in. (0.48 m)
Seat Pitch	30 in. (0.76 m)
Seat Width	16 in.(0.41 m)
Under Seat Storage	13 in. x 18.5 in. x 6 in. (0.33m x 0.47m x 0.15m)
Preloaded Baggage	6.2 cu. ft. per passenger (0.176 m³)

57 in. (1.45m)

54 in. (1.37m)

473.5 in (12.03m)

BT1213A
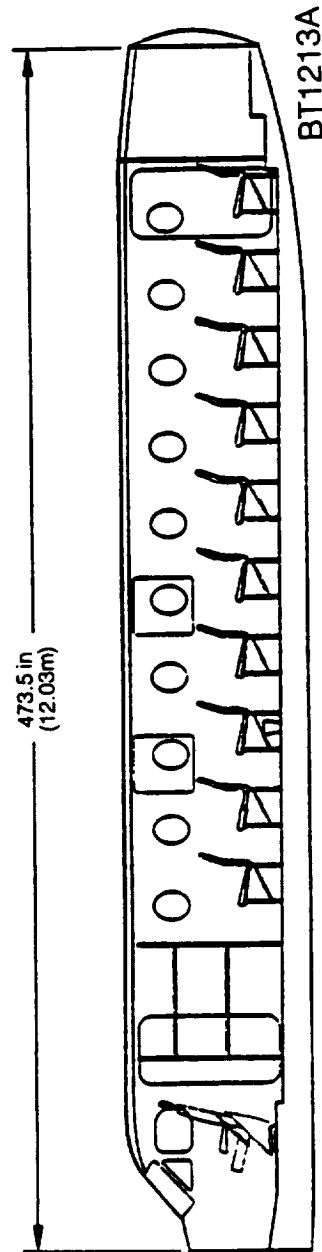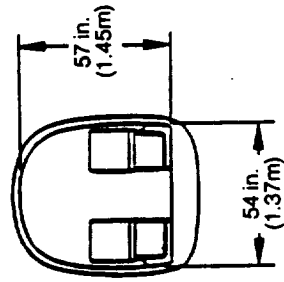
Figure 2. Fuselage Interior

70

SIZING MISSION PROFILE
FULL PAYLOAD

RESERVE FUEL

45 MIN AT MAX ENDURANCE SPEED
ALT = 10,000 FT (3048m)

CRUISE AT M = 0.373
ALT = 10,000 FT (3048m)

DESCENT

CLIMB AT
MAXIMUM RATE
OF CLIMB

RAMP

RAMP

TAXI
AND
TAKEOFF

APPROACH
AND
LAND

600 N. MI
(1111 km)

BLOCK TIME AND FUEL
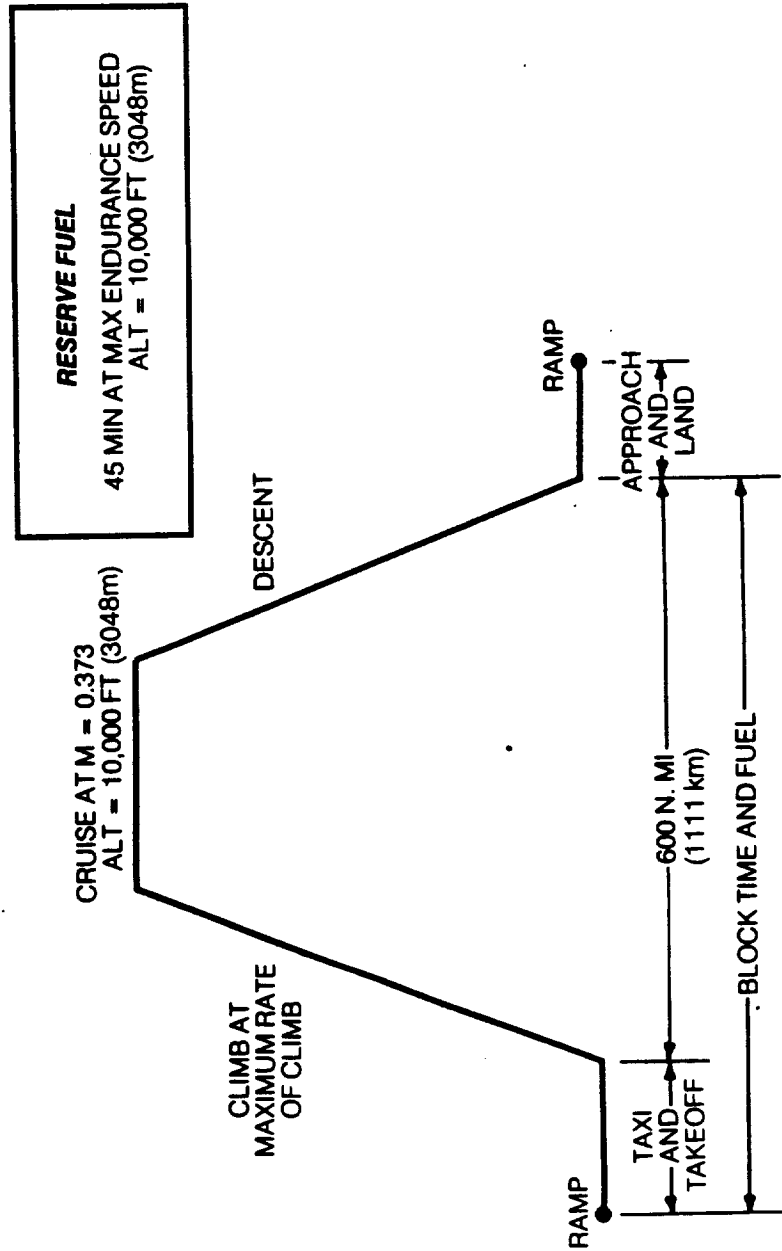
BT1215

Figure 3.   Sizing Mission Profile

71

GROSS WEIGHT = 12930. PASSENGERS = 19. PLUS CREW

Category	Parameter	Symbol	Value	Units
FUSELAGE	LENGTH	(ELF)	51.82	FT
	WIDTH	(SWF)	5.55	FT
	WETTED AREA	(SF)	773.	SQFT
	DELTA P	(DELP)	6.80	PSI
WING	ASPECT RATIO	(AR)	9.00	
	AREA	(SW)	255.1	SQFT
	SPAN	(B)	50.0	FT
	GEOM. MEAN CHORD	(CBARW)	5.39	FT
	QUARTER CHORD SWEEP	(DLWC4)	0.0	DEG
	TAPER RATIO	(SLW)	0.416	
	ROOT THICKNESS	(TCRT)	0.160	
	TIP THICKNESS	(TCT)	0.113	
	WING LOADING	(WS)	50.7	PSF
	WING FUEL VOLUME	(VFW)	525.2	GAL
	STR.SPAN/ROOT TCK	(BSTROT)	36.58	
HOR. TAIL	ASPECT RATIO	(ARHT)	5.00	
	AREA	(SHT)	57.2	SQFT
	SPAN	(BHT)	16.92	FT
	MEAN CHORD	(CBARHT)	3.51	FT
	THICKNESS/CHORD	(TCHT)	0.100	
	MOMENT ARM	(ELTH)	26.4	FT
	VOLUME COEFF.	(VBARH)	1.181	
VERT. TAIL	ASPECT RATIO	(ARVT)	1.18	
	AREA	(SVT)	41.0	SQFT
	SPAN	(BVT)	6.97	FT
	MEAN CHORD	(CBARVT)	5.99	FT
	THICKNESS/CHORD	(TCVT)	0.120	
	MOMENT ARM	(ELTV)	24.3	FT
	VOLUME COEFF.	(VBARV)	0.078	
ENG.NACELLES	LENGTH	(ELN)	11.18	FT
	MEAN DIAMETER	(DBARN)	2.83	FT
	NUMBER ENGINES	(ENP)	2.0	
	WETTED AREA		90.64	SQFT EACH
	LOCATION		7.9 FT. FROM A/C CENTERLINE	
ENGINE	POWER/ENGINE	(HPMSLS)	848.	SHP
	STATIC THRUST/WT.	(TOW)	0.412	
	MEAN DIAMETER	(FT)	1.147	FT
	MEAN LENGTH	(FT)	2.881	FT
PROPELLER	DIAMETER	(DPROP)	9.17	FT
	RPM	(RPM)	1700.	
	MAX. TIPSPEED	(TIPSPD)	816.	FPS
	NO. BLADES	(BL)	3.	
	ACT.FACT./BLADE	(AF)	110.0	
	INT.LIFT COEFF.	(CLI)	0.500	

Figure 4.   Reference Aircraft Dimensions

72

PROPULSION GROUP		
PRIMARY ENGINES	(HEP)	718.
PRIMARY ENGINE INSTL.	(HPEII)	126.
FUEL SYSTEM	(HFSS)	197.
PROPULSOR HEIGHT	(HPROP)	166.
GEAR BOX HEIGHT	(HTGB)	-
TOTAL PROP.GROUP HT.	(HP)	1207.

STRUCTURES GROUP			
WING	(HH)	703.	
HOR. TAIL	(HHT)	186.	
VERT. TAIL	(HVT)	90.	
FUSELAGE	(HB)	1665.	(INCL. 0.0 LBS A.T.M.)
LANDING GEAR	(HLG)	540.	
PRIMARY ENG. SECTION	(HPES)	316.	
GROUP HEIGHT INC.	(DELHST)	0.	
TOTAL STRUC.GROUP HT.	(HST)	3420.	

FLIGHT CONTROLS GROUP		
COCKPIT CONTROLS	(HCC)	32.
FIXED WING CONTROLS	(HCFH)	177.
SAS	(HSAS)	0.
GROUP HEIGHT INC.	(DELHFC)	0.
TOTAL CONTROL HT.	(HFC)	209.

HT. OF FIXED EQUIPMENT	(HFE)	2162.

HEIGHT EMPTY	(HE)	6998.

FIXED USEFUL LOAD	(HFUL)	340. (INC. CREW)

OPERATING HEIGHT EMPTY	(OHE)	7338.

PAYLOAD	(HPL)	3800. (PAX.VOL.= 19. DESIGN PAX= 19.)

FUEL	(HFA)	1792. (HFR= 1792.)(HFTP= 0.)

GROSS HEIGHT	(HG)	12930.

Figure 5.   Reference Aircraft Group Weights

73

AERODYNAMIC DATA

DESIGN MACH = 0.373   DESIGN ALTITUDE = 10000.   DESIGN Q (PSF) =142.19

DESIGN RE.NUM. PER FT. = 2.001E+06   FLATPLATE CF AT RE=10E7 IS 0.00267

DRAG BREAKDOWN	FLATPLATE AREA(SQFT)	CDO	WETTED AREA(SQFT)
WING	1.5915	0.00624	432.01
FUSELAGE	2.1006	0.00823	772.56
VERT.TAIL	0.2426	0.00095	82.10
HOR.TAIL	0.3578	0.00140	114.50
ENGINE NAC.	0.6495	0.00255	197.29
TIP TANKS	0.0000	0.00000	0.00
INCREMENTAL	4.0438	0.01585	0.00
TOTAL	8.9858	0.03522	1599.25

MEAN SKIN FRICTION COEF.= 0.005619

AERODYNAMIC COEFF.

A1	0.7074
A2	-0.1159
A3	0.0655
A4=.75X(T/C)	0.1158
A5=CDO--	0.0264
A6	2.1733
K=ST/(PI.SER.ART)	0.0462
3-D LIFT SLOPE AT CRUISE MACH (CLALPH)	6.0924 PER RADIAN
OSWALD FACTOR (SEE)	0.7634
SINB	0.9754
UFAC	1.0155
HGAP/B	0.1019
LHT/LWING	0.0427
DEL/ELTH	0.0570

CRUISE CD = 0.0352 + 0.0462 CL2 (ASSUMES MINIMUM WING PROFILE DRAG)

RETRACTABLE LANDING GEAR CD INC.=0.02185

LOW SPEED LIFT/DRAG-GR.UP(IF R10.G.E.

	FLAPS UP			TAKEOFF			LANDING		
ALPHA	CL	CD	L/D	CL	CD	L/D	CL	CD	L/D
-2.00000	0.01182	0.03906	0.33718	0.40794	0.05588	8.29197	0.81701	0.09978	8.19092
0.00000	0.20407	0.03710	5.50050	0.67979	0.06640	10.23751	1.00966	0.10949	9.22103
2.00000	0.39632	0.04255	9.31429	0.87204	0.07750	11.25193	1.20191	0.12309	9.76405
4.00000	0.58857	0.05141	11.44799	1.06428	0.09213	11.55251	1.39415	0.14054	9.92007
6.00000	0.78083	0.06372	12.25437	1.25653	0.11028	11.39450	1.58640	0.16182	9.80574
8.00000	0.97306	0.07948	12.24320	1.44878	0.13195	10.97906	1.77865	0.18693	9.51510
10.00000	1.16531	0.09869	11.80760	1.64103	0.15714	10.44292	1.97090	0.21566	9.13057
11.68369	1.35756	0.12136	11.18596	1.01569	0.18305	9.91088	2.13274	0.24315	8.77128
11.68369	1.36220	0.12195	11.16989	1.01569	0.18305	9.91088	2.13274	0.24315	8.77128
11.68369	1.36220	0.12195	11.16989	1.01569	0.18305	9.91088	2.13274	0.24315	8.77128

DFLAP=	0.00	DFLAP=	15.00	DFLAP=	35.00
CLMAX= 1.36220		CLMAX= 1.81569		CLMAX= 2.13274	

Figure 6. Reference Aircraft Aerodynamic Data

Figure 7. Reference Aircraft Performance : Take-Off Phase

ACCELERATE TO MAX RATE OF CLIMB SPEED. MACH NO. = 0.210

TIME (HRS)	RANGE (NM)	FUEL USED (LBS)	WEIGHT (LBS)	ALT. (FT)	TAS (KTS)	EAS (KTS)	MACH NO.	MACH DIV	THRUST (LBS)	FUEL FLOW (LB/HR)
0.166	0.00	44.1	12886.	500.	130.	129.	0.197	0.603	3344.	841. 2700.0 862.0
0.167	0.11	44.8	12885.	500.	130.	130.	0.210	0.615	3223.	842. 2700.0 865.2

END OF ACCELERATION SEGMENT
TIME= 0.167 HRS FUEL USED= 44.8 LBS WEIGHT= 12885. LBS RANGE= 0.1 NM 2700.0 863.2

CLIMB TO 10000. FT. AT MAXIMUM RATE OF CLIMB

TIME (HRS)	RANGE (NM)	FUEL USED (LBS)	WEIGHT (LBS)	ALT. (FT)	TAS (KTS)	EAS (KTS)	MACH NO.	MACH DIV	CL	CD	ALPHA (DEG)	GAMMA (DEG)	FUS. ANGLE (DEG)	R/C (FPM)	THRUST (LBS)	FUEL FLOW (LB/HR)
0.167	0.	35.	12885.	500.	138.	138.	0.210	0.617	0.7817	0.0650	6.00	7.00	12.00	1716.	2684.	720. 713.3
0.171	1.	40.	12882.	1000.	140.	138.	0.211	0.617	0.7817	0.0650	5.99	7.01	12.00	1724.	2726.	730. 730.5
0.181	2.	55.	12874.	2000.	142.	138.	0.215	0.617	0.7813	0.0650	5.99	7.01	12.00	1752.	2674.	720. 725.3
0.191	3.	62.	12860.	3000.	144.	138.	0.219	0.617	0.7809	0.0649	5.98	7.02	12.00	1781.	2676.	724. 736.3
0.200	5.	69.	12861.	4000.	146.	138.	0.223	0.617	0.7804	0.0649	5.97	7.03	12.00	1810.	2678.	729. 747.9
0.209	6.	76.	12854.	5000.	148.	138.	0.228	0.617	0.7800	0.0649	5.95	7.05	12.00	1840.	2680.	735. 760.5
0.218	7.	82.	12847.	6000.	150.	137.	0.232	0.617	0.7817	0.0650	5.97	7.03	12.00	1863.	2667.	733. 762.6
0.227	9.	89.	12841.	7000.	151.	136.	0.233	0.615	0.8004	0.0664	6.16	6.84	12.00	1819.	2593.	714. 743.9
0.236	10.	95.	12834.	8000.	151.	134.	0.234	0.612	0.8235	0.0682	6.40	6.60	12.00	1758.	2524.	695. 725.4
0.246	12.	102.	12828.	9000.	151.	132.	0.235	0.609	0.8515	0.0704	6.68	6.32	12.00	1679.	2460.	677. 707.2
0.256	13.	109.	12821.	10000.	150.	129.	0.236	0.605	0.8800	0.0727	6.98	6.02	12.00	1600.	2396.	659. 689.2

END OF CLIMB TO 10000. FT
TIME= 0.256 HRS FUEL USED= 109. LBS WEIGHT= 12821. LBS RANGE= 13. NM 2700.0 689.2 1700.0 0.799

Figure 8. Reference Aircraft Performance : Accelerate and Climb Phase

76

ACCELERATE TO SPECIFIED SPEED.   MACH NO. = 0.375

TIME (HRS)	RANGE (NM)	FUEL USED (LBS)	WEIGHT (LBS)	ALT. (FT)	TAS (KTS)	EAS (KTS)	MACH NO.	MACH DIV	THRUST (LBS)	FUEL FLOW (LB/HR)
0.256	13.88	108.7	12821.	10000.	150.	129.	0.236	0.604	2396.	659. 2700.0 689.2
0.278	17.81	124.1	12806.	10000.	238.	205.	0.373	0.666	1763.	679. 2700.0 727.9

END OF ACCELERATION SEGMENT
TIME= 0.278 HRS   FUEL USED=   124.1 LBS   WEIGHT= 12806. LBS   RANGE= 18. NM   2700.0 727.9

ACCELERATE TO NORMAL POWER SPEED.   MACH NO. = 0.374

TIME (HRS)	RANGE (NM)	FUEL USED (LBS)	WEIGHT (LBS)	ALT. (FT)	TAS (KTS)	EAS (KTS)	MACH NO.	MACH DIV	THRUST (LBS)	FUEL FLOW (LB/HR)
0.256	13.88	108.7	12821.	10000.	150.	129.	0.236	0.604	2396.	659. 2700.0 689.2
0.278	17.82	124.1	12806.	10000.	239.	205.	0.374	0.666	1762.	679. 2700.0 727.9

END OF ACCELERATION SEGMENT
TIME= 0.278 HRS   FUEL USED=   124.1 LBS   WEIGHT= 12806. LBS   RANGE= 18. NM   2700.0 727.9

ACCELERATE TO BEST SPEC. RANGE SPEED.   MACH NO. = 0.289

TIME (HRS)	RANGE (NM)	FUEL USED (LBS)	WEIGHT (LBS)	ALT. (FT)	TAS (KTS)	EAS (KTS)	MACH NO.	MACH DIV	THRUST (LBS)	FUEL FLOW (LB/HR)
0.256	13.88	108.7	12821.	10000.	150.	129.	0.236	0.604	2396.	659. 2700.0 689.2
0.261	14.01	112.4	12817.	10000.	165.	159.	0.289	0.638	2121.	666. 2700.0 701.9

END OF ACCELERATION SEGMENT
TIME= 0.261 HRS   FUEL USED=   112.4 LBS   WEIGHT= 12817. LBS   RANGE= 14. NM   2700.0 701.9

ACCELERATE TO MAX. ENDURANCE SPEED.   MACH NO. = 0.266

TIME (HRS)	RANGE (NM)	FUEL USED (LBS)	WEIGHT (LBS)	ALT. (FT)	TAS (KTS)	EAS (KTS)	MACH NO.	MACH DIV	THRUST (LBS)	FUEL FLOW (LB/HR)
0.256	13.88	108.7	12821.	10000.	150.	129.	0.236	0.604	2396.	659. 2700.0 689.2
0.259	13.94	110.7	12819.	10000.	170.	146.	0.266	0.626	2234.	663. 2700.0 696.0

END OF ACCELERATION SEGMENT
TIME= 0.259 HRS   FUEL USED=   110.7 LBS   WEIGHT= 12819. LBS   RANGE= 14. NM   2700.0 696.0

Figure 9.   Reference Aircraft Performance : Accelerate to Cruise Phase

CRUISE PERFORMANCE SUMMARY
FOR

OWE = 7338., PAYLOAD = 3000., FUEL AVAIL = 1792., MTMISN = 12930.

		AT SPECIFIED SPEED		AT NORMAL POWER		AT BEST SPEC. RANGE		AT MAX. ENDURANCE	
		START CRUISE	END CRUISE	START CRUISE	END CRUISE	START CRUISE	END CRUISE	START CRUISE	END CRUISE
TIME	HRS.	0.278	2.664	0.278	2.687	0.261	3.756	0.259	4.026
RANGE	N.MI	18.	587.	18.	593.	14.	660.	14.	654.
FUEL USED	LBS.	124.	1507.	124.	1521.	112.	1521.	111.	1521.
HEIGHT	LBS.	12806.	11423.	12806.	11406.	12817.	11408.	12819.	11408.
ALTITUDE	FT.	10000.	10000.	10000.	10000.	10000.	10000.	10000.	10000.
TAS	KTS.	238.5	238.5	238.0	238.0	164.8	164.8	169.9	169.9
EAS	KTS.	205.0	205.0	205.2	205.2	158.8	158.8	146.0	146.0
MACH NO.		0.3733	0.3733	0.3737	0.3737	0.2592	0.2592	0.2660	0.2660
DIV. MACH		0.6664	0.6708	0.6665	0.6710	0.6391	0.6466	0.6266	0.6355
ANGLE ATTACK	DEG.	1.411	1.030	1.404	1.019	3.909	3.246	5.043	4.255
FUSE. ANGLE	DEG.	0.411	0.030	0.404	0.019	2.909	2.246	4.043	3.255
CL		0.3535	0.3153	0.3528	0.3143	0.5897	0.5249	0.6971	0.6204
L/D		8.612	7.914	8.600	7.895	11.273	10.731	11.794	11.416
FUEL FLOW	LB/HR	586.4	574.3	586.5	575.3	411.7	395.3	383.8	365.0
BREG. FACTOR	N.MI.	5212.	4747.	5216.	4738.	5755.	5336.	5679.	5303.
SPEC. RANGE	NM/LB	0.40673	0.41528	0.40789	0.41502	0.44870	0.46740	0.44276	0.46452
SHP/ENG		621.8	604.1	623.1	605.3	304.5	362.8	344.9	320.5
T.I.T. (R)		2560.0	2540.6	2560.0	2542.1	2279.9	2249.9	2231.7	2197.7
PROP. EFF.		0.6936	0.6934	0.6937	0.6935	0.6666	0.6623	0.6525	0.6459
PROP. RPM		1700.0	1700.0	1700.0	1700.0	1700.0	1700.0	1700.0	1700.0
TIPSPEED	FPS	816.0	816.0	816.0	816.0	816.0	816.0	816.0	816.0

Figure 10. Reference Aircraft Performance : Cruise Summary

78

DESCENT FROM CRUISE AT SPECIFIED SPEED CONDITION
(U=NO CONSTRAINT; R= 500. FPM CABIN; A= -6.00 FUS. ANGLE; S=PHO OR VMO)

TIME (HRS)	RANGE (NM)	FUEL USED (LBS)	WEIGHT (LBS)	ALT. (FT)	TAS (KTS)	EAS (KTS)	MACH NO.	MACH DIV	CL	CD	ALPHA (DEG)	GAMMA (DEG)	FUS. ANGLE (DEG)	R/S (FPM)	THRUST (LBS)	FUEL FLOW (LB/HR)	
2.664	587.	1507.	11423.	10000.	224.	193.	0.350	0.666	0.3540	0.0421	1.44	-6.44	-6.00	2547.	78.	187.	74.1 A
2.670	588.	1508.	11422.	9000.	222.	194.	0.346	0.667	0.3487	0.0419	1.39	-6.39	-6.00	2506.	93.	192.	76.3 A
2.677	590.	1510.	11420.	8000.	219.	195.	0.341	0.667	0.3464	0.0418	1.37	-6.37	-6.00	2465.	103.	200.	79.4 A
2.684	591.	1511.	11419.	7000.	217.	195.	0.336	0.668	0.3438	0.0417	1.35	-6.35	-6.00	2432.	115.	208.	82.5 A
2.691	593.	1512.	11417.	6000.	214.	196.	0.331	0.668	0.3411	0.0417	1.33	-6.33	-6.00	2396.	127.	216.	85.8 A
2.698	594.	1514.	11416.	5000.	212.	197.	0.326	0.668	0.3383	0.0416	1.31	-6.31	-6.00	2361.	140.	225.	89.2 A
2.705	596.	1516.	11414.	4000.	210.	198.	0.321	0.669	0.3354	0.0415	1.28	-6.28	-6.00	2326.	154.	233.	92.6 A
2.712	597.	1517.	11412.	3000.	207.	199.	0.317	0.669	0.3325	0.0414	1.26	-6.26	-6.00	2292.	169.	243.	96.3 A
2.720	599.	1519.	11410.	2000.	205.	199.	0.312	0.669	0.3294	0.0413	1.23	-6.23	-6.00	2259.	184.	252.	100.0 A
2.727	600.	1521.	11408.	1000.	203.	200.	0.306	0.670	0.3262	0.0412	1.20	-6.20	-6.00	2226.	200.	262.	103.8 A

END OF DSCNT TO 1000. FT
TIME= 2.727 HRS   FUEL USED= 1521. LBS   WEIGHT= 11408. LBS   RANGE= 600. NM   2560.0   103.8   1105.0   0.558

RESERVE FUEL = 271.0 LBS.   HOLDING: TIME= 45. MIN. ALTITUDE= 10000. MACH= 0.256 FUEL= 271.0
                            ALTERNATE : DISTANCE= 0. N.MI. ALTITUDE= 10000. MACH= 0.000 FUEL= 0.0

RANGE = 600.2   BLOCK TIME= 2.727   USED FOR DESIGN RANGE AND COST

Figure 11.   Reference Aircraft Performance : Descent Phase

BT1212

46 in.
(1.17 m)

19.0 in. (0.48 m)

19.6 in.
(0.50 m)
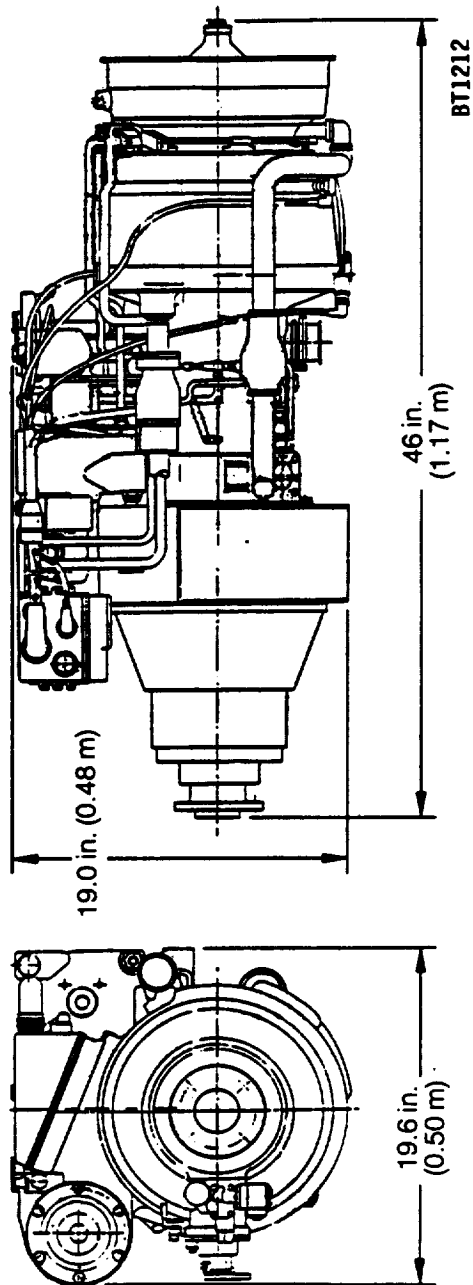
Figure 12.   SECT Reference Engine

--- COST DATA ---
GASP SHORTHAUL METHOD

OPERATING COST FOR SPECIFIED SPEED AND 10000. ALTITUDE

ENGINES   NUMBER = 2. TYPE = 6   WEIGHT OF 1 ENGINE= 359.   WEIGHT OF 1 PROP = 83. LBS   TOTAL MAN. TIME= 9.9 MIN.

EMPTY WEIGHT= 6998.   AIRFRAME WEIGHT= 6114.

HORSEPOWER/ENGINE= 848. CRUISE SPEED= 240. KTS

TOTAL AIRCRAFT COST= 2440759.   AIRFRAME COST= 2074300.   COST OF 1 ENGINE= 177988.   COST OF 1 PROP.= 5242.

RANGE= 100. N.M.   BLOCK FUEL= 295. LBS   BLOCK TIME= 0.6288 HRS.

	\$1.00/GAL.				\$2.00/GAL.	
	\$	LABOR	MATERIAL	%	\$	%
UTILIZATION	2800.					
FLYING OPERATIONS						
FLIGHT CREW	40.623			18.8	40.623	15.5
FUEL,OIL,AND TAXES(1.000\$/G)	46.177			21.3	92.354	35.2
INSURANCE	8.222			3.8	8.222	3.1
DIRECT MAINTENANCE						
AIRFRAME	31.743	14.679	17.064	14.7	31.743	12.1
ENGINE	29.445	9.075	20.370	13.6	29.445	11.2
MAINTENANCE BURD.	19.004			8.8	19.004	7.2
DEPRECIATION	41.158			19.0	41.158	15.7
TOTAL DOC (\$/TRIP)	216.372			100.0	262.549	100.0
(\$/B.HR.)	344.078				417.540	
(\$/N.MI.)	2.164				2.625	
(C/ASSM)	9.903	(19. SEATS)			12.014	

Figure 13   GASP Shorthaul Output: 65% Payload Mission

GASP SHORTHAUL METHOD
ECONOMIC MISSION
65% PAYLOAD
100 N.MI. (185 km) STAGE LENGTH

FUEL PRICE = 1.00 $/G   FUEL PRICE = 2.00 $/G

First pie chart (216.37 $/TRIP):
- FUEL, OIL, & TAXES 21.3%
- FLIGHT CREW 18.8%
- AIRFRAME MAINTENANCE 14.7%
- ENGINE MAINTENANCE 13.6%
- MAINTENANCE BURDEN 8.8%
- DEPRECIATION 19.0%
- INSURANCE 3.8%

216.37 $/TRIP

Second pie chart (262.55 $/TRIP):
- FUEL, OIL, & TAXES 35.2%
- FLIGHT CREW 15.5%
- AIRFRAME MAINTENANCE 12.1%
- ENGINE MAINTENANCE 11.2%
- MAINTENANCE BURDEN 7.2%
- DEPRECIATION 15.7%
- INSURANCE 3.1%

262.55 $/TRIP
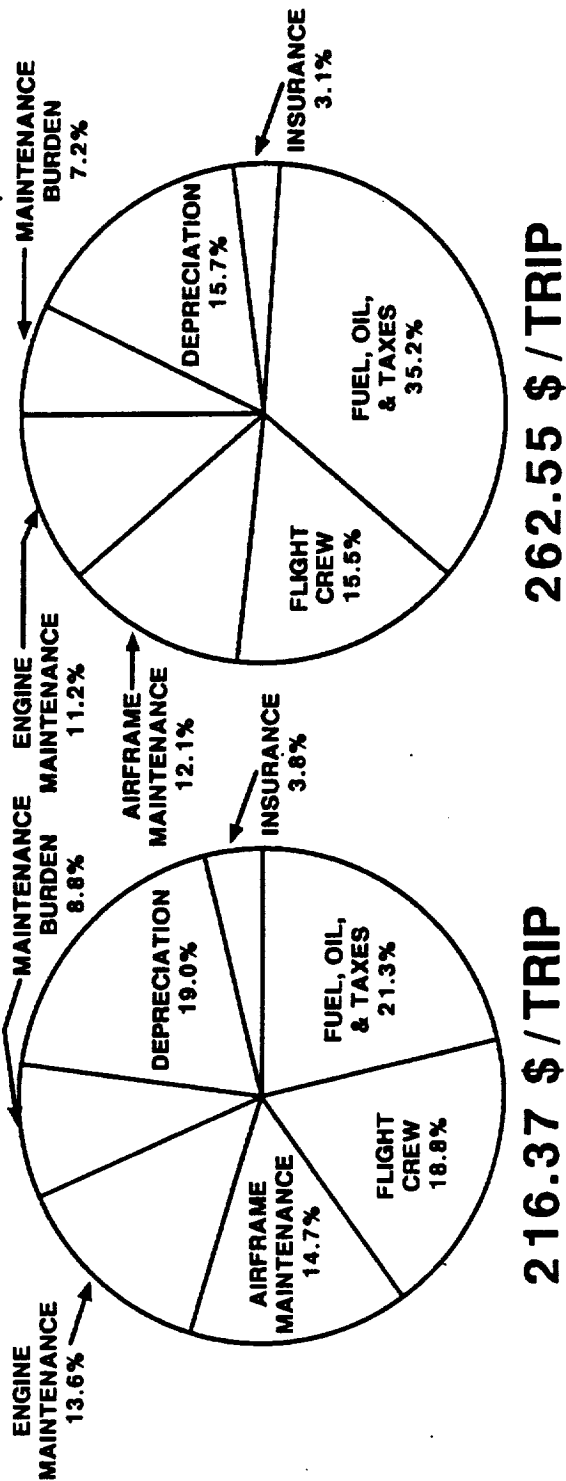
Figure 14.   Reference Aircraft DOC Breakdown

82

Figure 15.   Take-Off Noise Limits

83

FAR Part 36
Aircraft Sideline Noise Limits
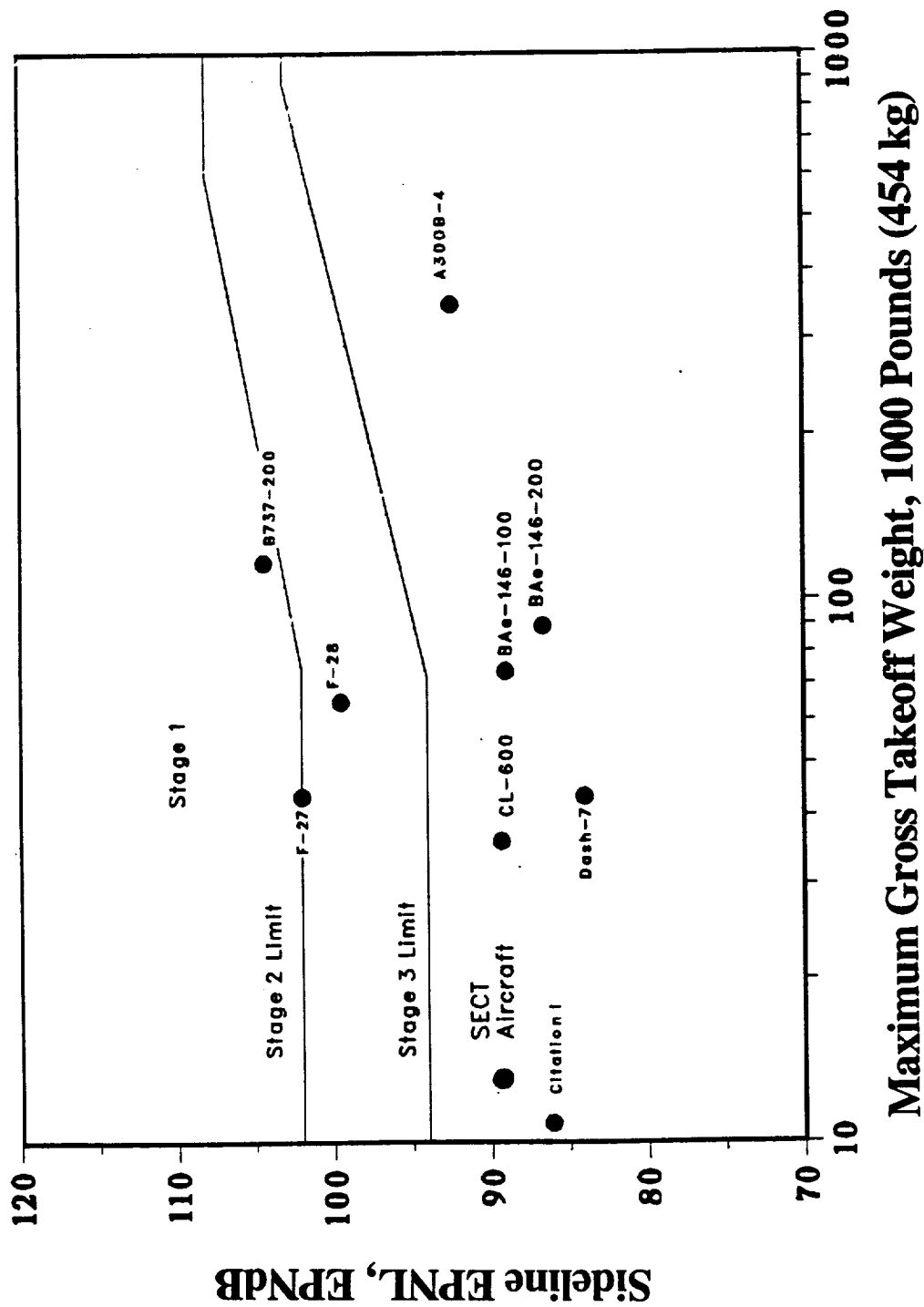
Figure 16.   Sideline Noise Limits

FAR Part 36
Aircraft Approach Noise Limits
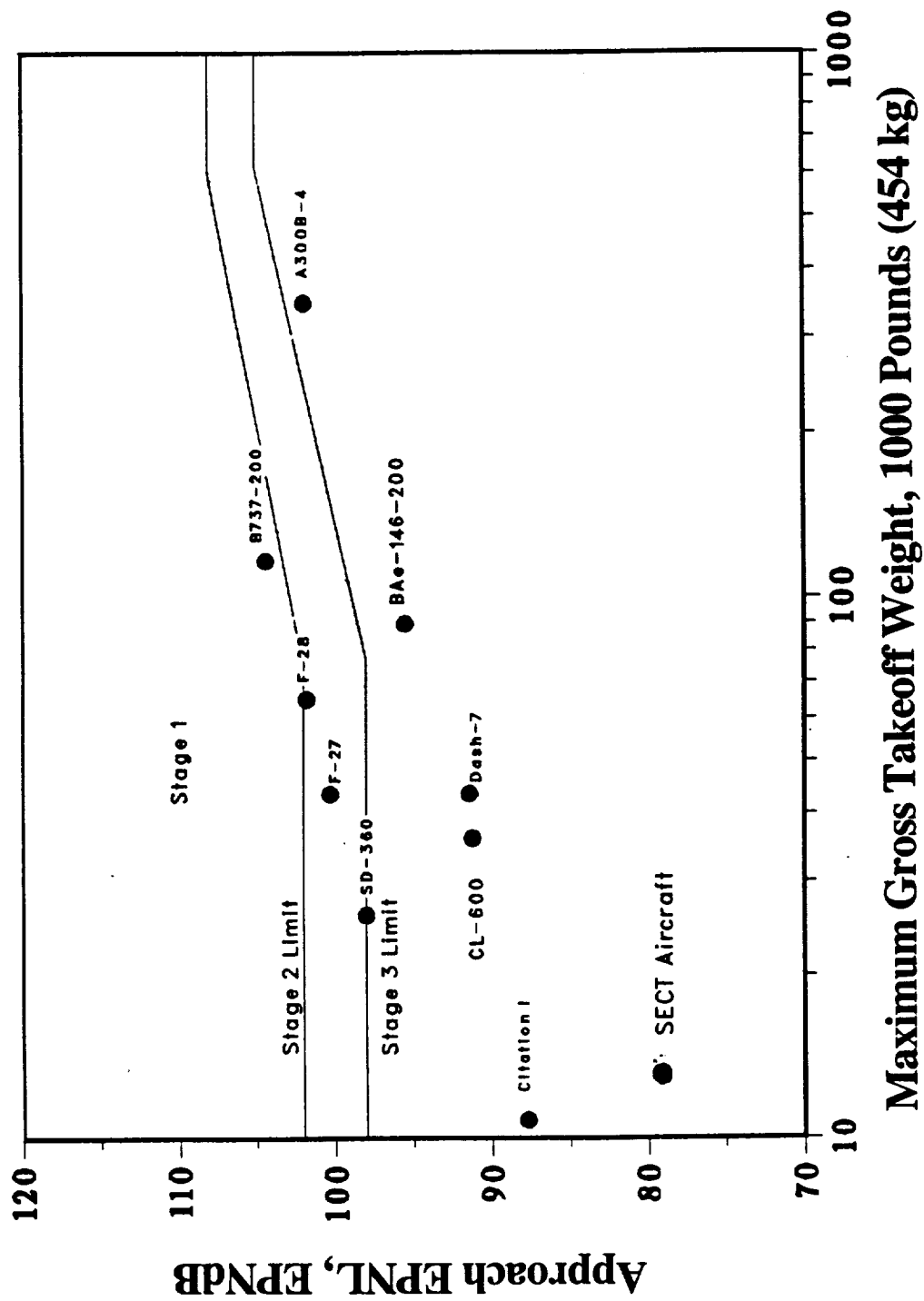
Figure 17. Approach Noise Limits

Estimated A - Weighted Sound Levels For Takeoff
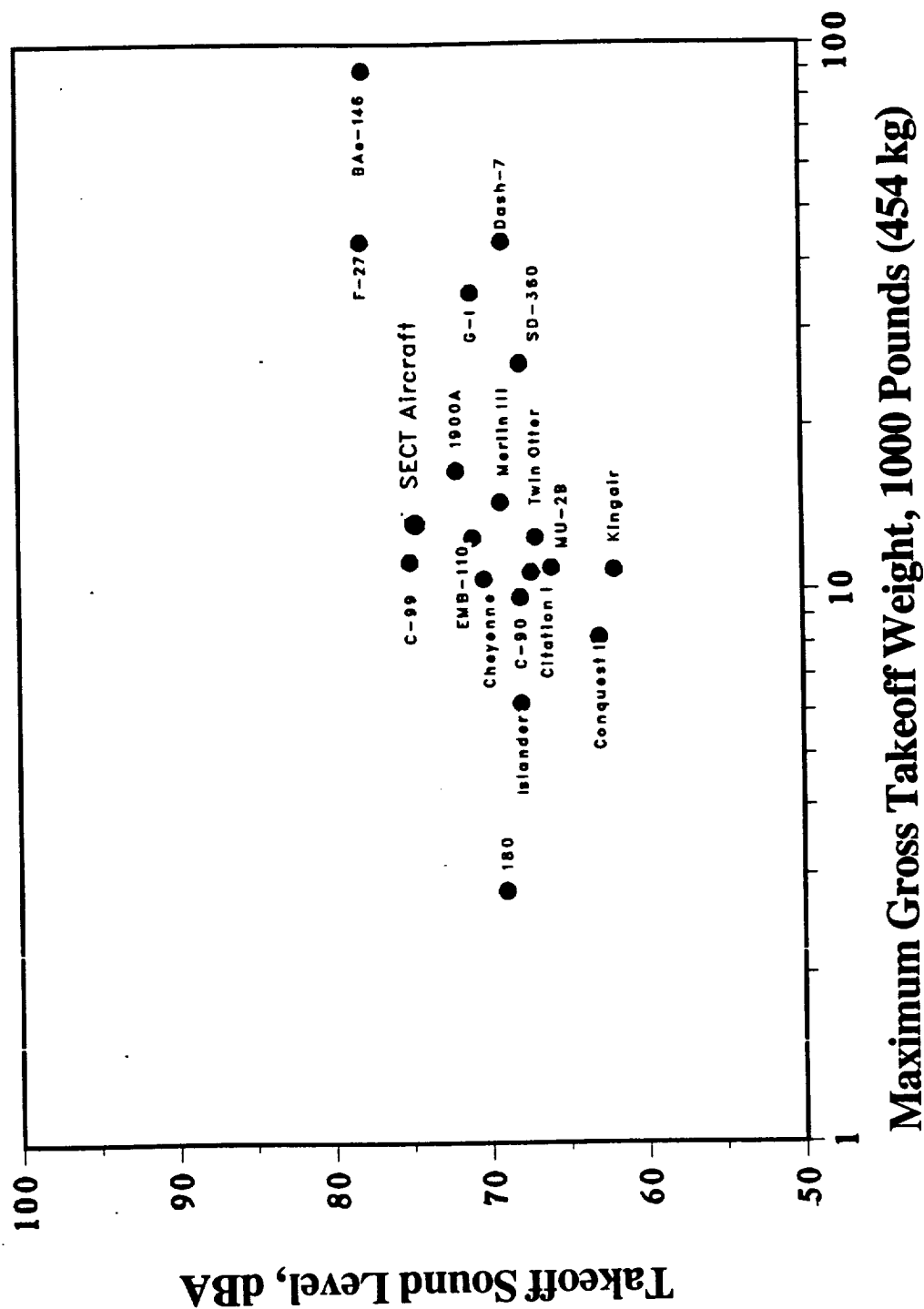
Figure 18.   Takeoff Sound Level

SMOKE VISIBILITY REQUIREMENTS
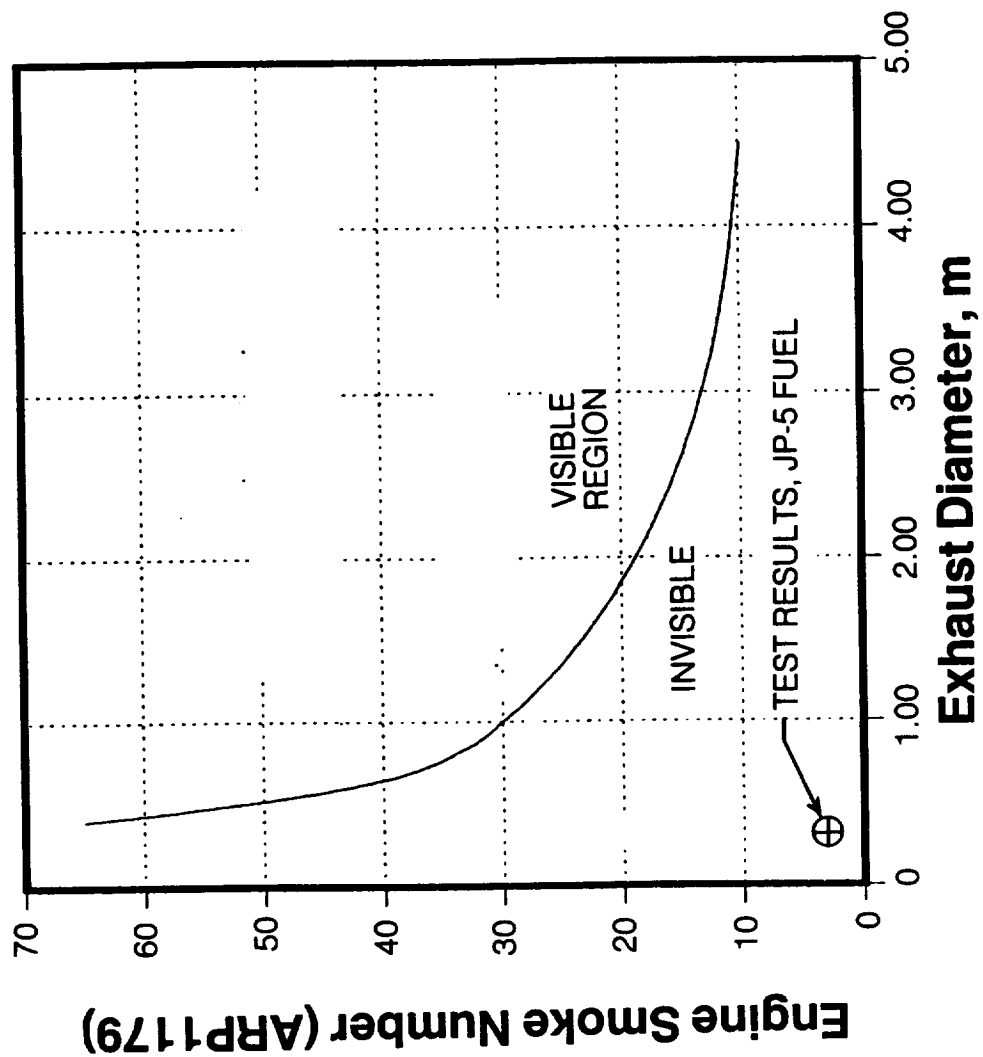
Figure 19.   Smoke Visibility

87
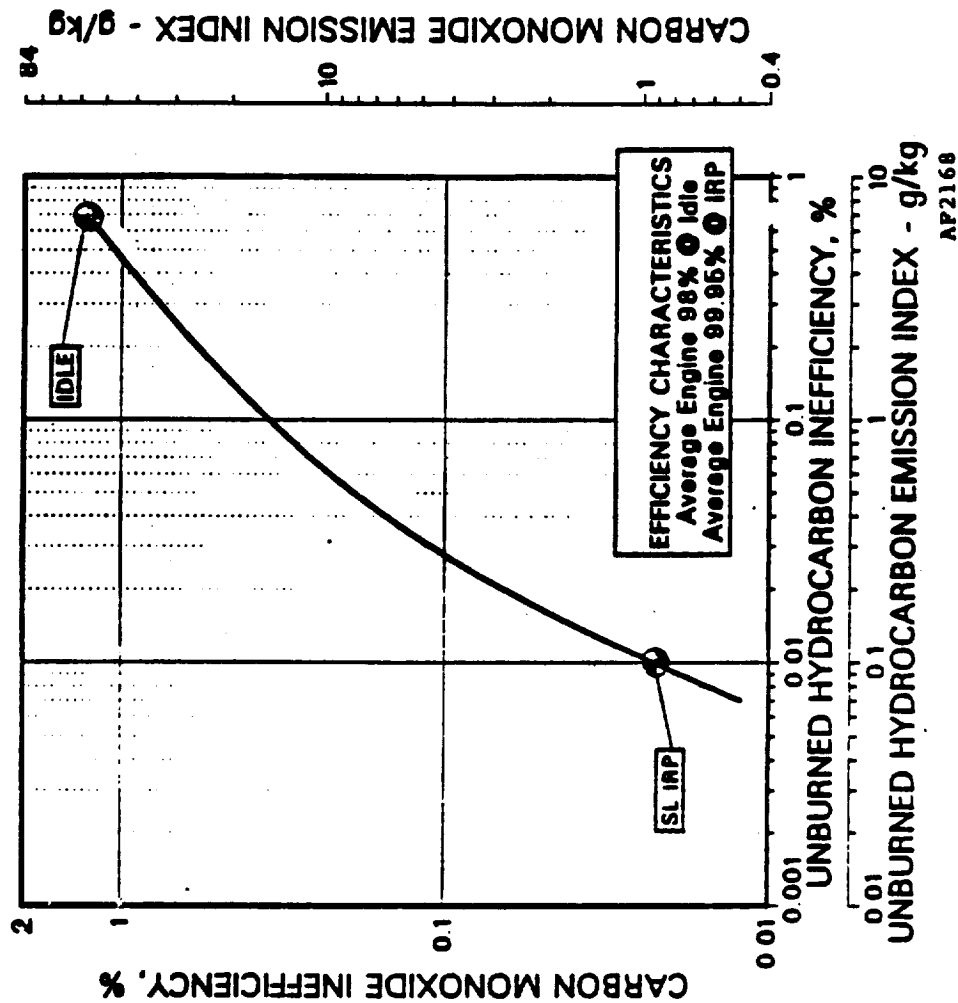
Figure 20. Combustion Efficiency

FUEL CONSUMPTION SENSITIVITY
DELTA WF (%) FOR A 10% DELTA IN PARAMETER
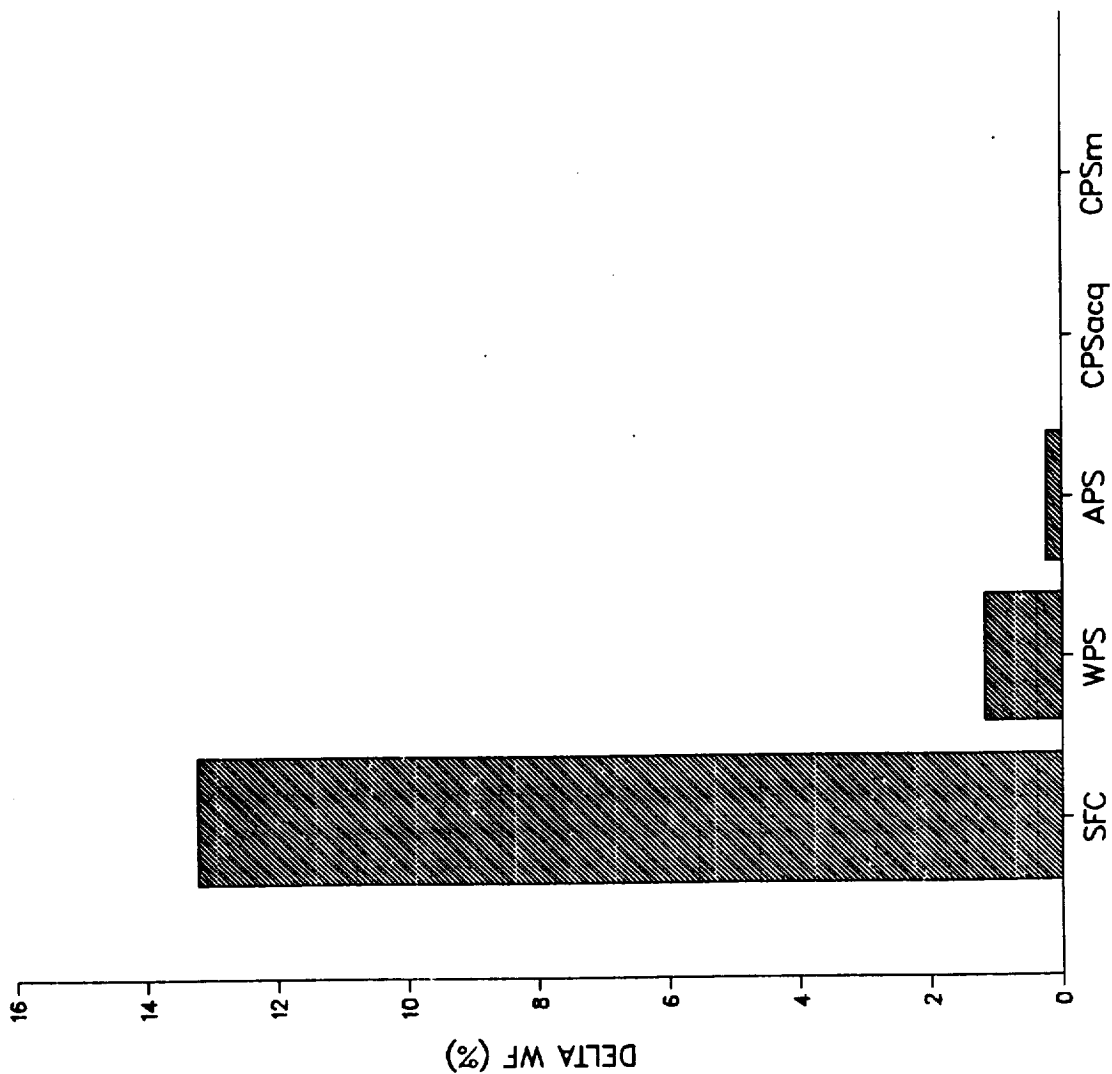
Figure 21. Aircraft Fuel Burn Sensitivity

A/C T/O GROSS WEIGHT SENSITIVITY
DELTA TOGW (%) FOR A 10% DELTA IN PARAMETER
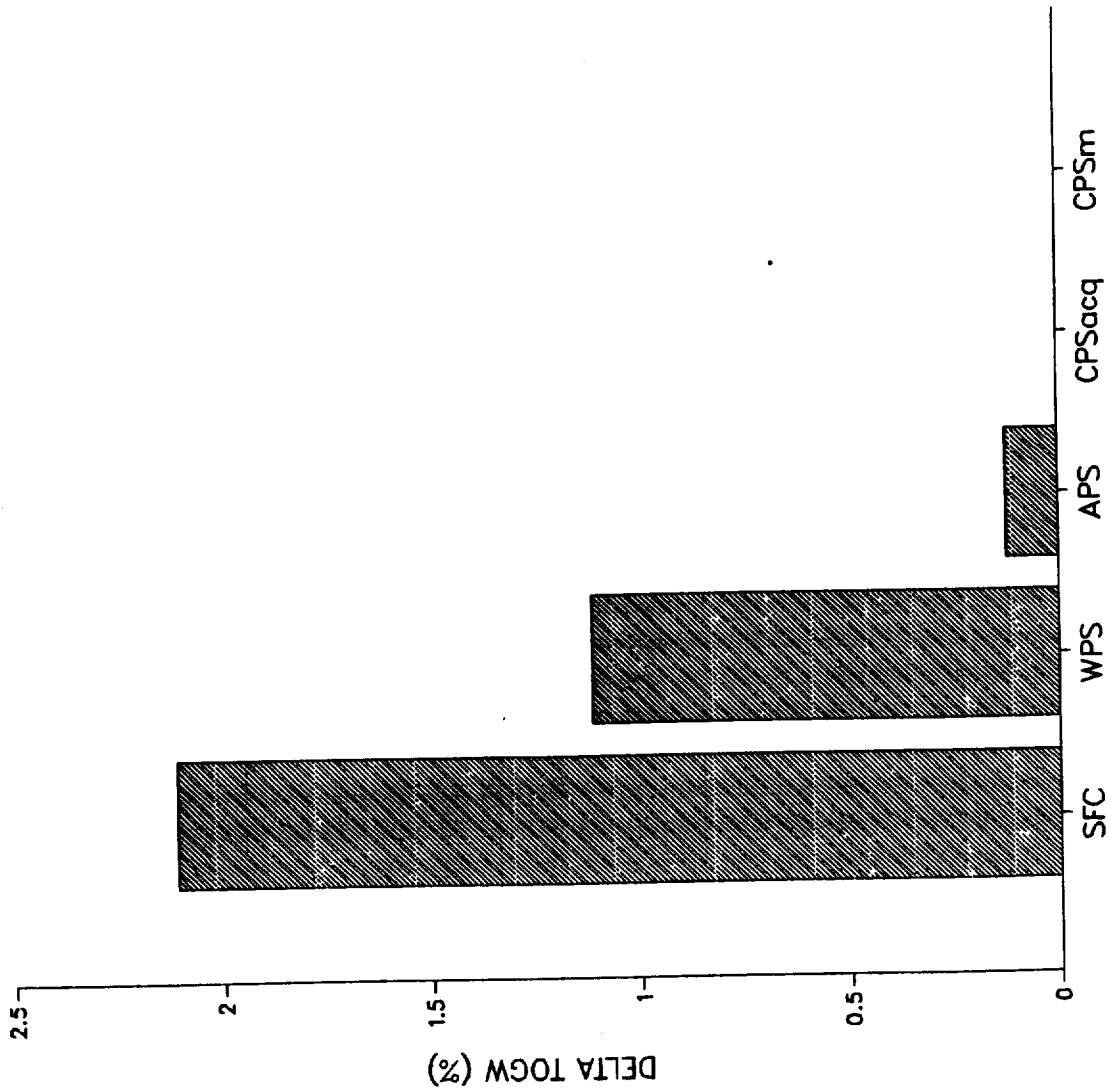
Figure 22. Aircraft Take-Off Gross Weight Sensitivity
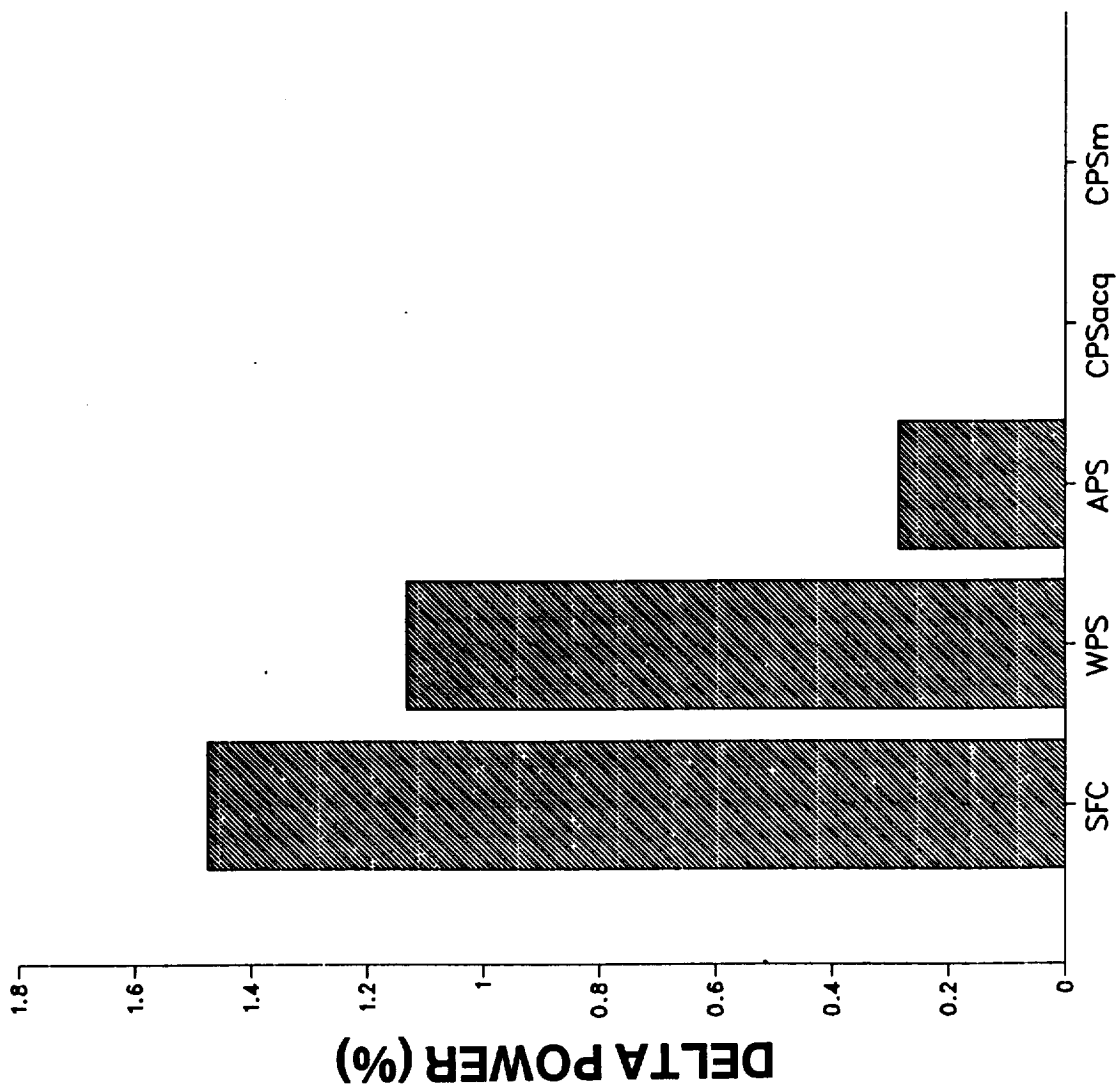
Figure 23.   Aircraft Takeoff Power Sensitivity

Figure 24. Aircraft Acquisition Cost Sensitivity
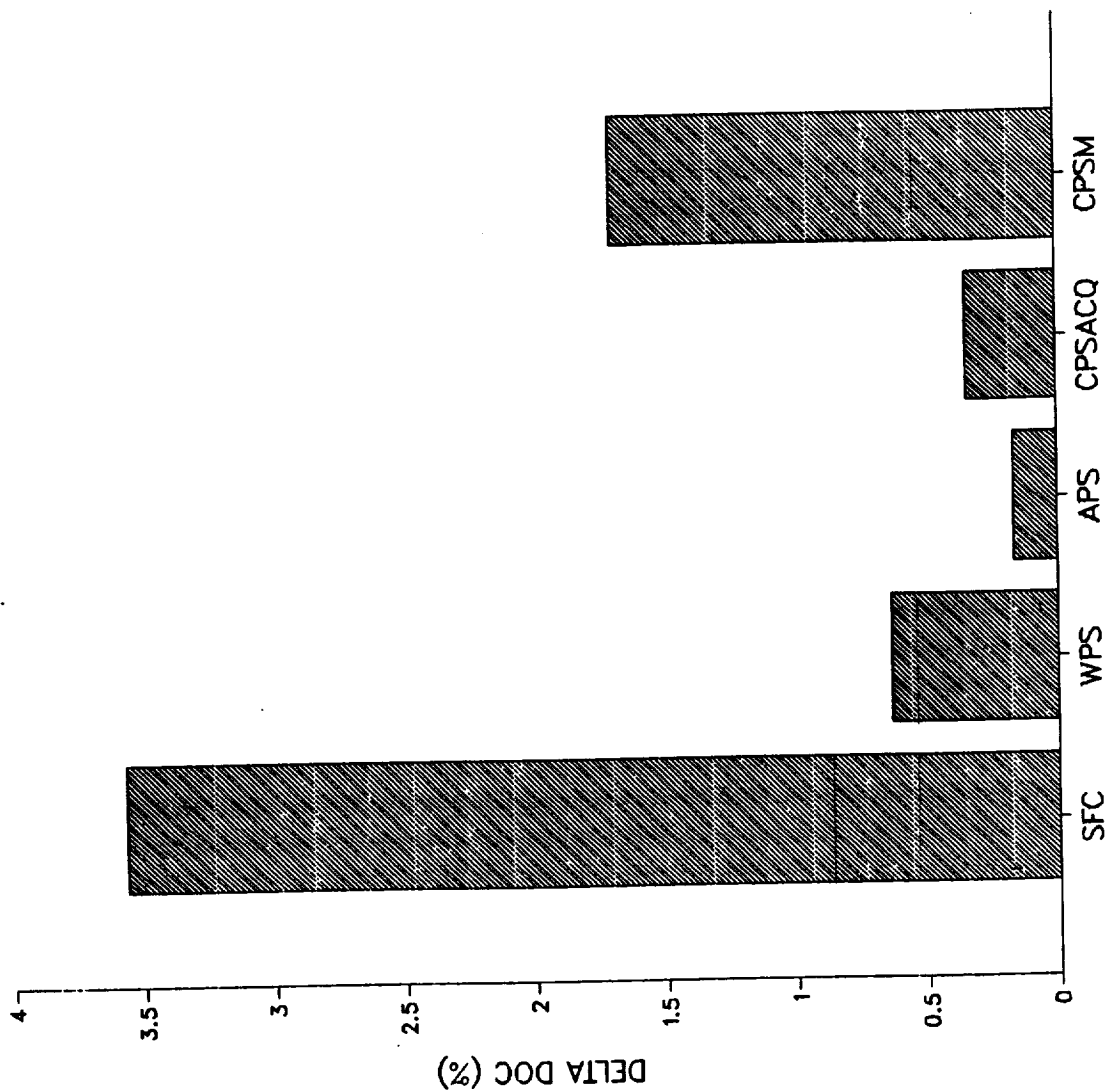
Figure 25. Aircraft DOC Sensitivity - $1.00 Per Gallon Fuel Price

93
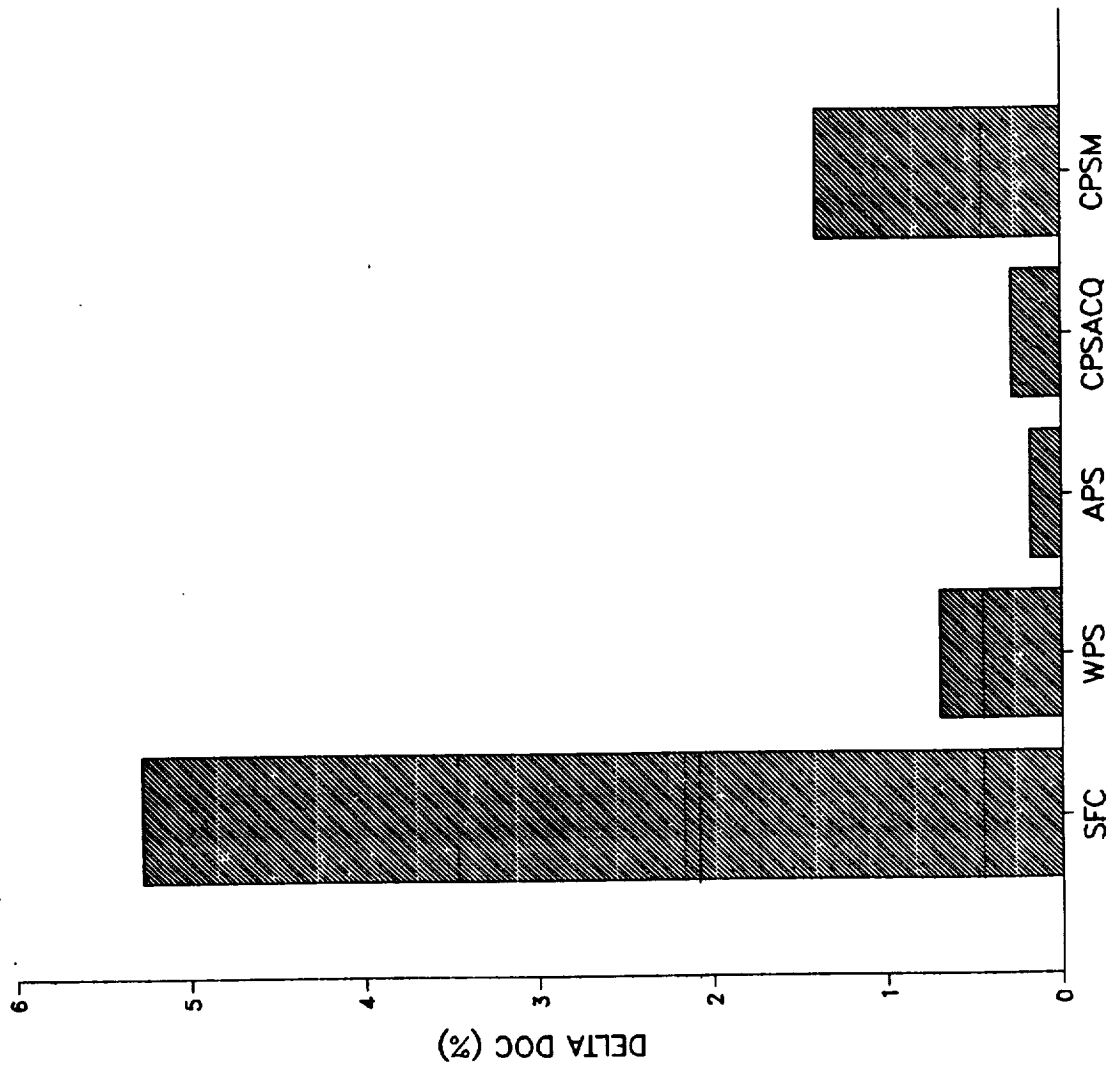
Figure 26. Aircraft DOC Sensitivity - $2.00 Per Gallon Fuel Price

COMPRESSOR EFFICIENCY
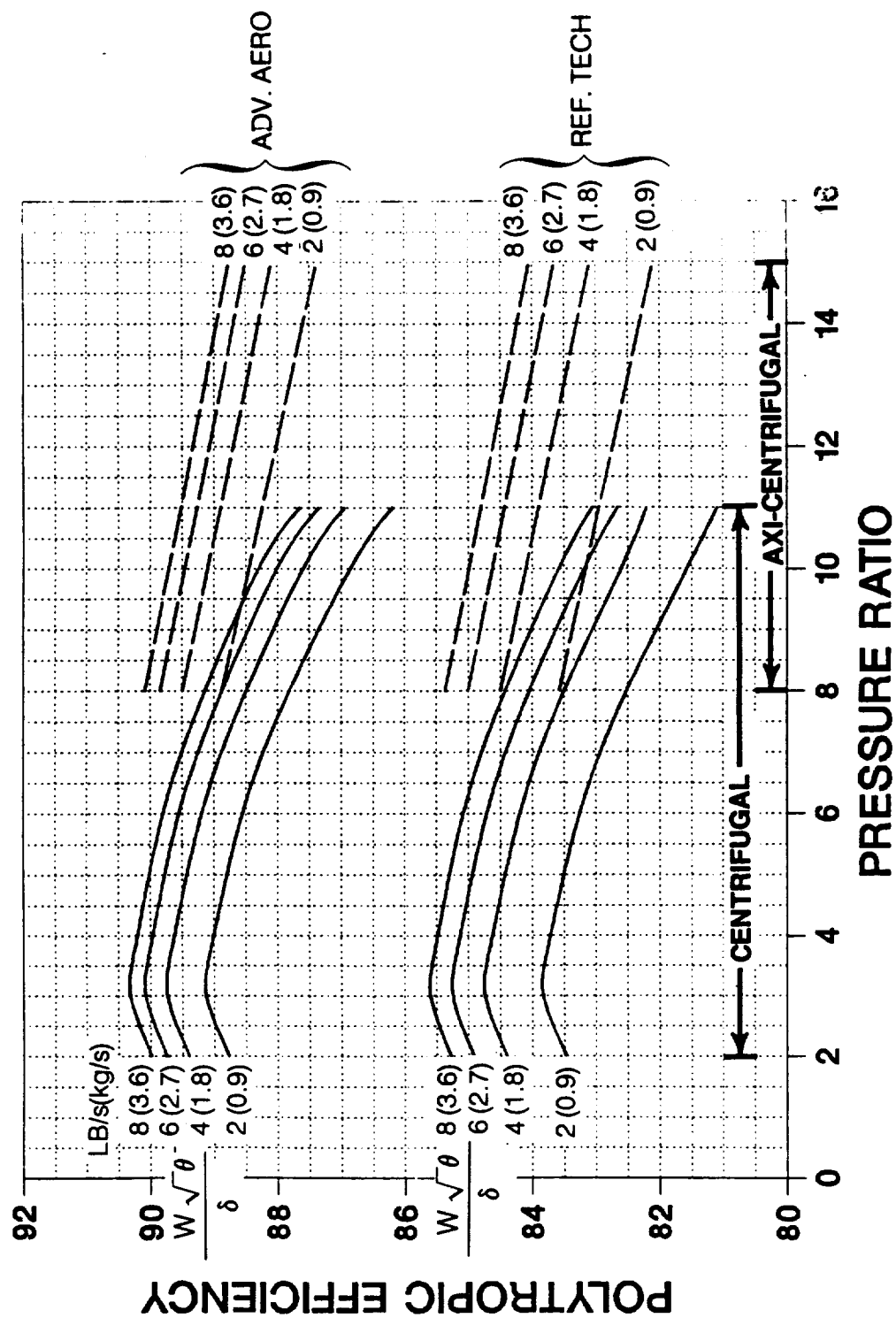
Figure 27. Compressor Efficiency

95

Figure 28. Gas Producer Turbine Efficiency
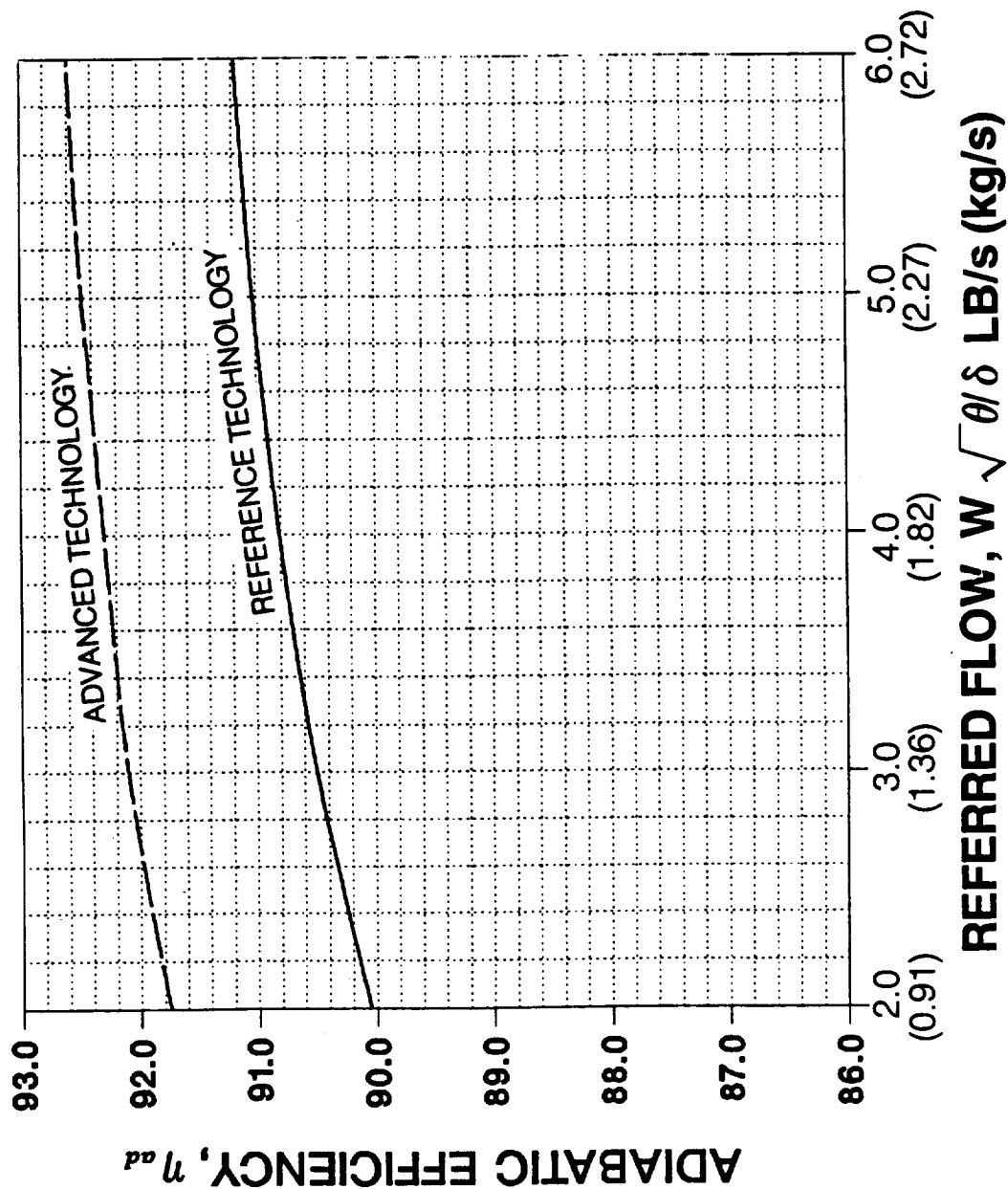
Figure 29. Power Turbine Efficiency

97

TURBINE BLADE COOLING PERFORMANCE

BLADE EFFECTIVENESS $\left(\dfrac{T_g - T_m}{T_g - T_c}\right)$

MASS FLOW RATE PARAMETER $\left(\dfrac{2W_c\ Cp_c}{h_g\ A_g}\right)$

ADVANCED TECHNOLOGY

REFERENCE TECHNOLOGY
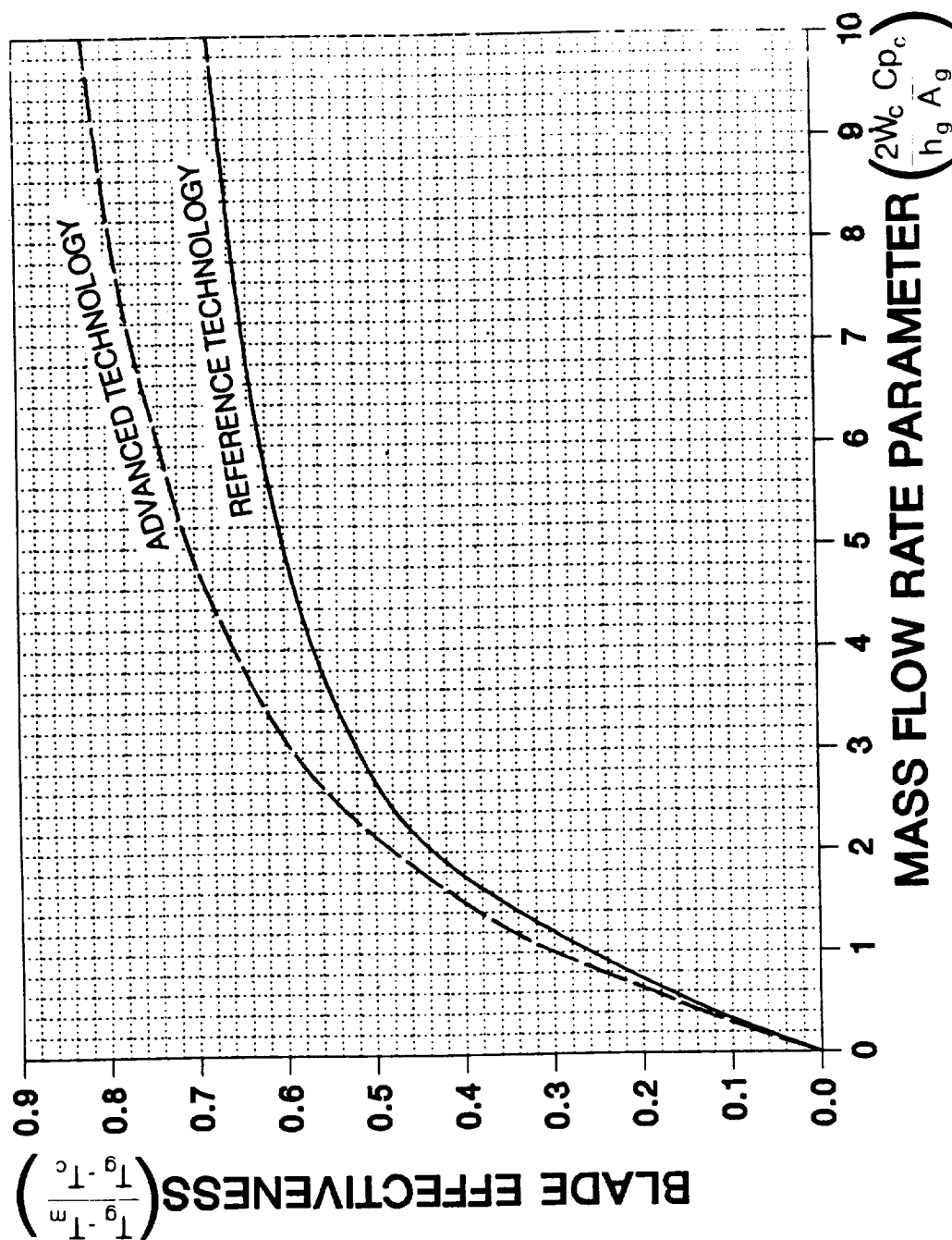
Figure 30.   Turbine Blade Cooling Performance

98
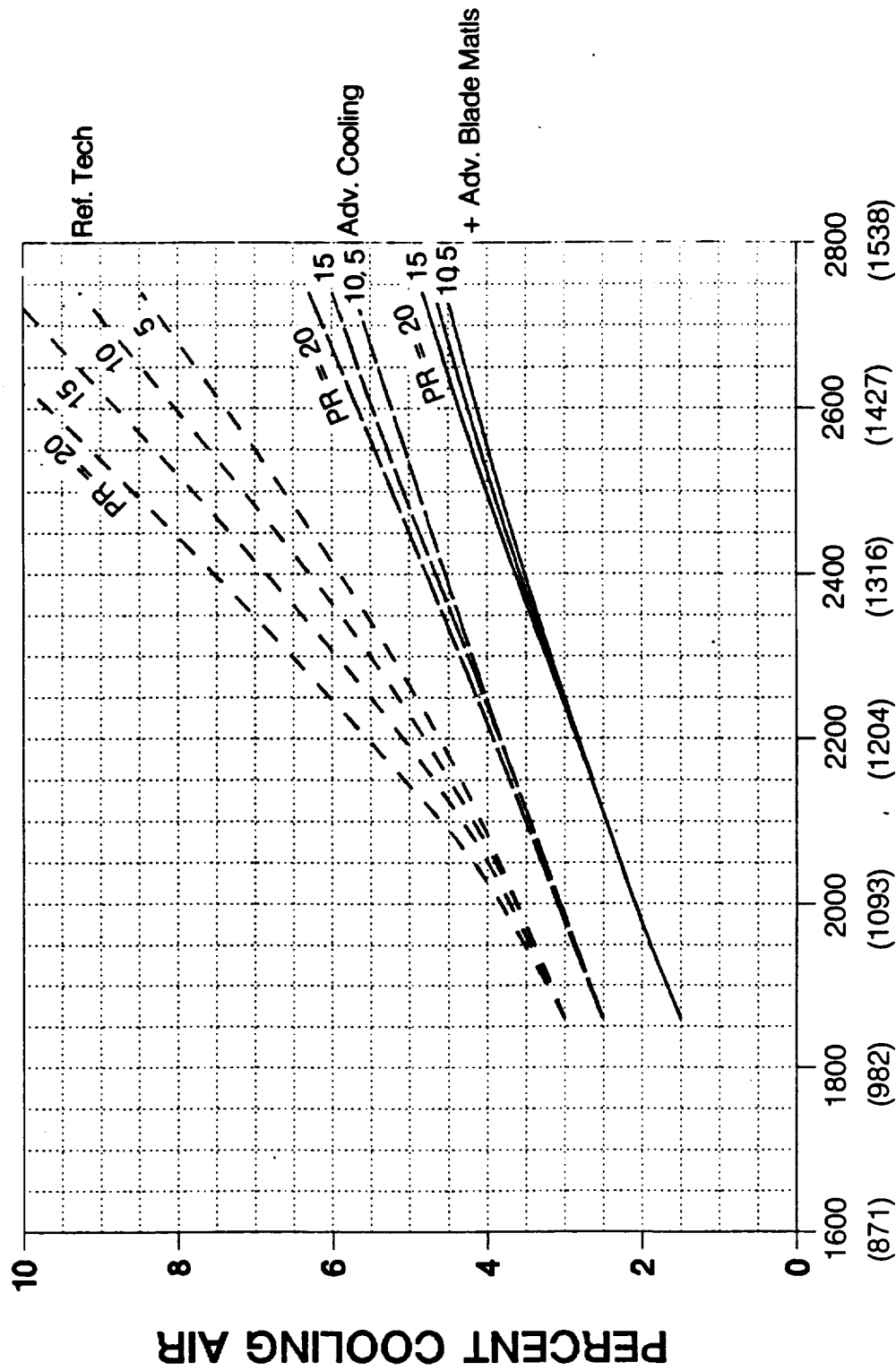
NOZZLE COOLING FLOW

Figure 31. Nozzle Cooling Flow

99
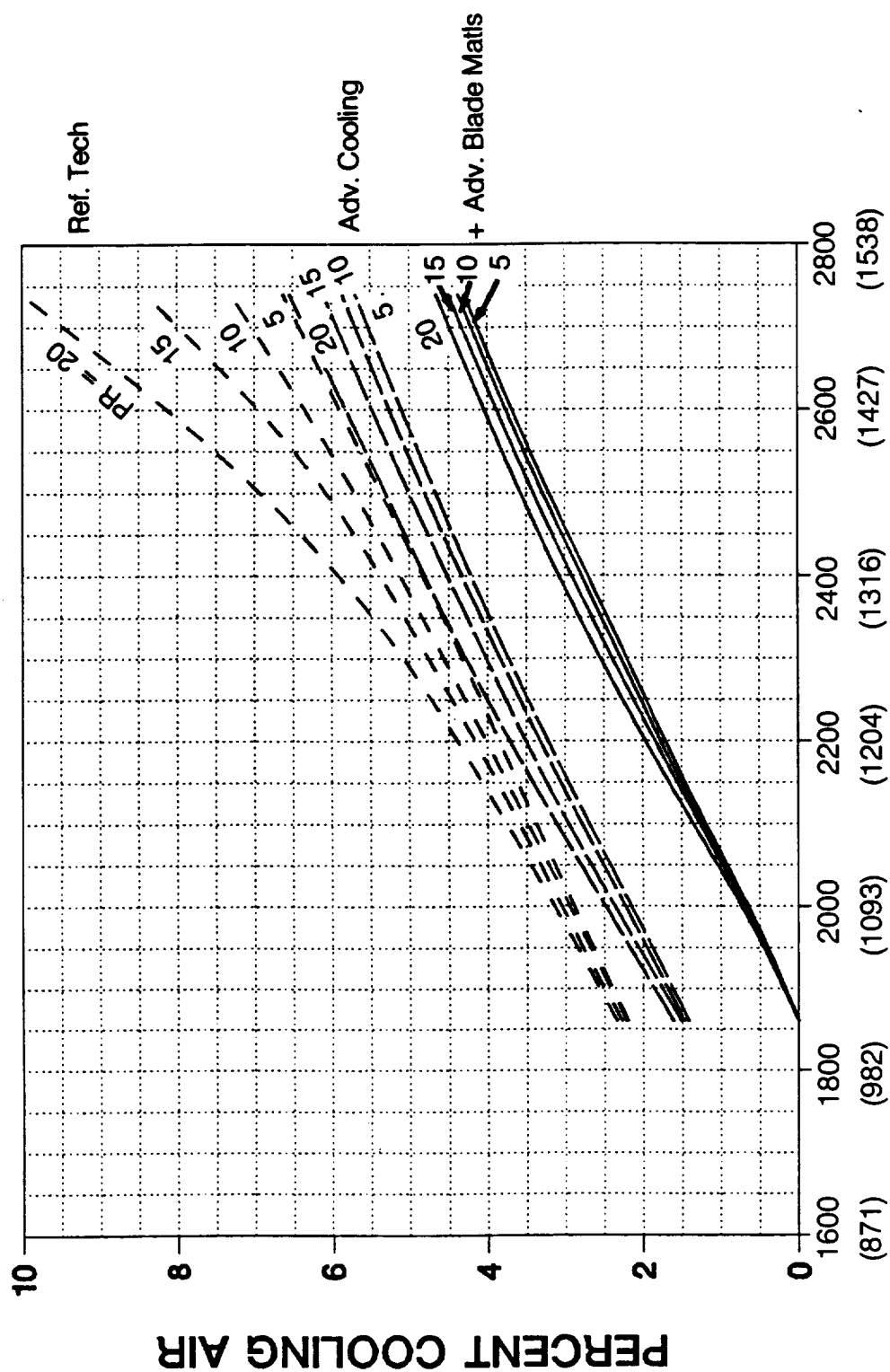
ROTOR COOLING FLOW

Figure 32. Rotor Cooling Flow

100

LYCOMING WAVEPLATE
RECUPERATOR CORE

AIR PASSAGE

GAS PASSAGE

AIR PASSAGE

EXHAUST GAS ⟶
HOT AIR ⟶
COLD AIR ⟶

AE1157
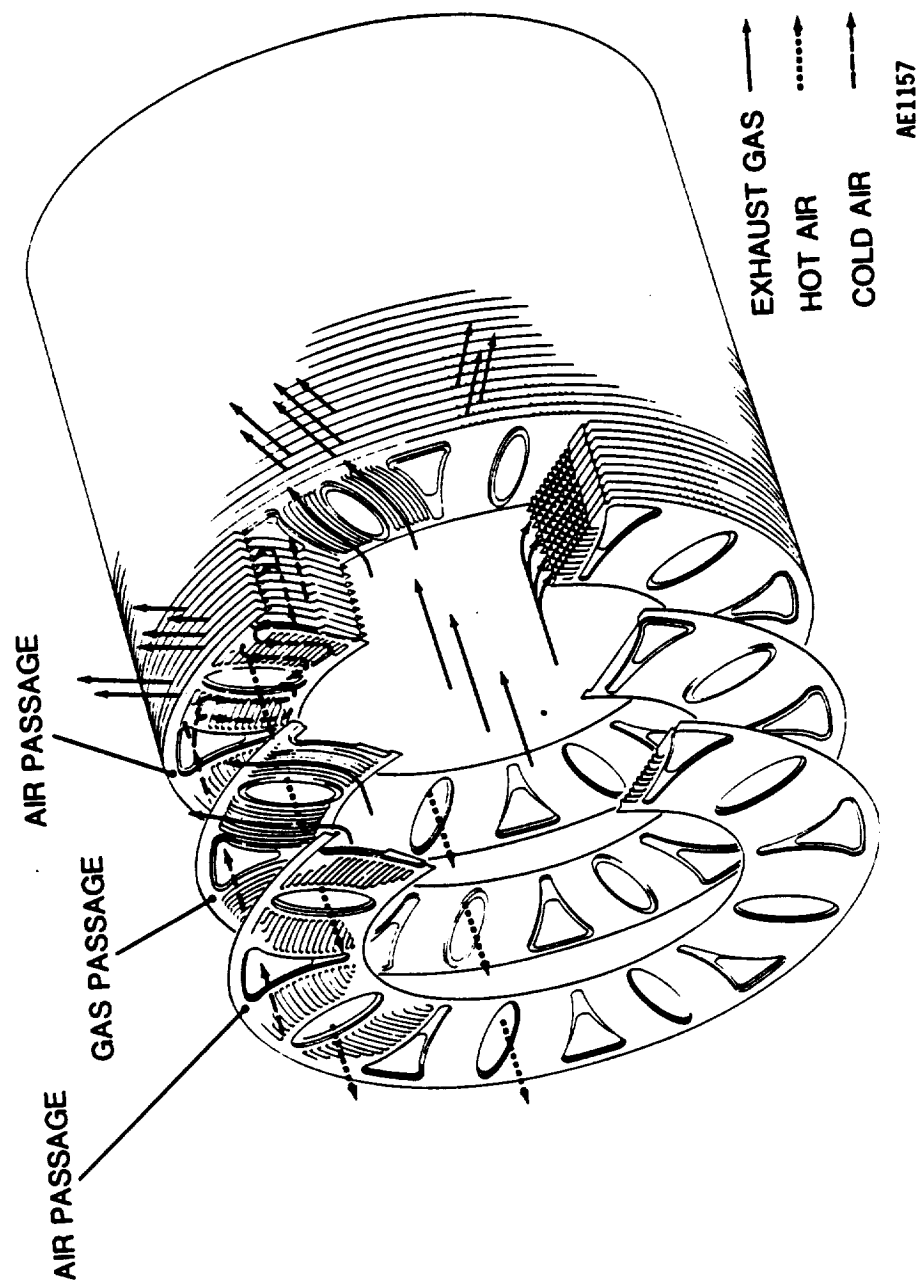
Figure 33.   Recuperator Core

101
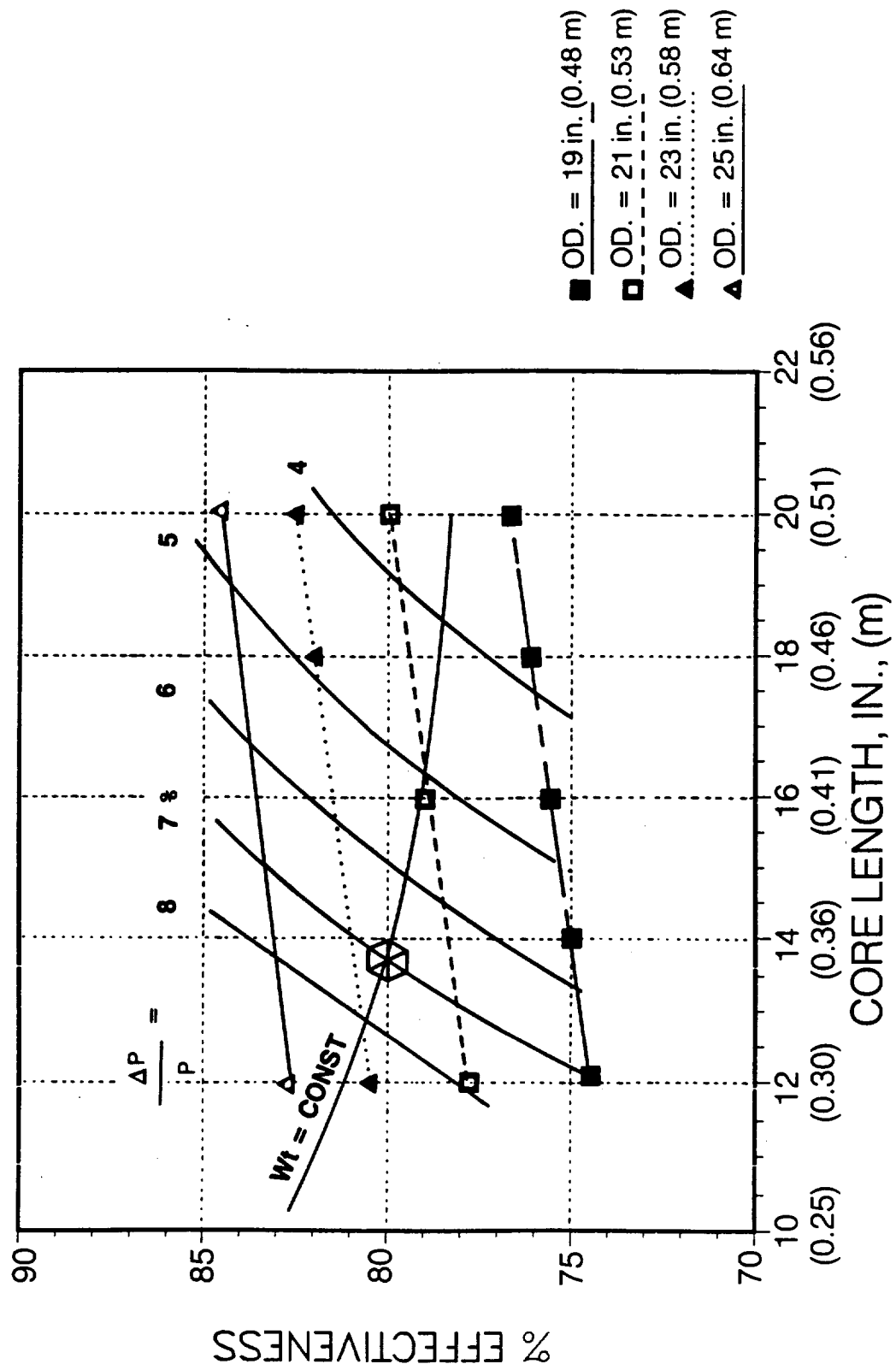
Figure 34. Recuperator Sizing Analysis

RECUPERATOR GEOMETRY
ε = 0.80
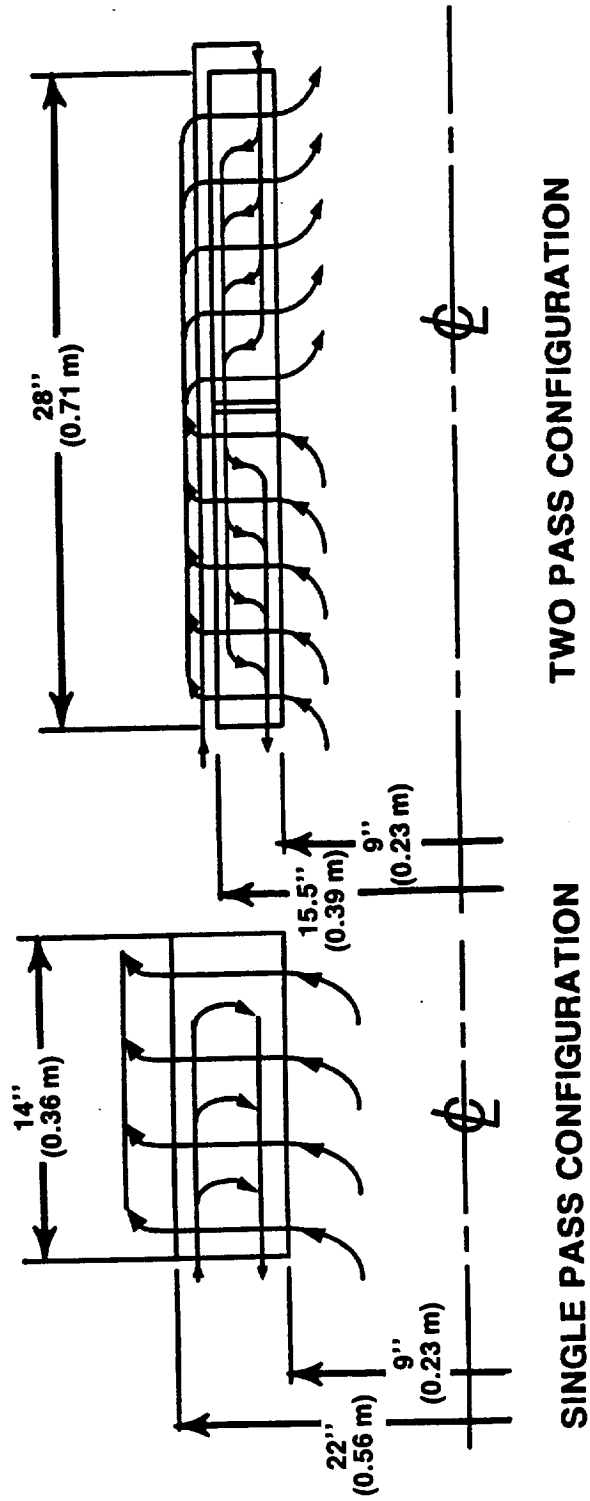
Figure 35. Recuperator Core Configurations
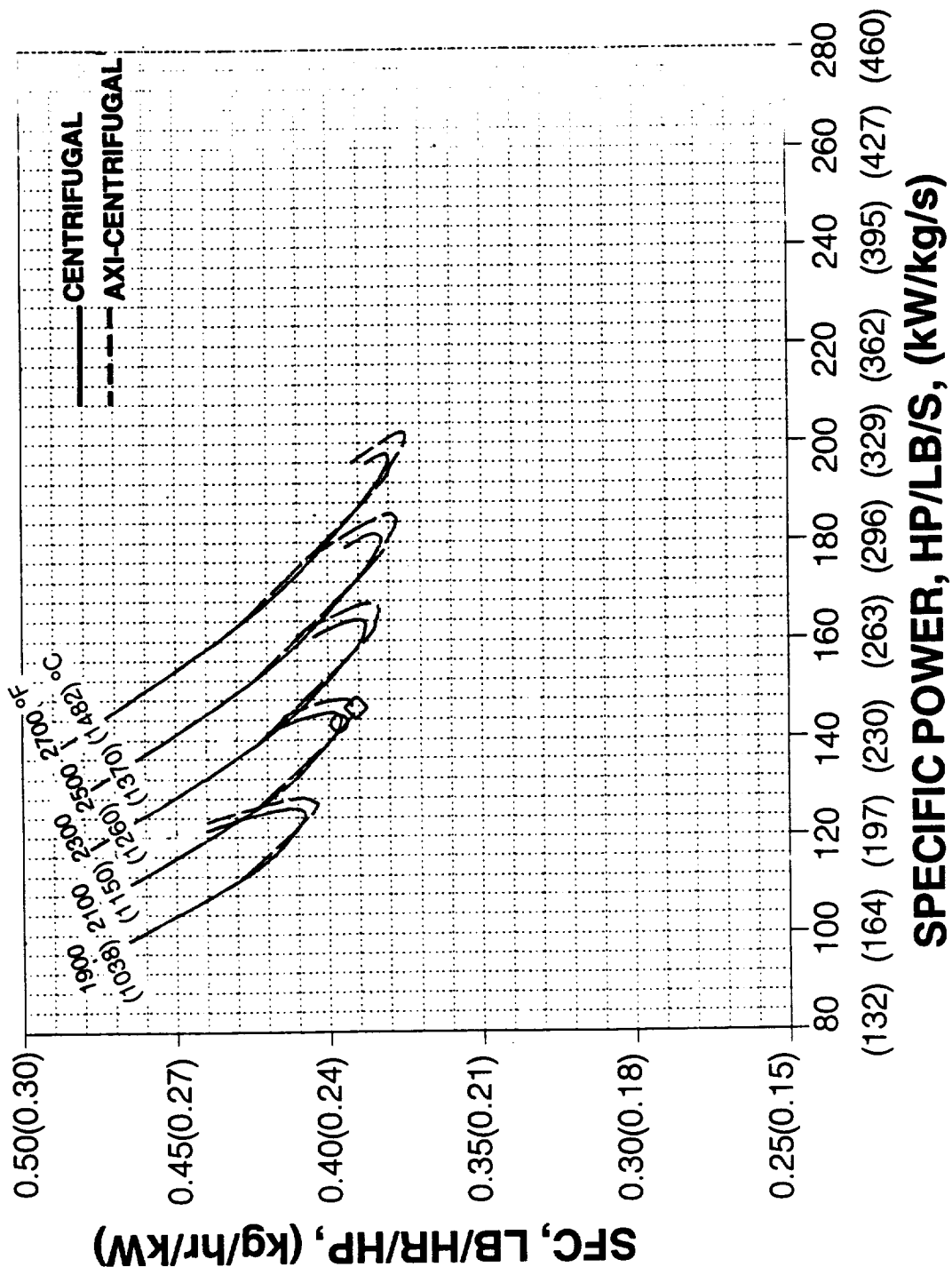
Figure 36. Reference Technology + Recuperator Cycle Performance, $\epsilon = 0.70$
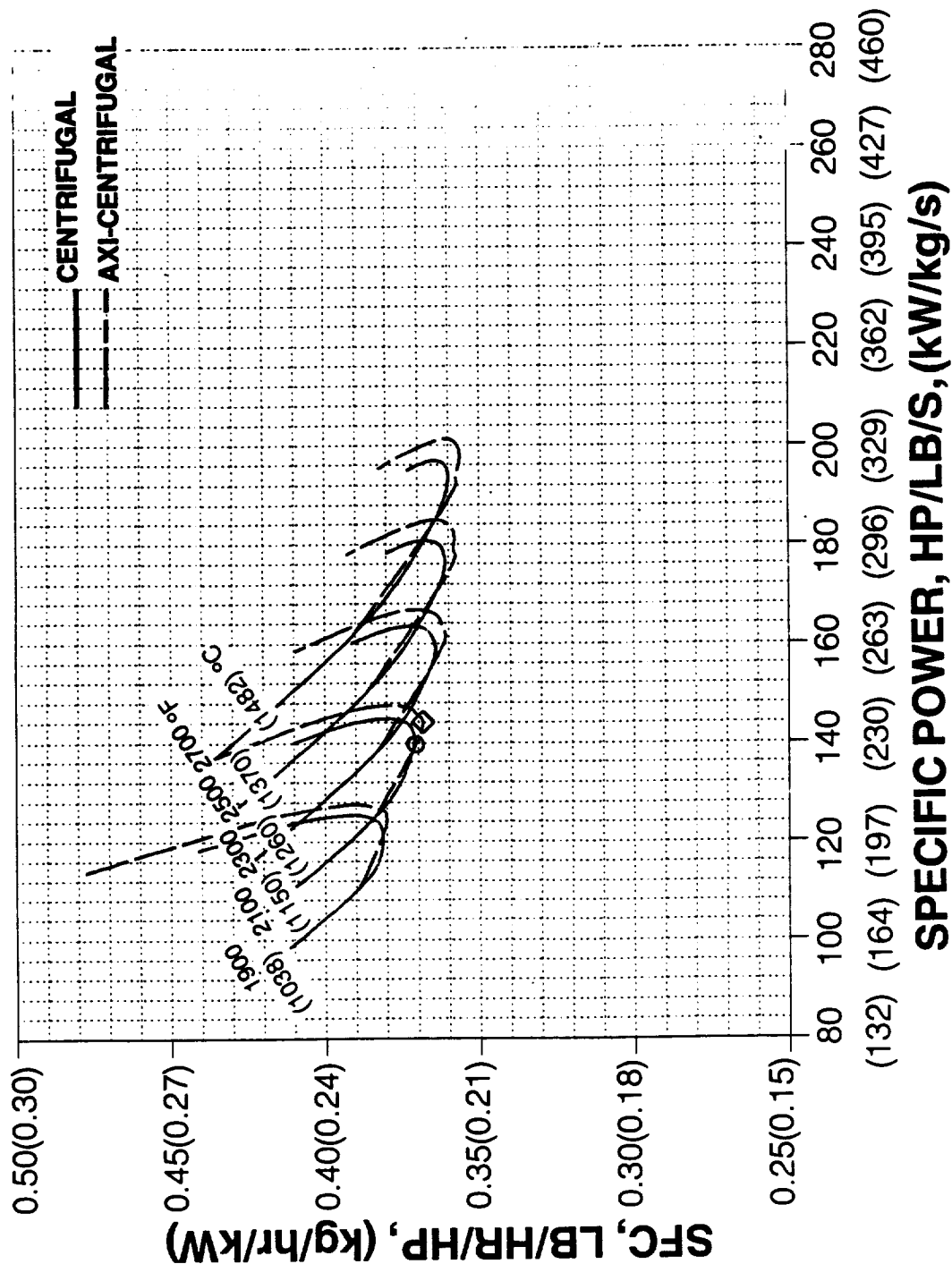
Figure 37. Reference Technology + Recuperator Cycle Performance, $\epsilon = 0.80$
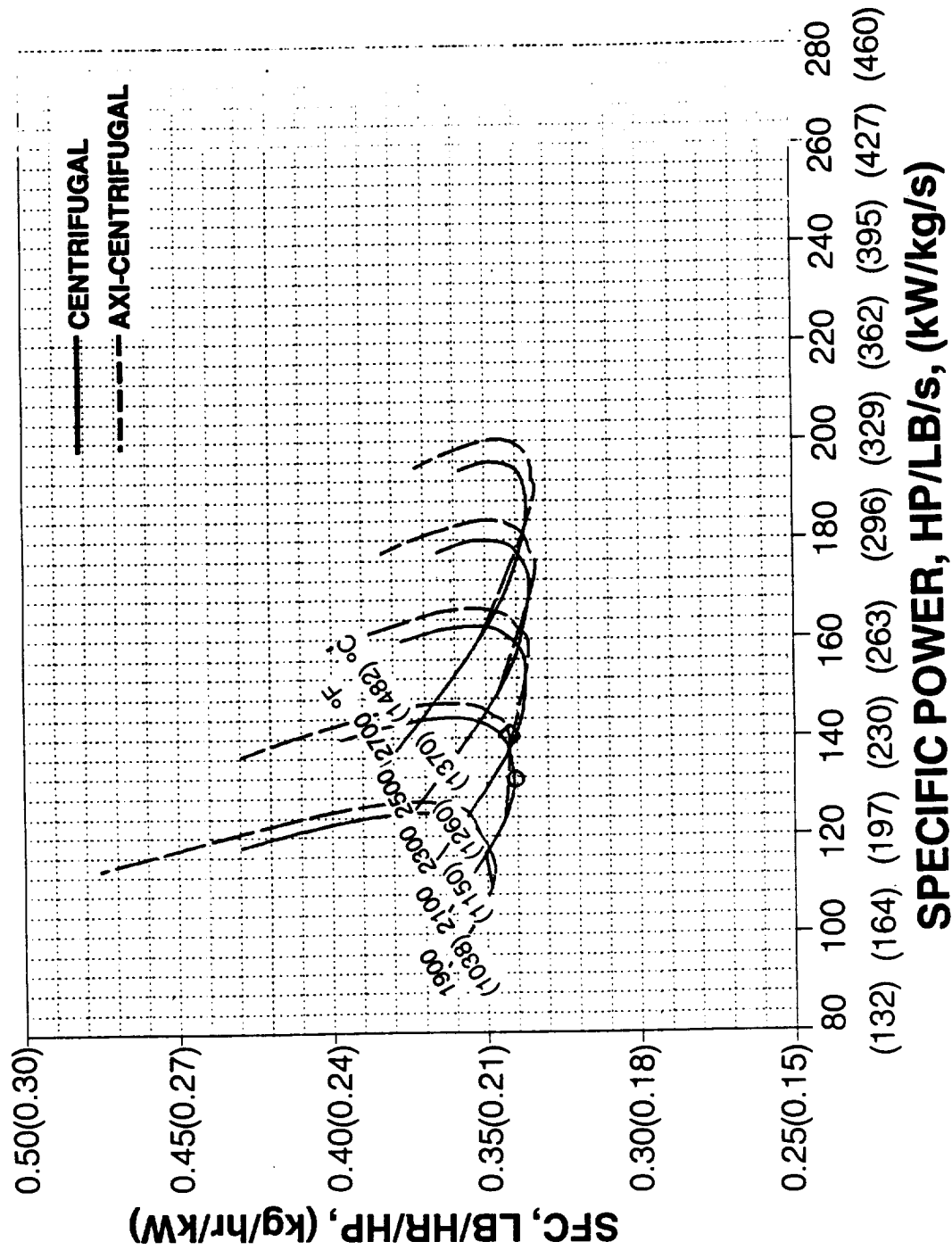
Figure 38.   Reference Technology + Recuperator Cycle Performance, ε = 0.90

Figure 39. Reference Technology + Recuperator Cycle Performance, $T_{4,0}$ = 2100°F (1150°C)

DESIGN POINT: M = 0.373, H = 10000. FT (3048 m)
ADVANCED AERO
T4.0 = 2100F (1150 C) EFFECTIVENESS = 0.70, 0.80, 0.90
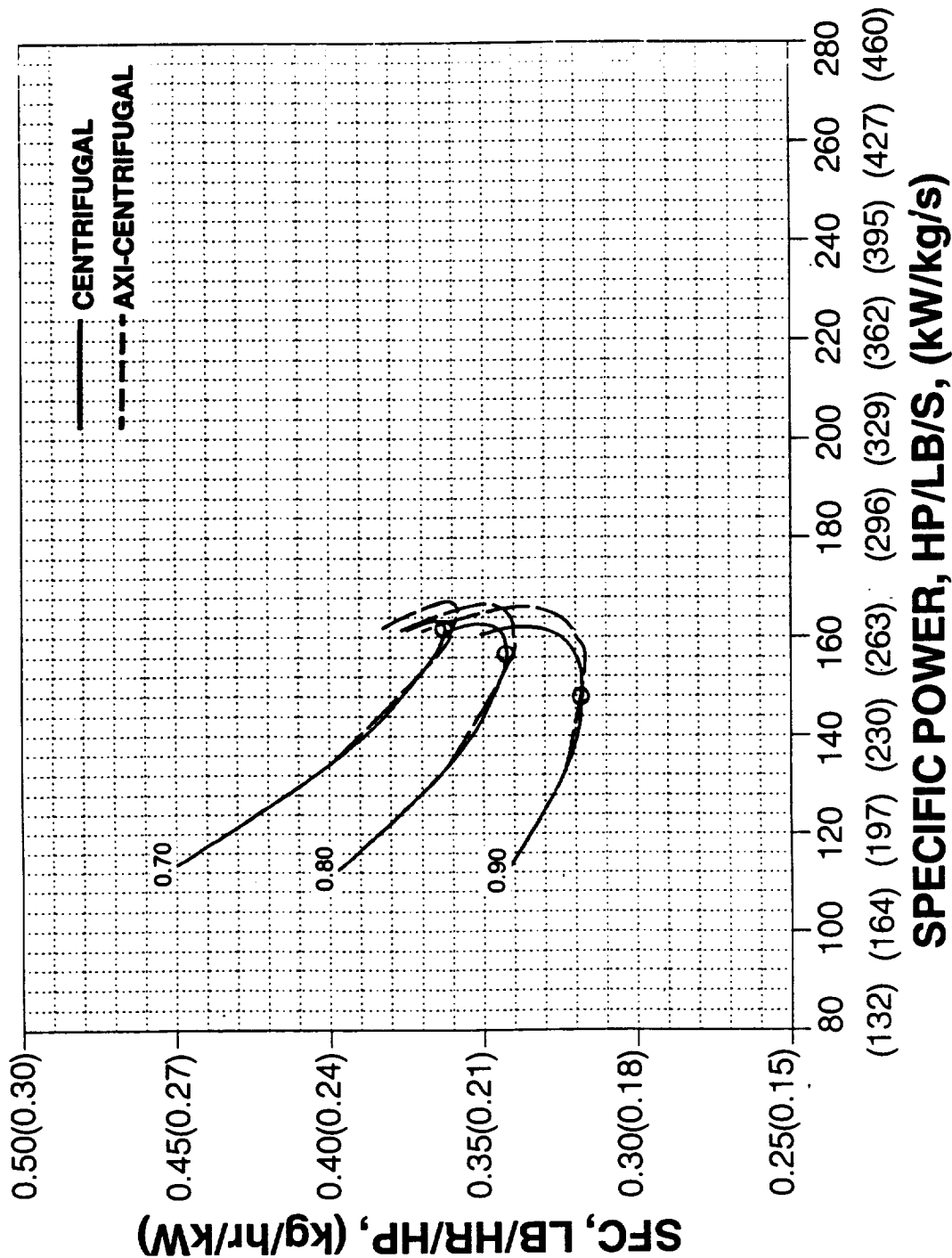
Figure 40. Advanced Aerodynamics Cycle Performance, $T_{4.0}$ = 2100°F (1150°C)

108
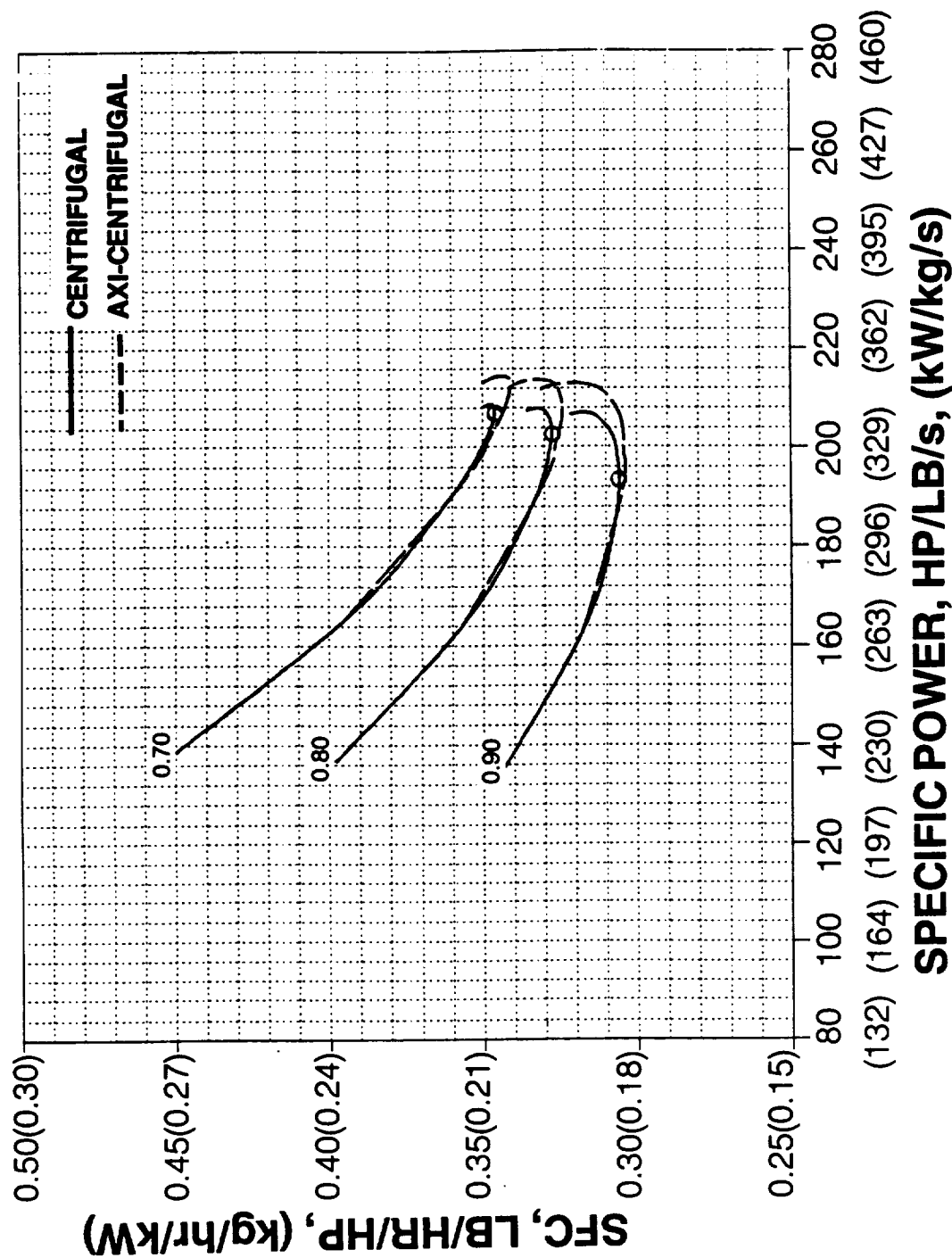
Figure 41. Advanced Aero + Cooling Cycle Performance, $T_{4.0}$ = 2500°F (1370°C)

109
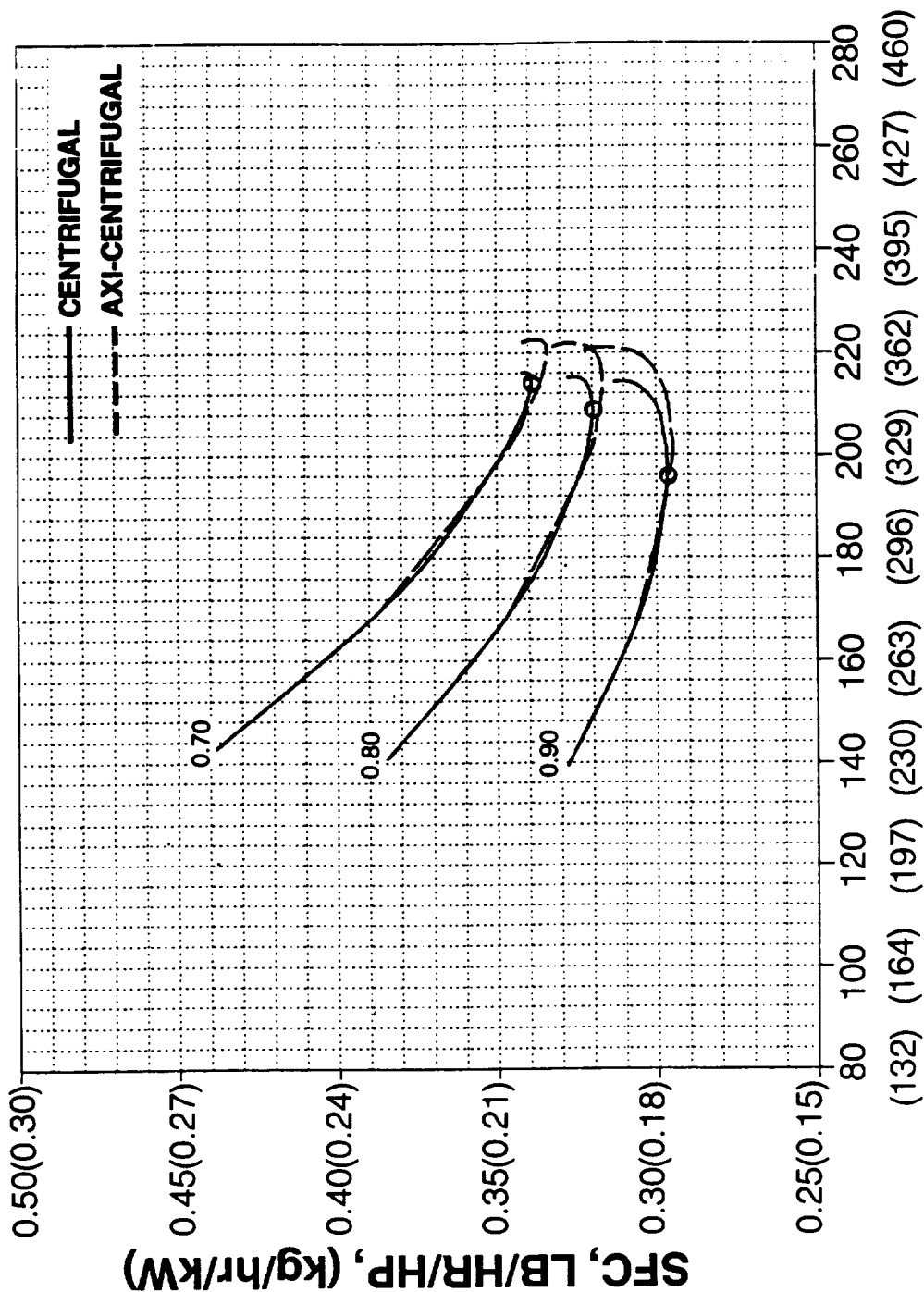
Figure 42.   Advanced Aero + Cooling + Blade Materials Cycle Performance, $T_{4.0}$ = 2500°F (1370°C)
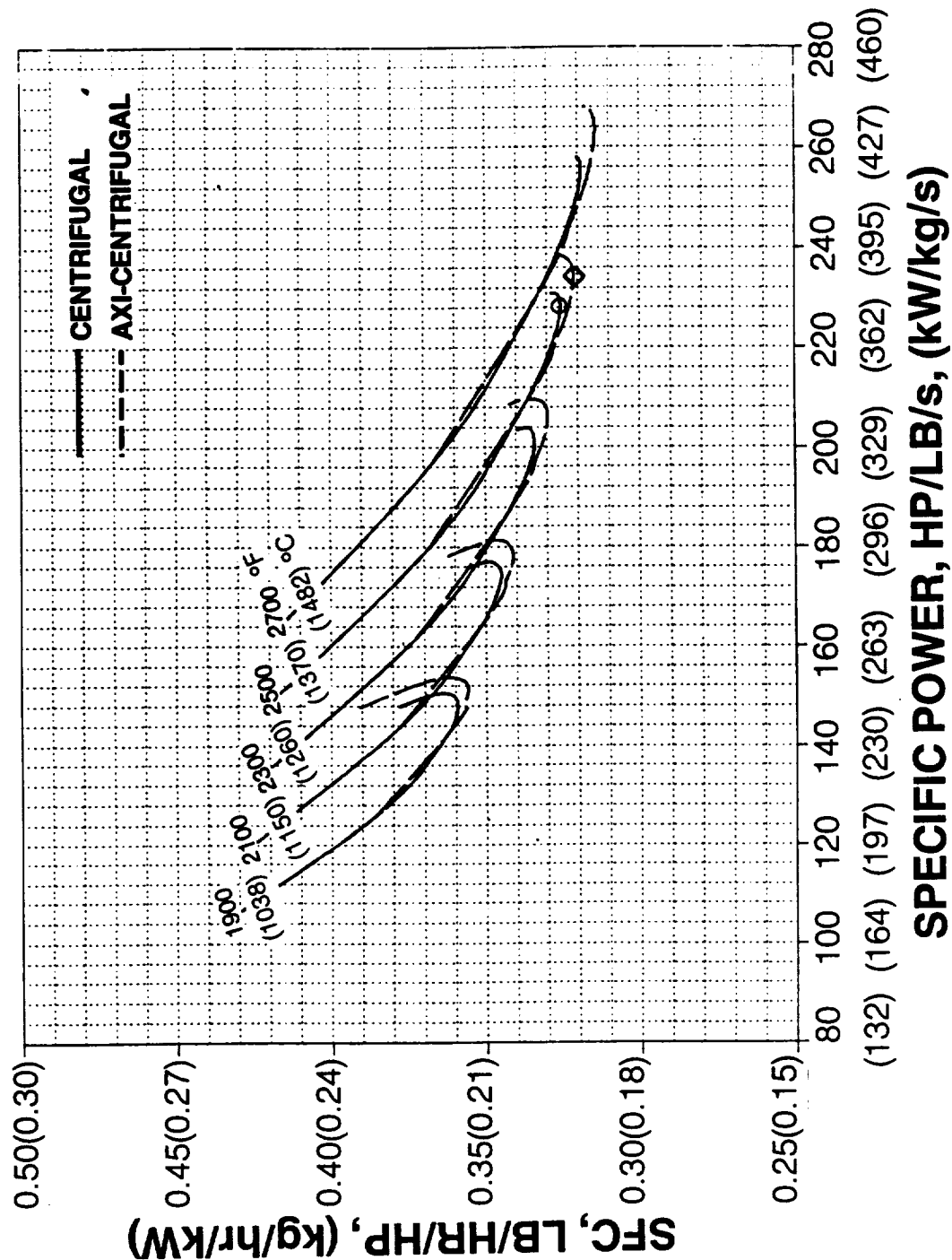
Figure 43.   Advanced Aero + Ceramics Cycle Performance, ε = 0.70

111
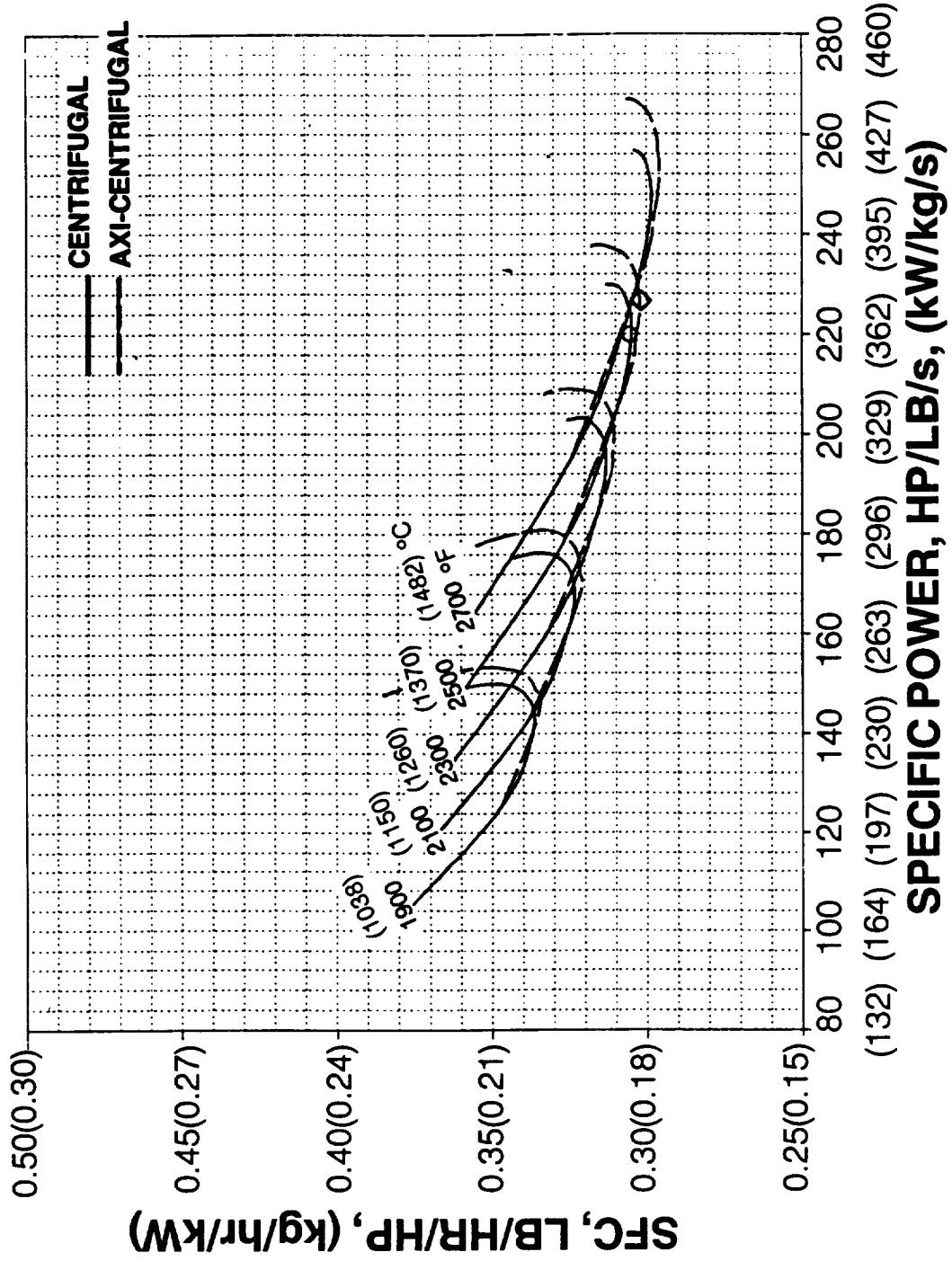
Figure 44.   Advanced Aero + Ceramics Cycle Performance, ε = 0.80
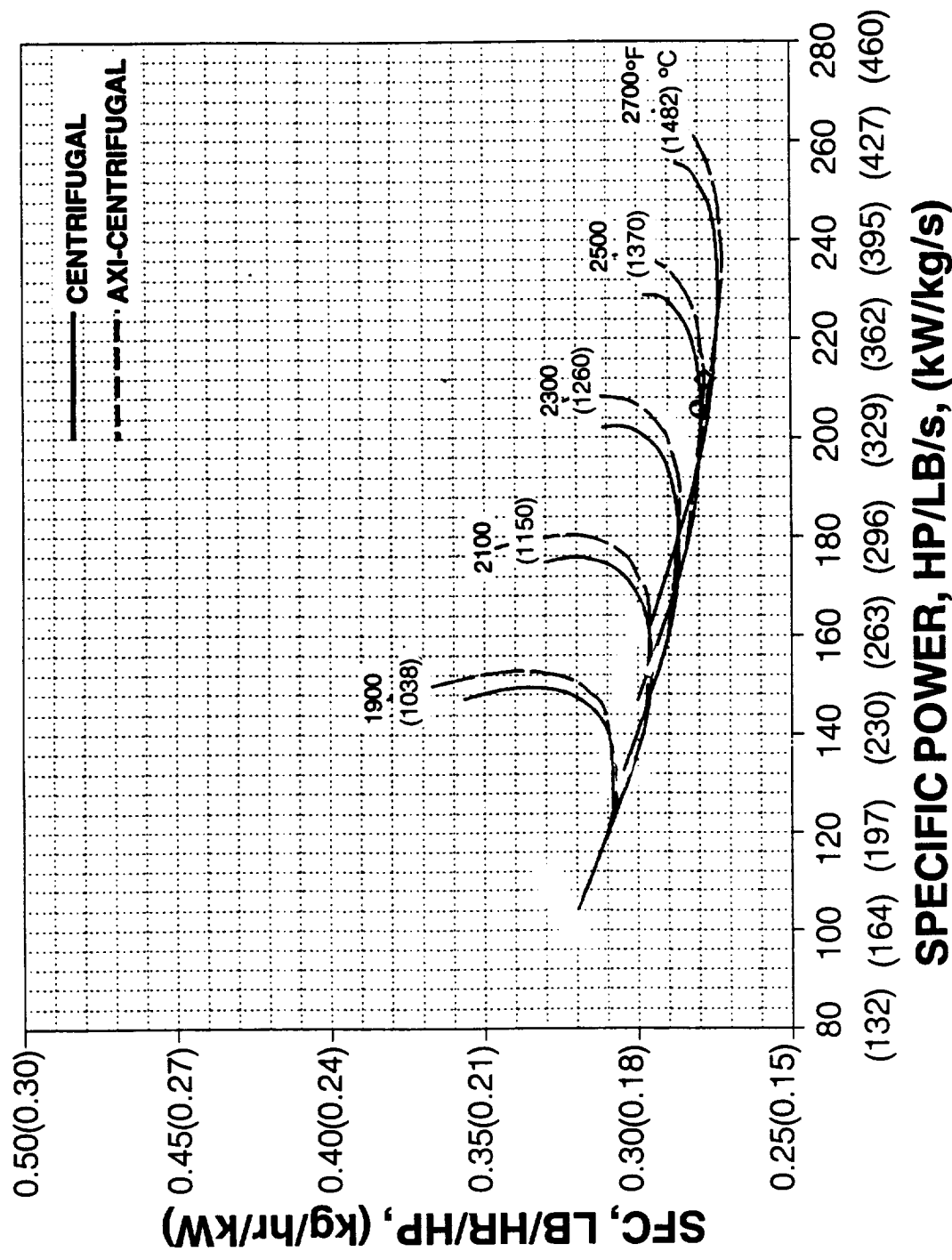
Figure 45.   Advanced Aero + Ceramics Cycle Performance, ϵ = 0.90

113

Figure 46. Advanced Aero + Ceramics Cycle Performance, $T_{4.0}$ = 2500°F (1370°C)
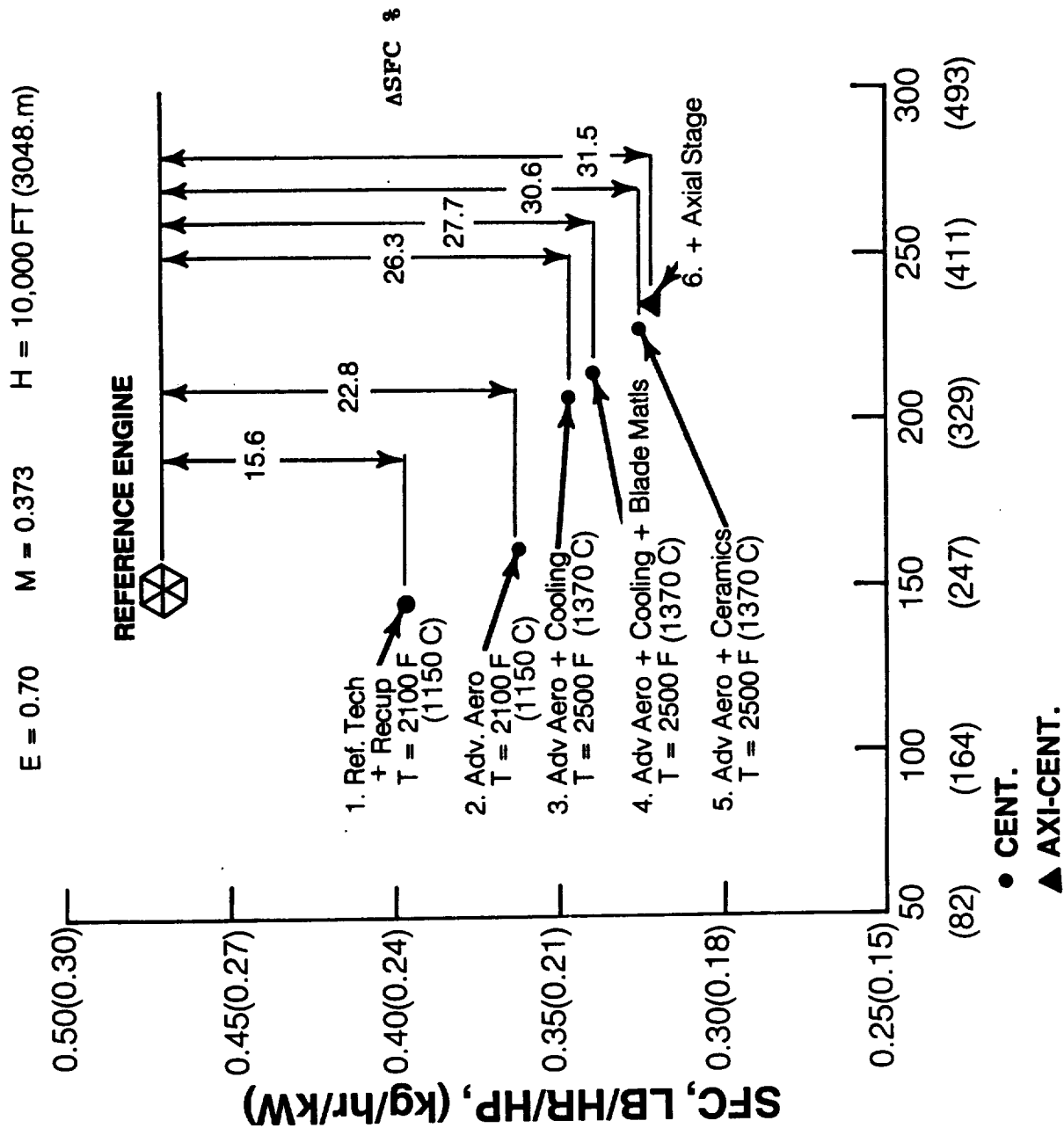
Figure 47. Summary of Engine Performance Gains, $\epsilon = 0.70$
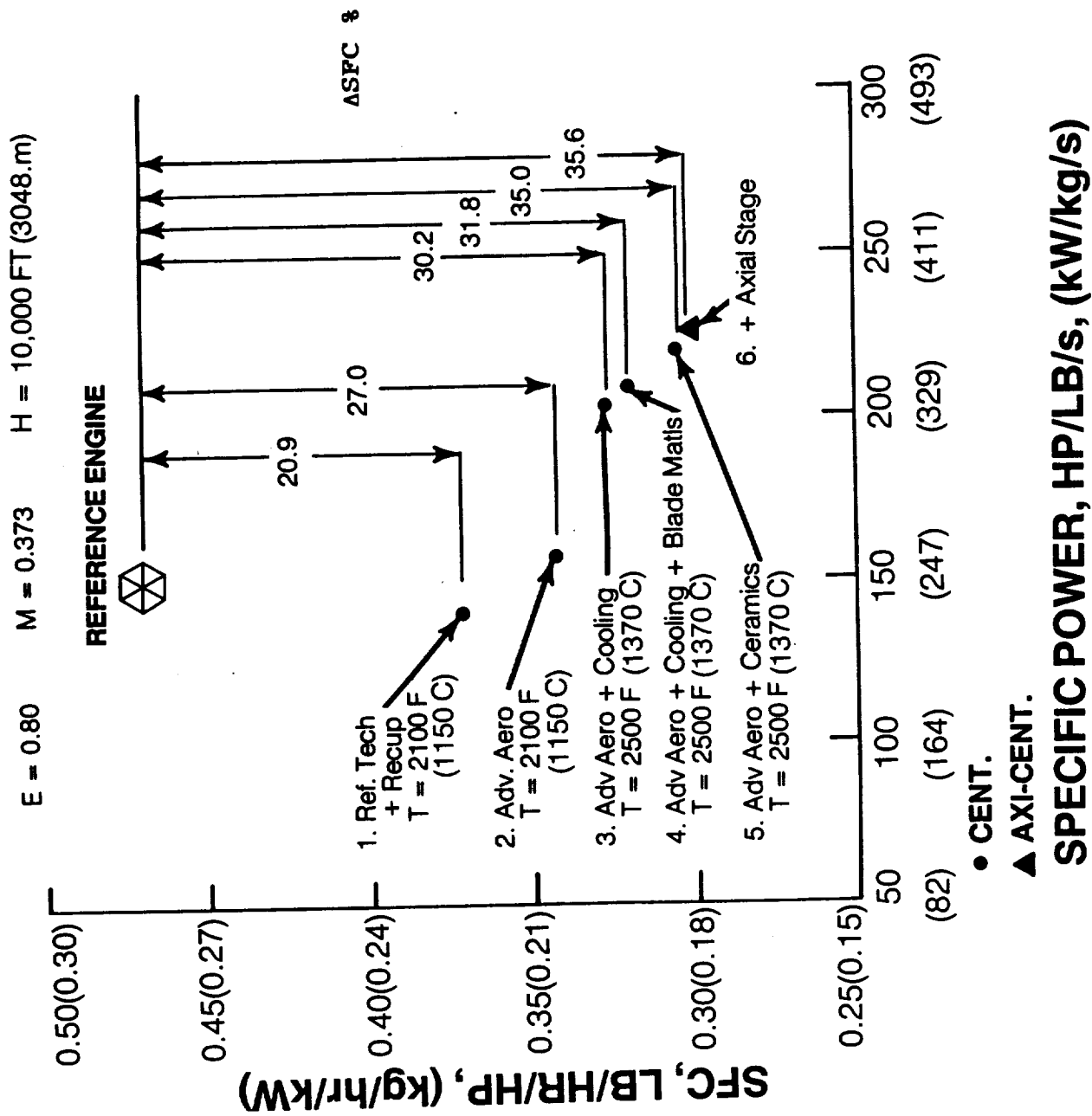
Figure 48. Summary of Engine Performance Gains, $\epsilon = 0.80$

BT1284A

116
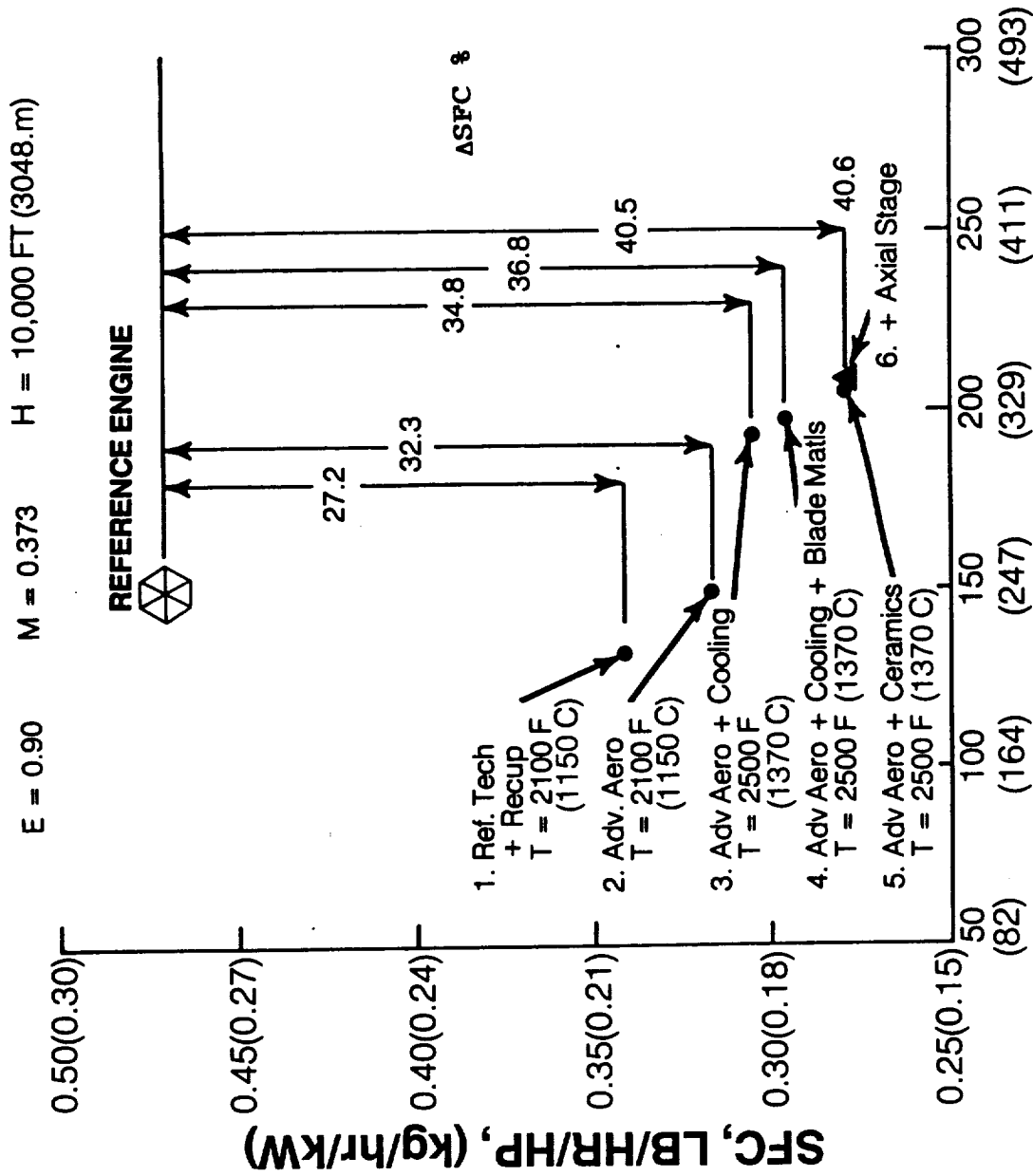
Figure 49. Summary of Engine Performance Gains, ε = 0.90

BT1285A

117

DESIGN POINT:

M = 0.373, H = 10000 FT (3048 m), SHP = 620 HP (462 kW)

MINIMUM SFC VS EFFECTIVENESS
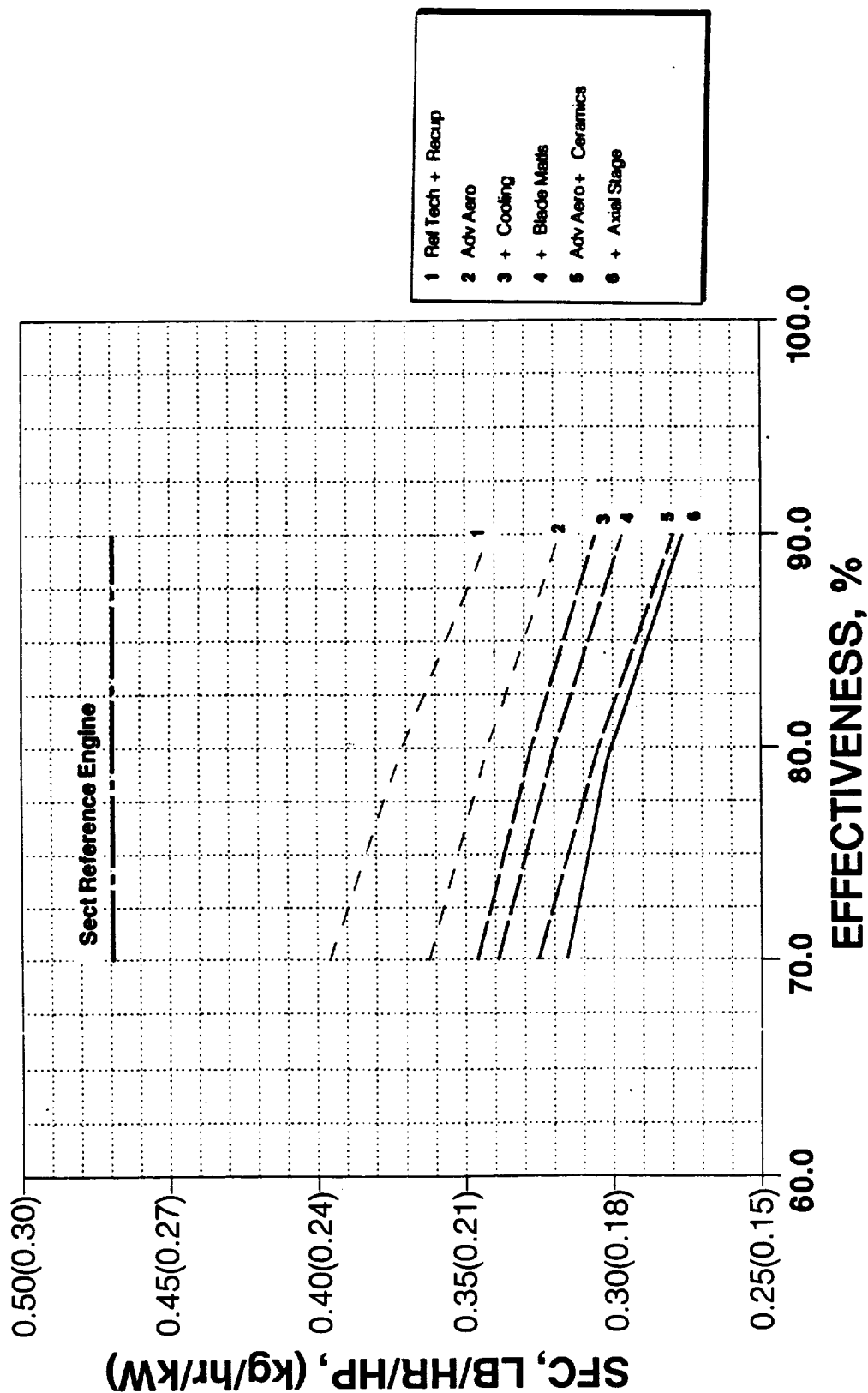
Figure 50.   Design Point Minimum SFC

DESIGN POINT:

M = 0.373, H = 10000 FT (3048 m), SHP = 620 HP (462 kW)

PRESSURE RATIO FOR MIN SFC

1	Ref Tech + Recup
2	Adv Aero
3	+ Cooling
4	+ Blade Matls
5	Adv Aero+ Ceramics

PRESSURE RATIO

Sect Reference Engine

EFFECTIVENESS, %
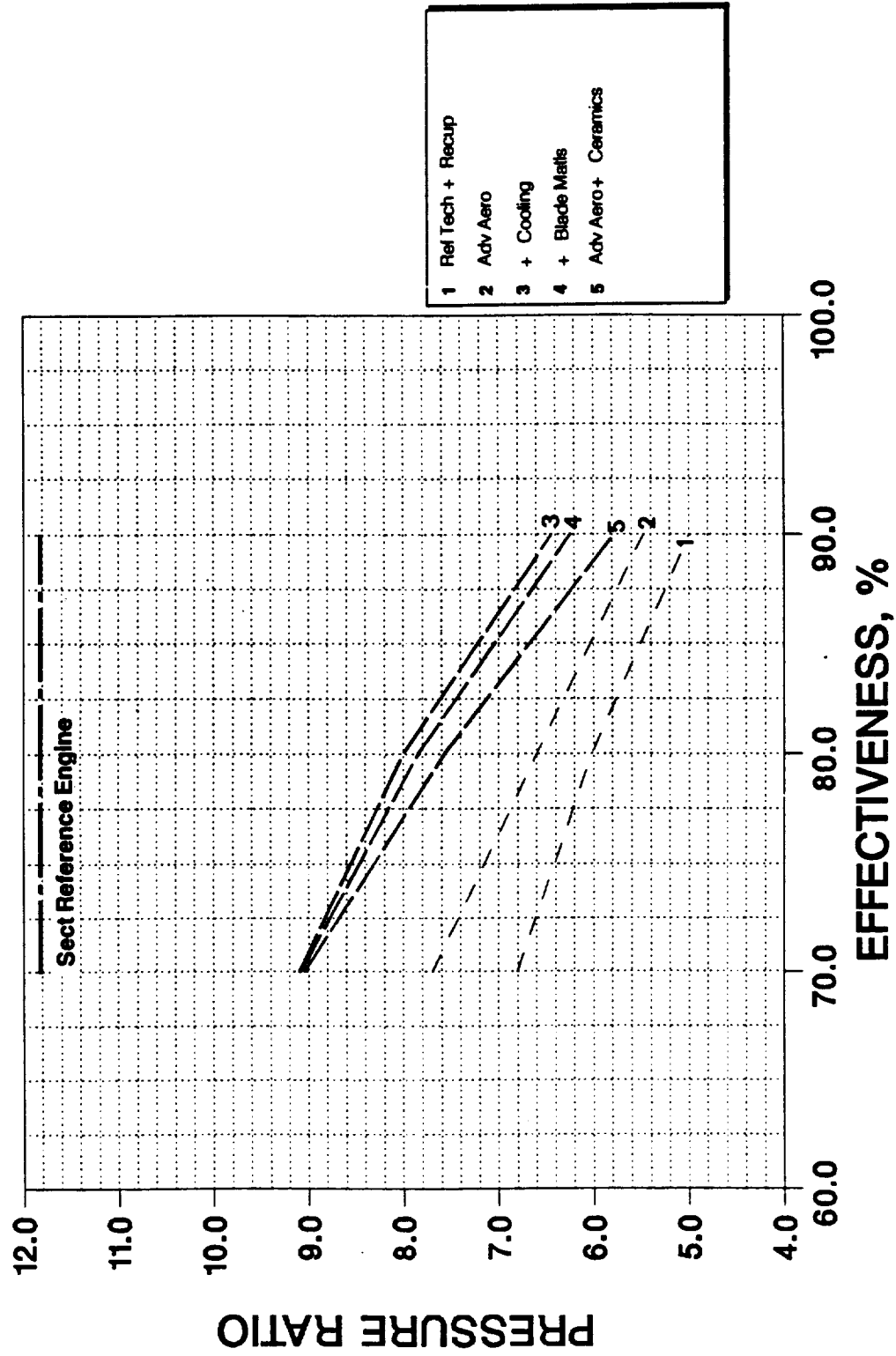
Figure 51. Design Point Pressure Ratio

DESIGN POINT:

M = 0.373, H = 10000 FT (3048 m), SHP = 620 HP (462 kW)

ROTOR COOLING FLOW RATE AT MIN SFC

Legend:
1 Ref Tech + Recup
2 Adv Aero
3 + Cooling
4 + Blade Matls
5 Adv Aero+ Ceramics
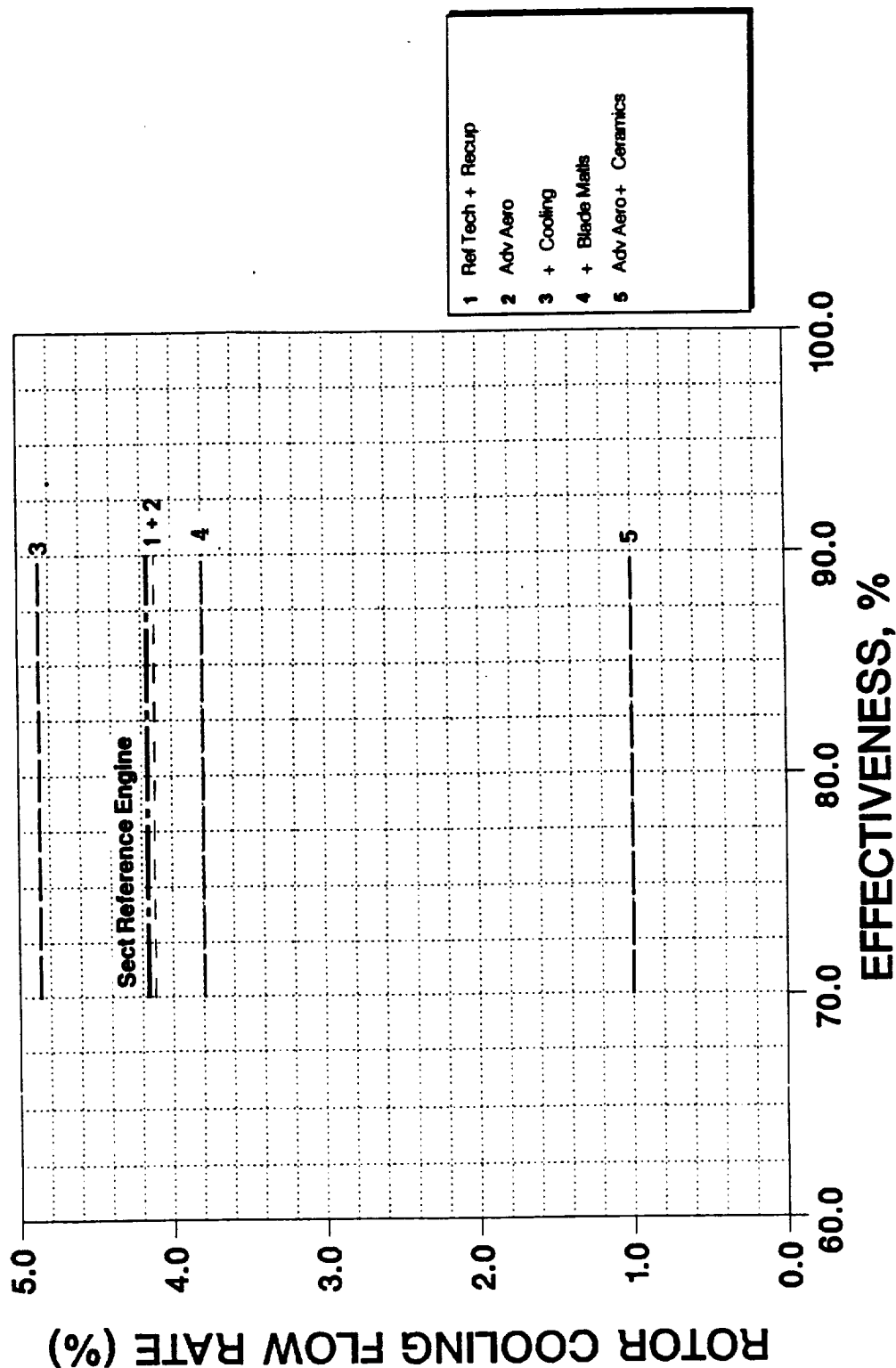
Figure 52.   Design Point Rotor Cooling Flow Rate

120

Figure 53.   Take-Off Rating Shaft Power

121

Figure 54. Take-Off Rating Cycle Pressure Ratio

Figure 55. Take-Off Rating Air Flow Rate

ENGINE PERFORMANCE AT T.O. RATING
UN-INSTALLED: SEA LEVEL/STATIC, STANDARD DAY
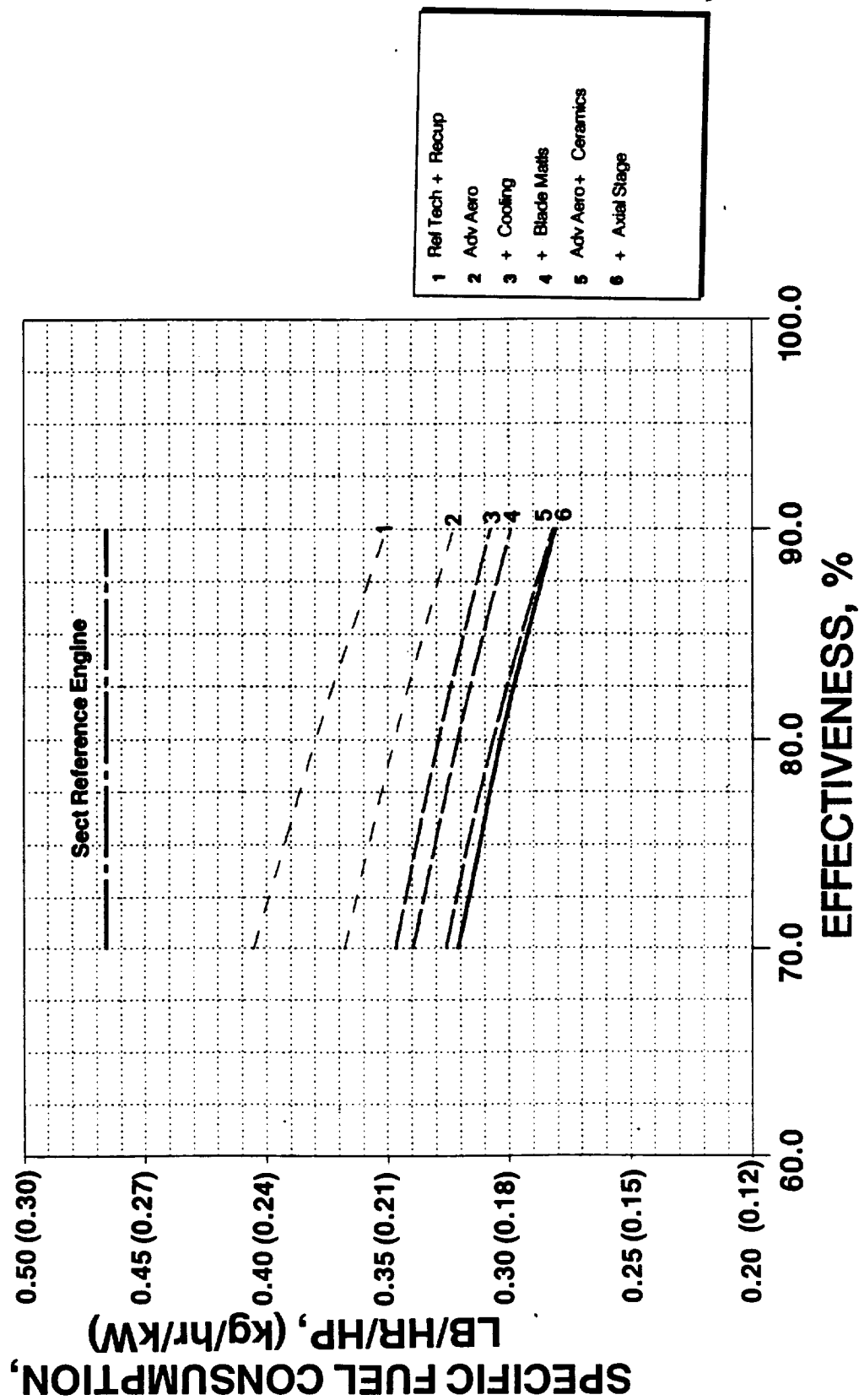
Figure 56.   Take-Off Rating Specific Fuel Consumption

124
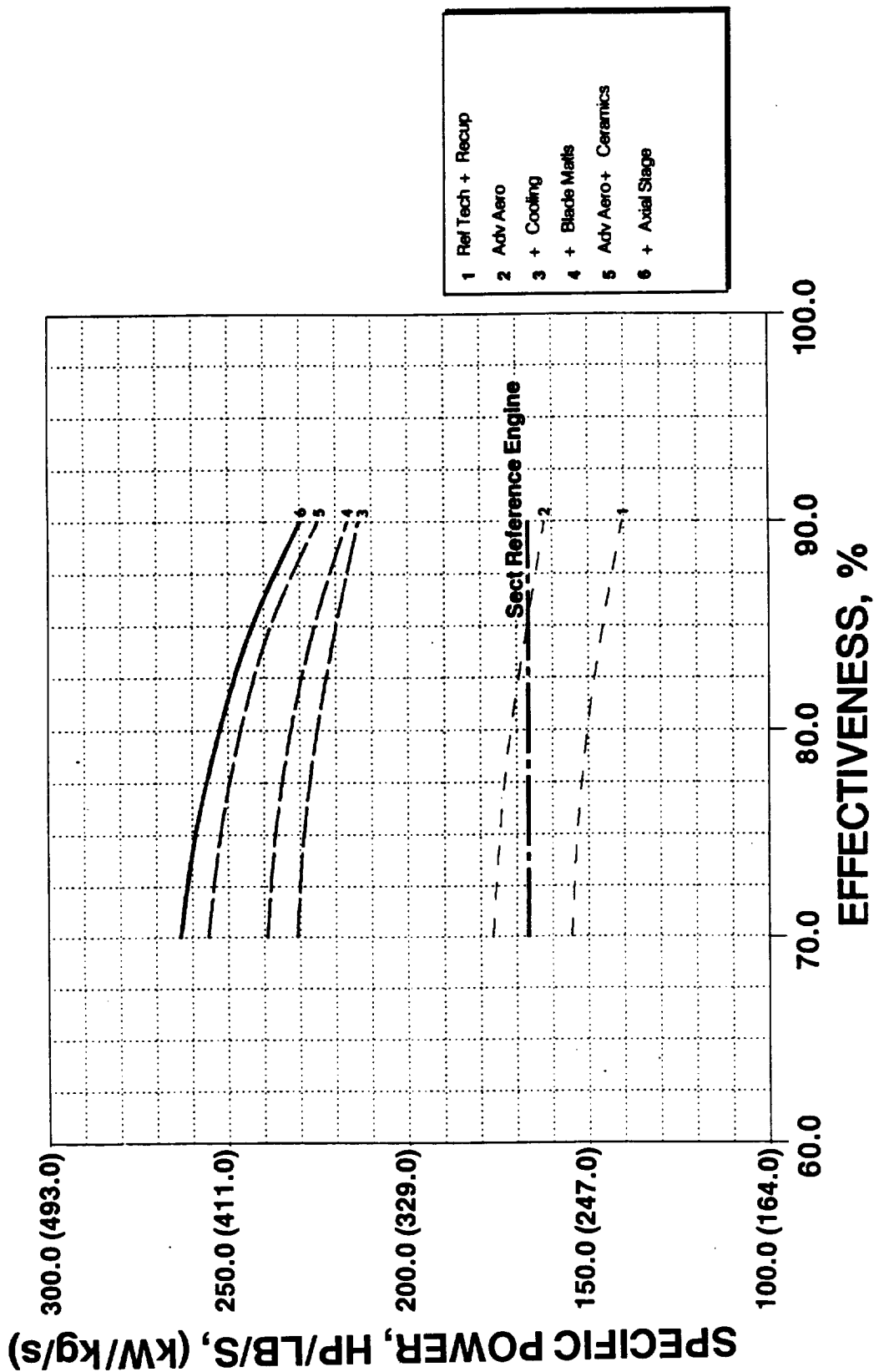
Figure 57.   Take-Off Rating Specific Power
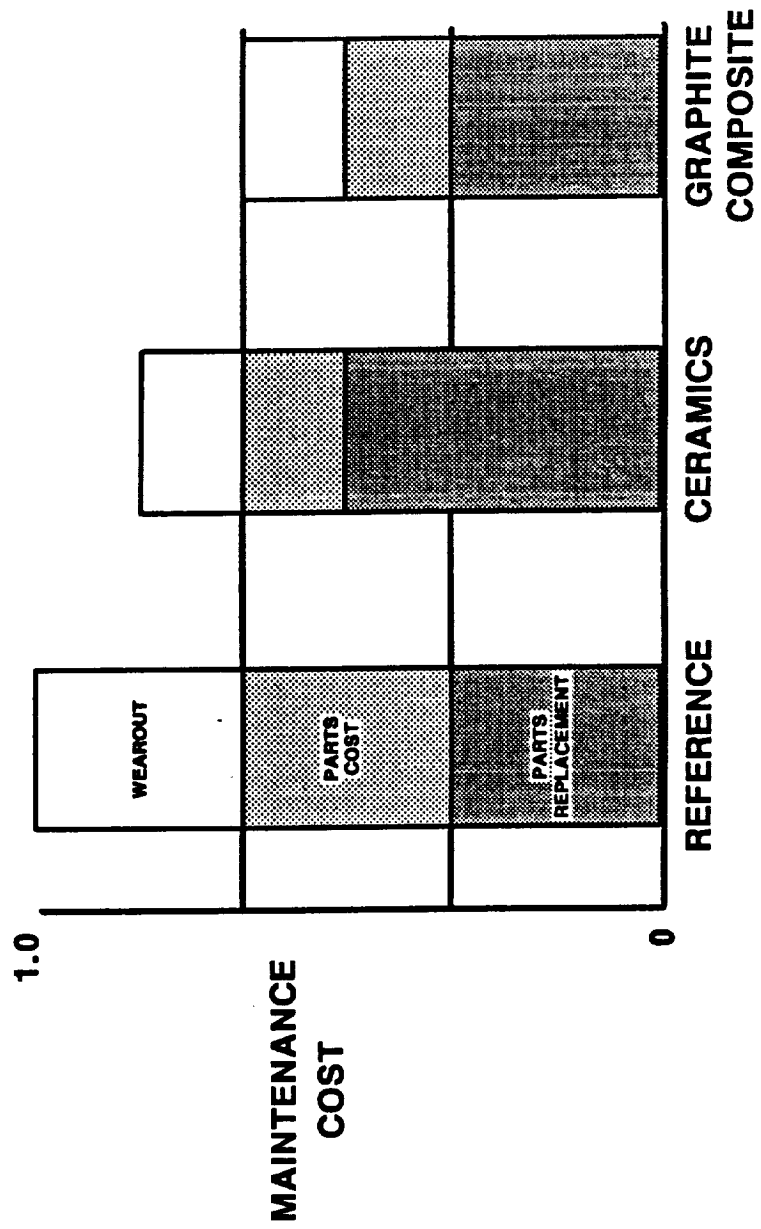
Figure 58. Materials Maintenance Impact

ENGINE SENSITIVITY TO RECUPERATOR EFFECTIVENESS
SINGLE-PASS HEAT EXCHANGER

1	Ref Tech + Recup
2	Adv Aero
3	+ Cooling
4	+ Blade Matls
5	Adv Aero + Ceramics
6	+ Axial Stage
7	+ Ceramic Recup
8	+ (PT/Case)
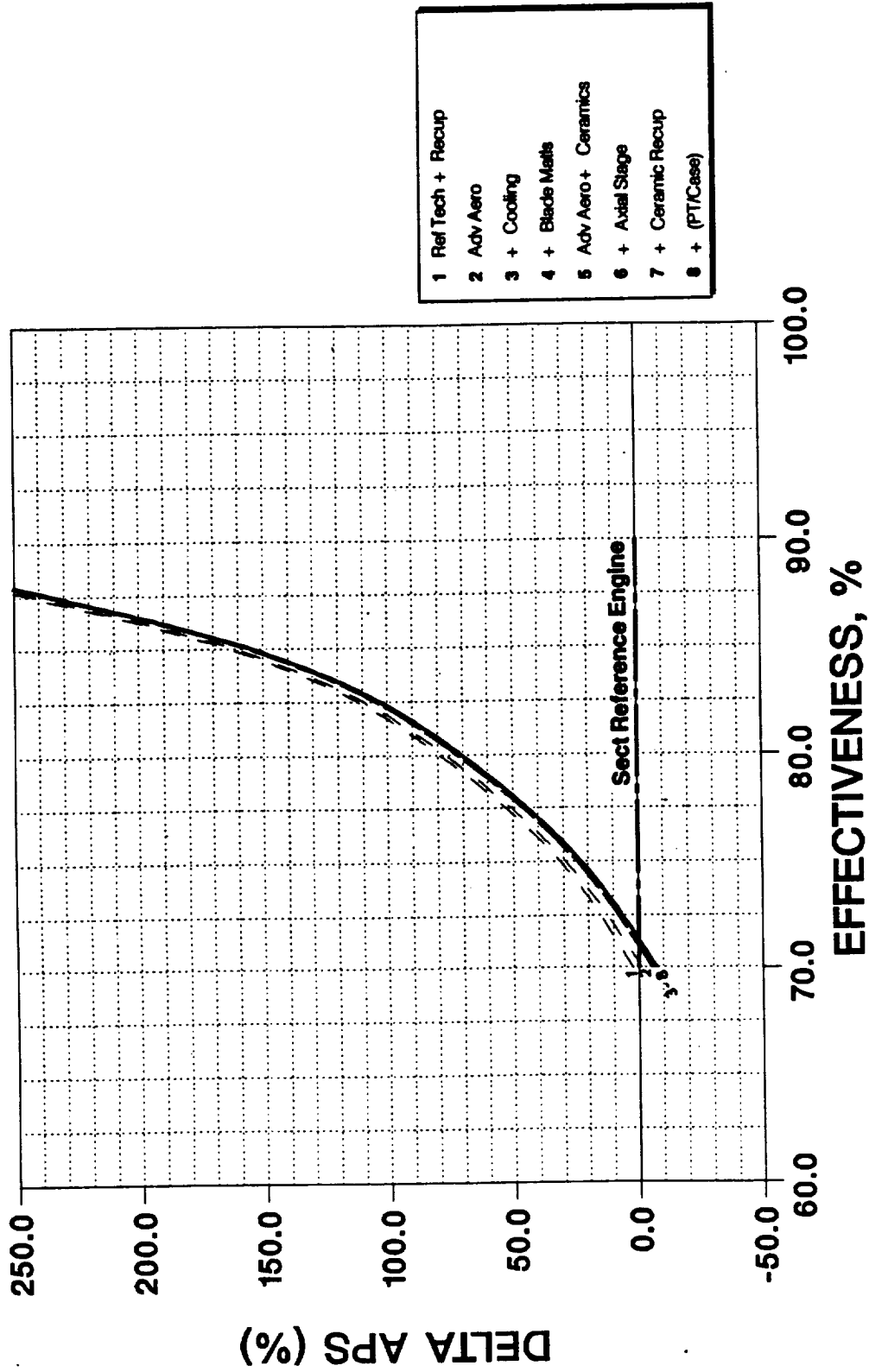
Figure 59. Propulsion System Δ Area, Single-Pass Recuperator
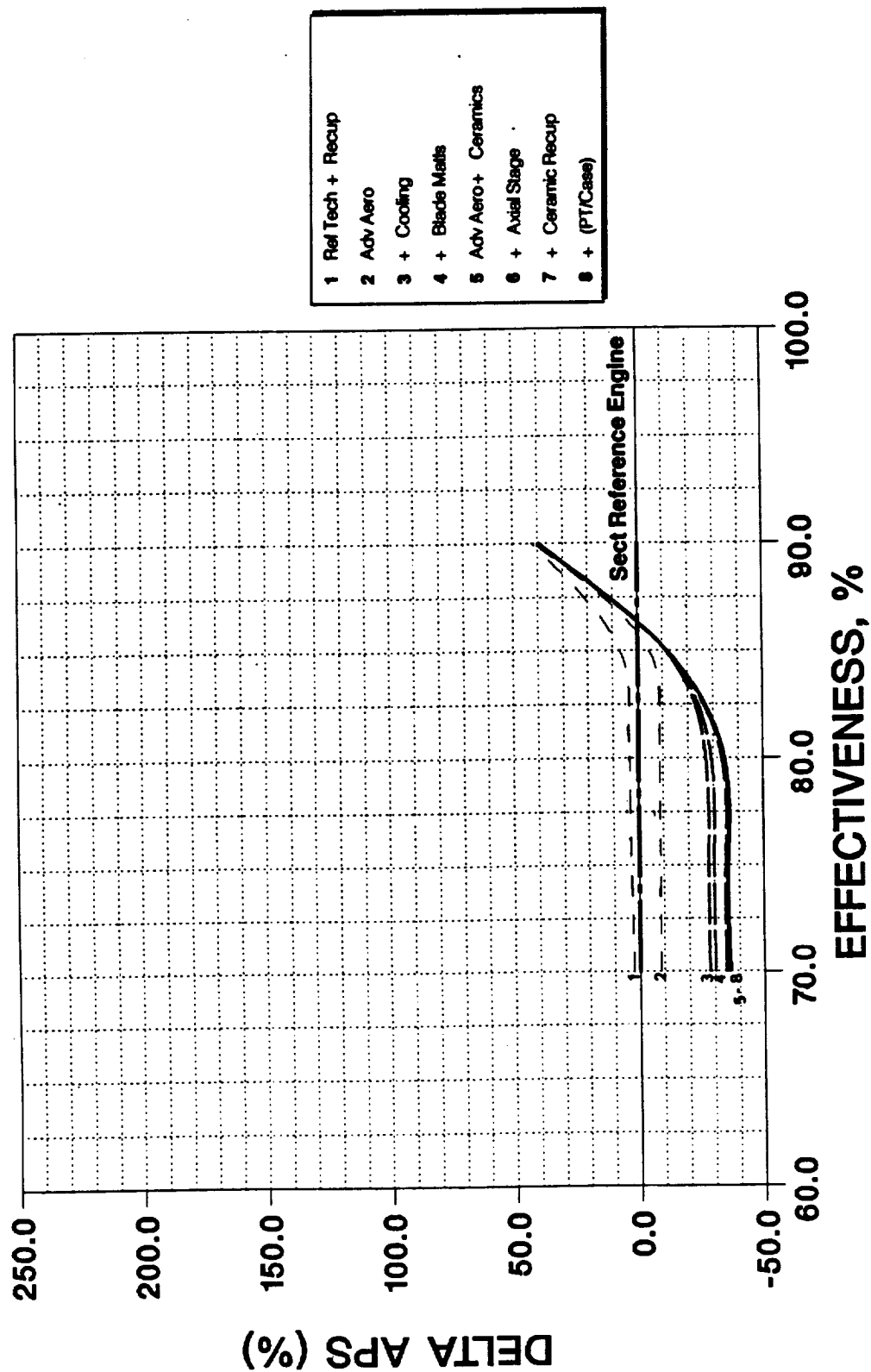
Figure 60. Propulsion System Δ Area, Two-Pass Recuperator
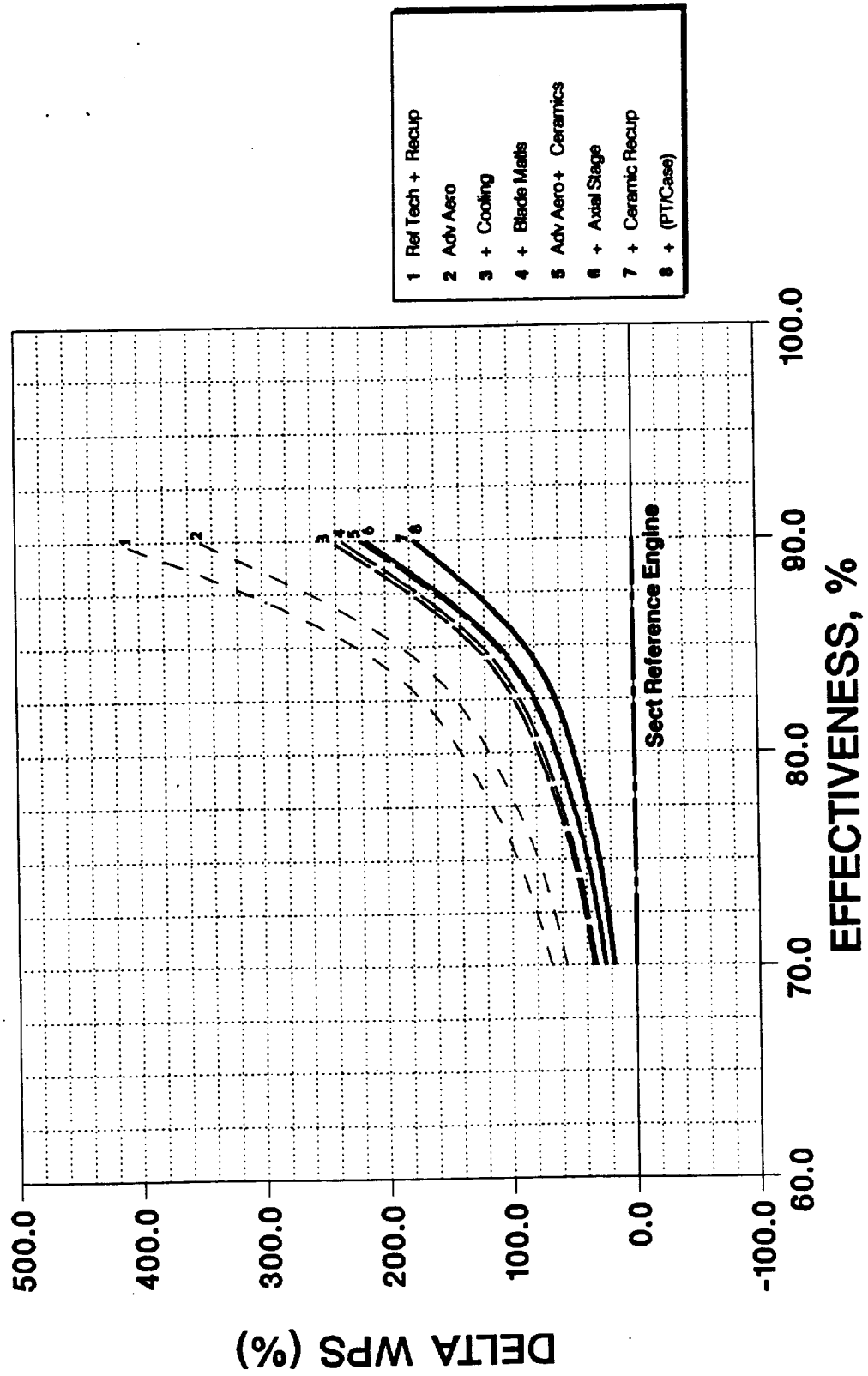
Figure 61. Propulsion System Δ Weight

ENGINE SENSITIVITY TO RECUPERATOR EFFECTIVENESS
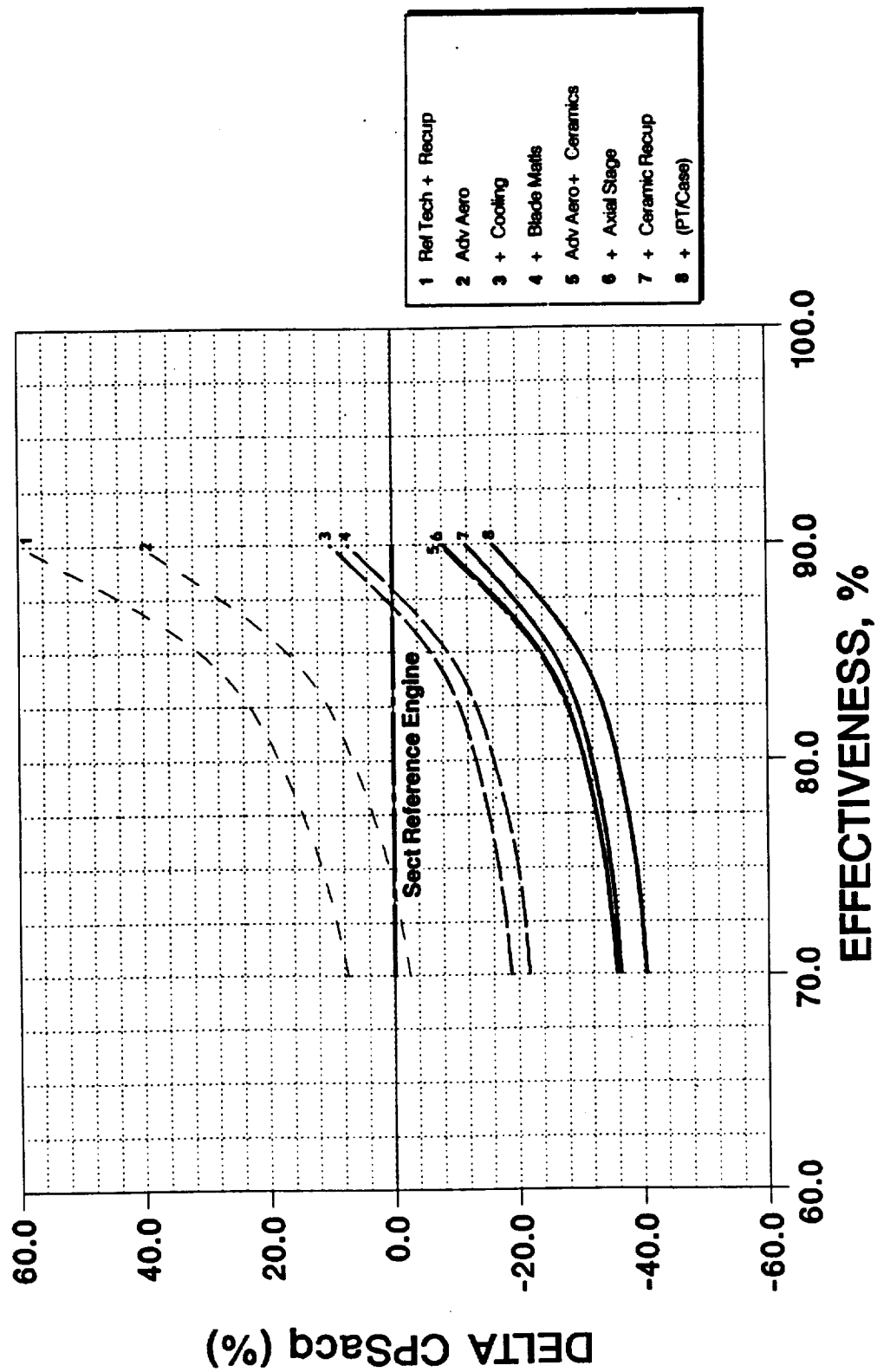
Figure 62. Propulsion System Δ Acquisition Cost
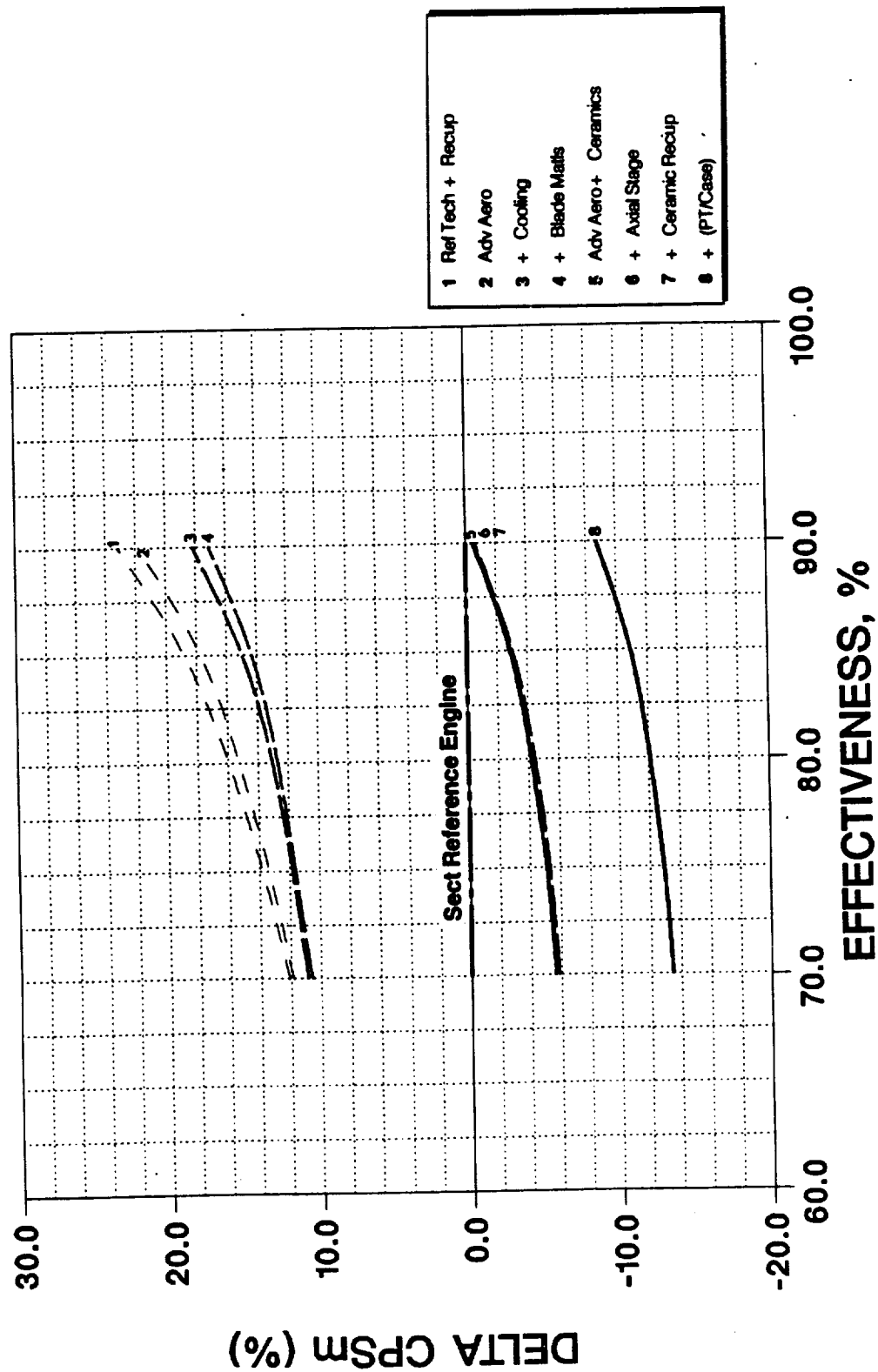
Figure 63.   Propulsion System ∆Maintenance Cost

A/C SENSITIVITY TO RECUPERATOR EFFECTIVENESS
TWO-PASS HEAT EXCHANGER

1	Ref Tech + Recup
2	Adv Aero
3	+ Cooling
4	+ Blade Matls
5	Adv Aero + Ceramics
6	+ Axial Stage
7	+ Ceramic Recup
8	+ (PT/Case)
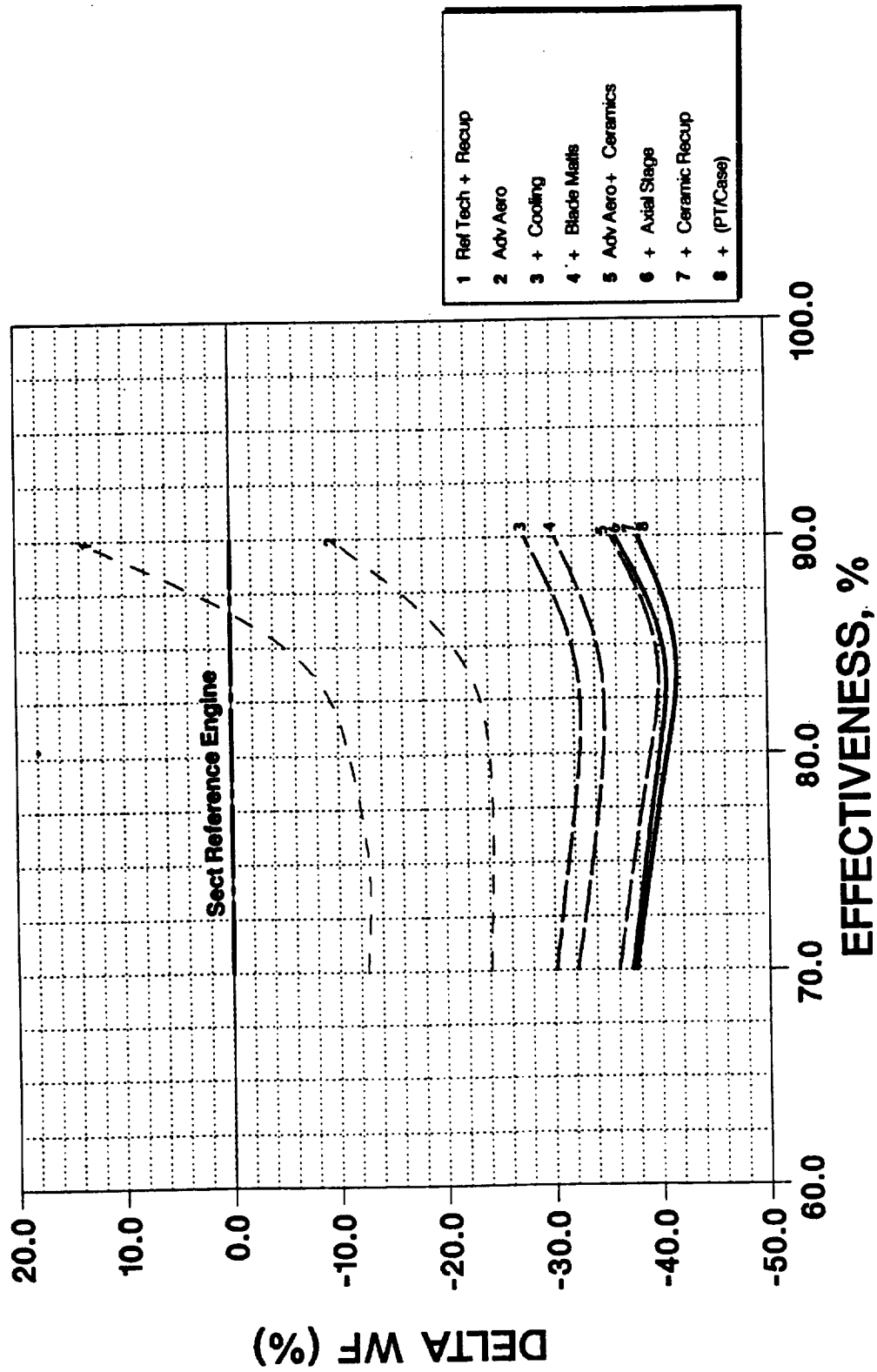
Figure 64. Aircraft Δ Fuel Burn
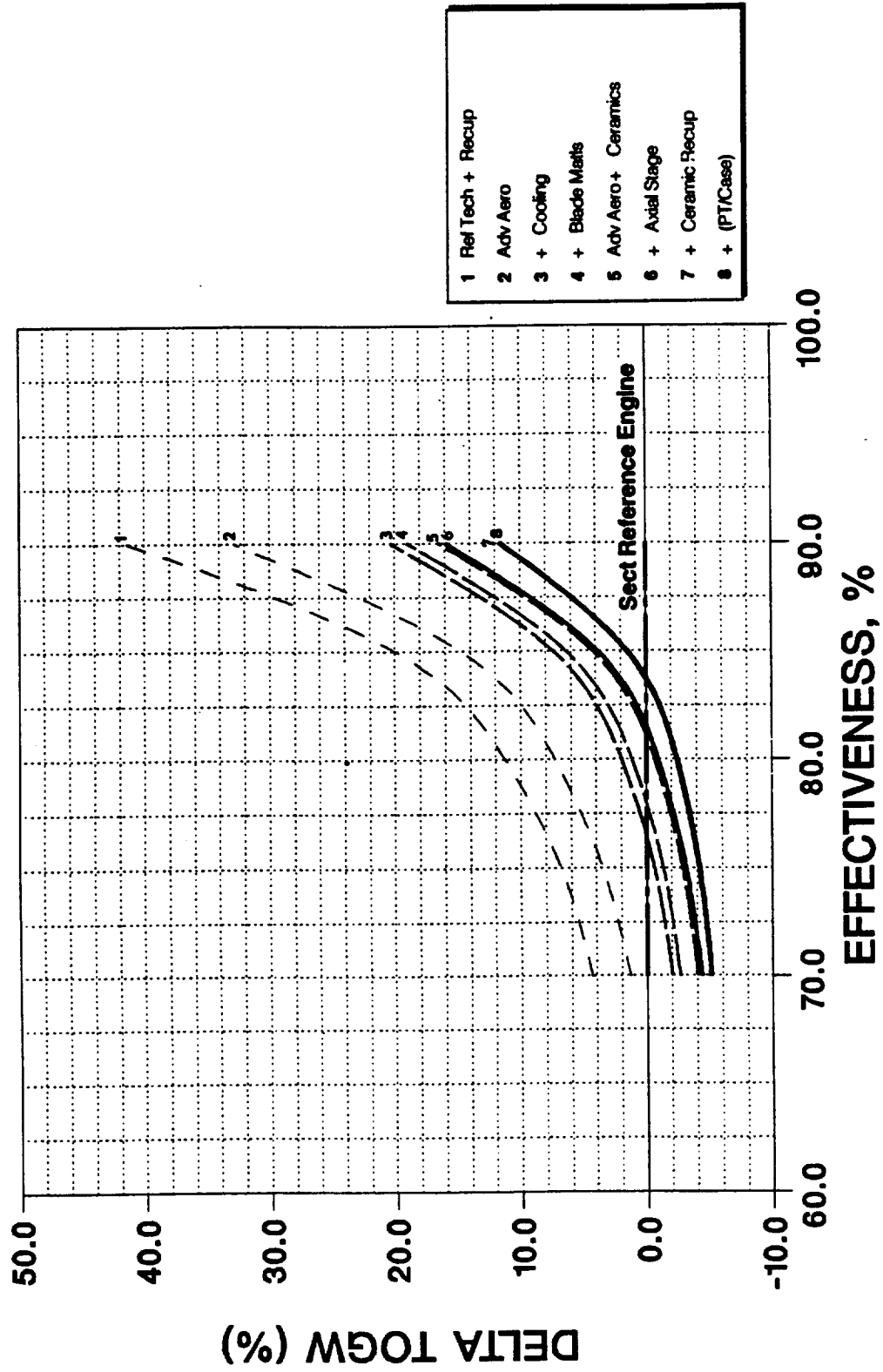
Figure 65. Aircraft Δ Take-Off Gross Weight

133
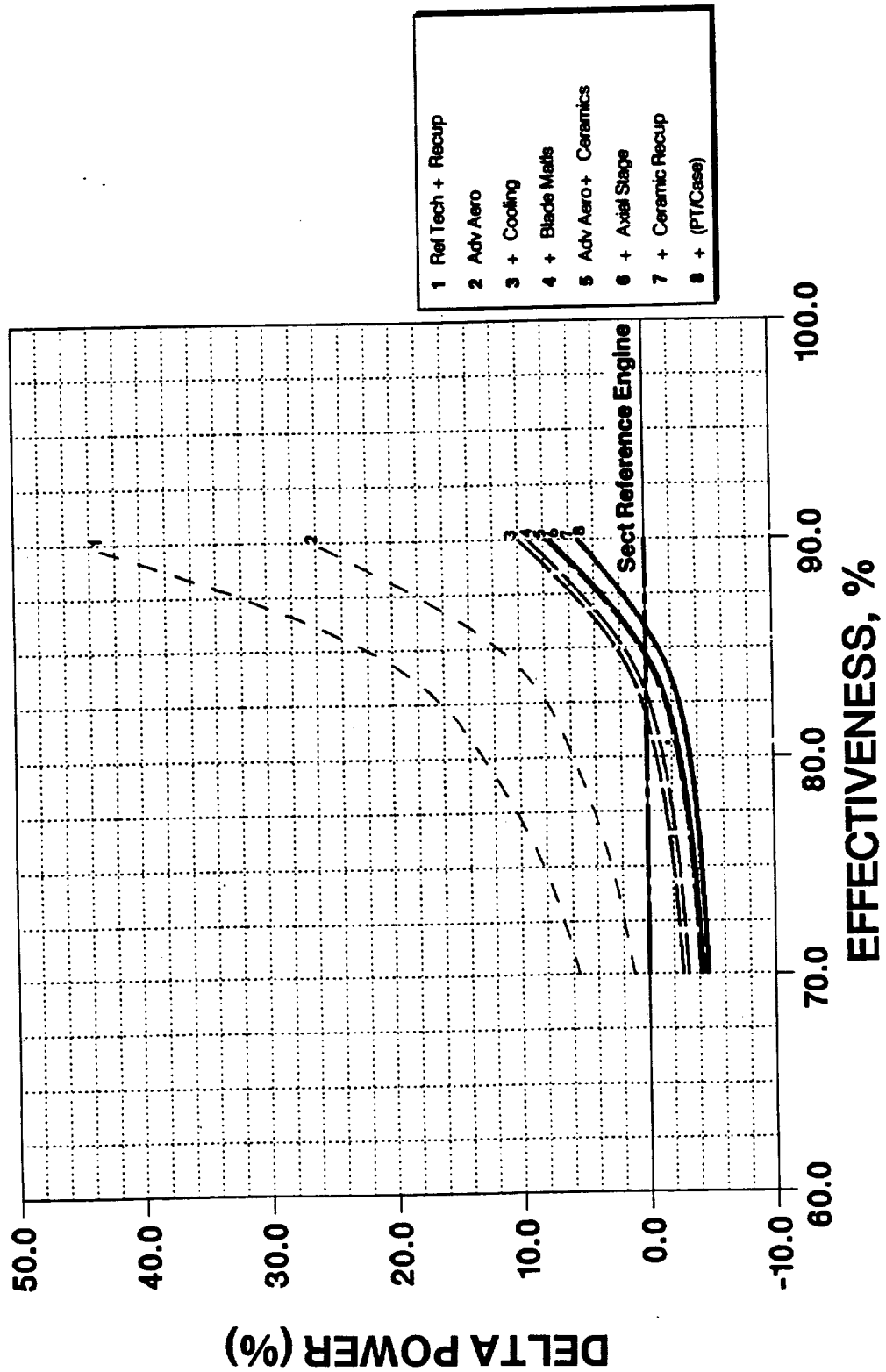
A/C SENSITIVITY TO RECUPERATOR EFFECTIVENESS
TWO-PASS HEAT EXCHANGER

Figure 66. Aircraft Δ Take-Off Power
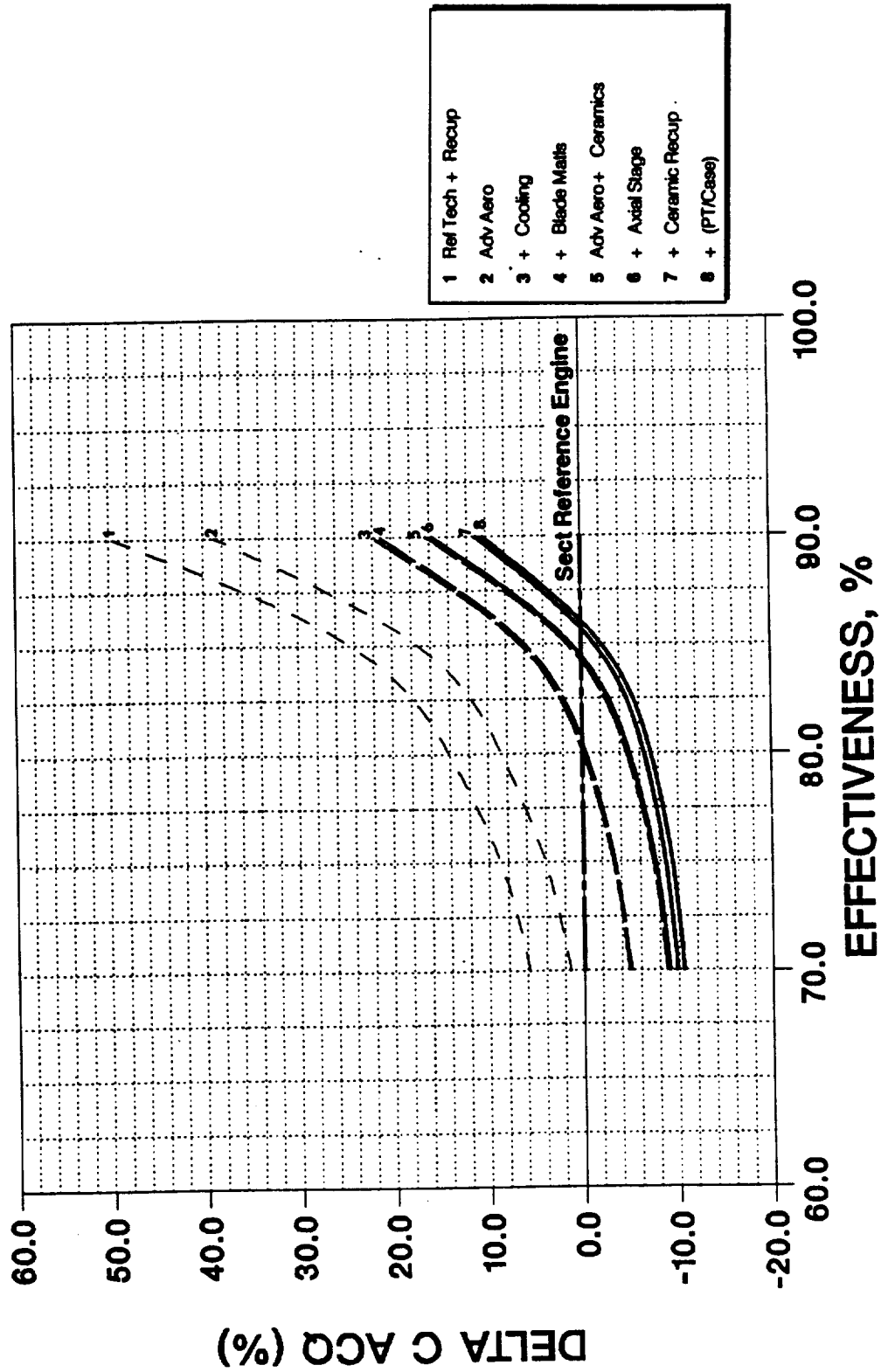
Figure 67. Aircraft Δ Acquisition Cost

A/C SENSITIVITY TO RECUPERATOR EFFECTIVENESS
TWO-PASS HEAT EXCHANGER
1.00 $/GALLON

1	Ref Tech + Recup
2	Adv Aero
3	+ Cooling
4	+ Blade Matls
5	Adv Aero + Ceramics
6	+ Axial Stage
7	+ Ceramic Recup
8	+ (PT/Case)

Sect Reference Engine.

EFFECTIVENESS, %

DELTA DOC (%)
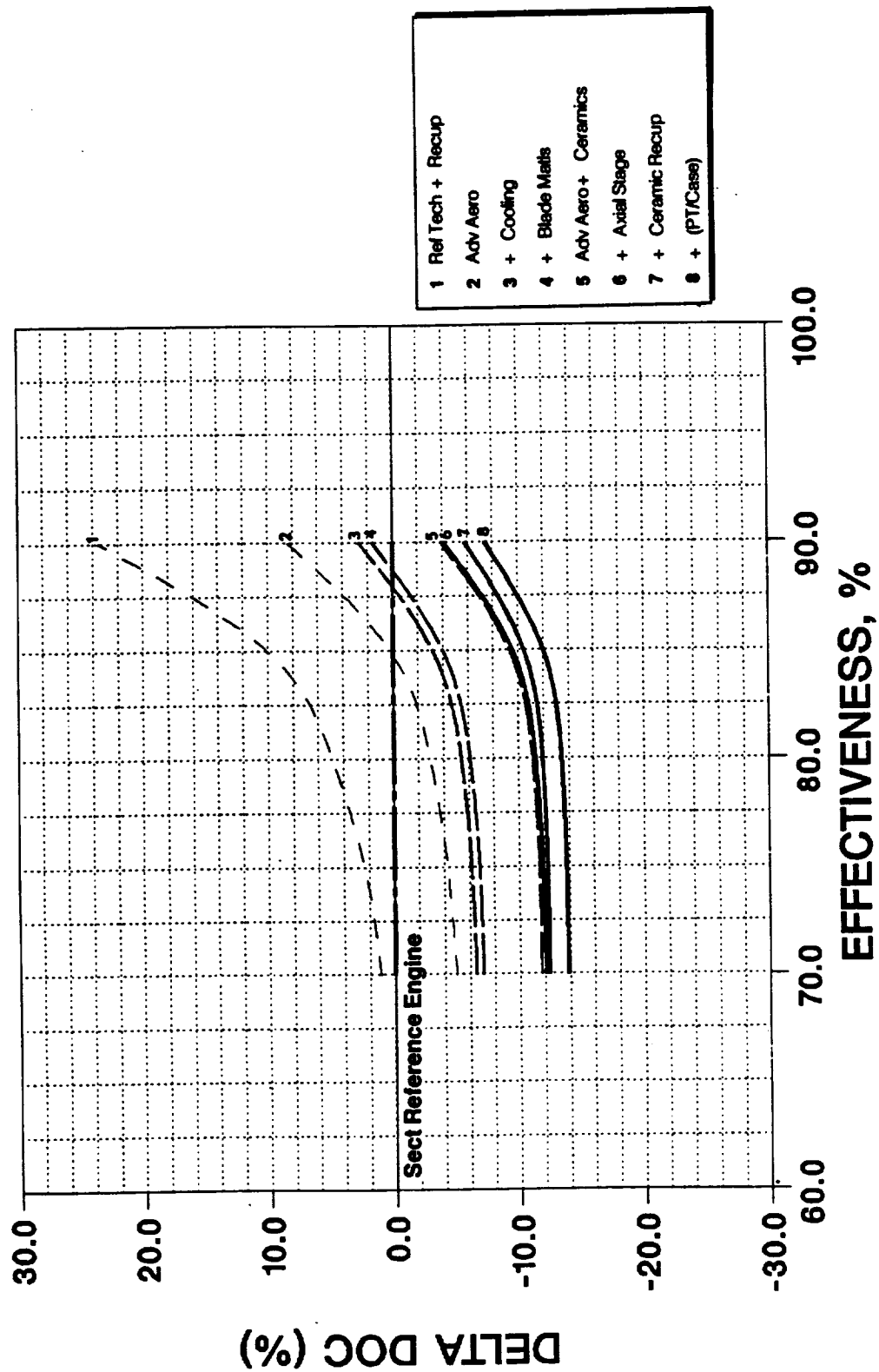
Figure 68. Aircraft Δ DOC, $1.00 Per Gallon Fuel Price

A/C SENSITIVITY TO RECUPERATOR EFFECTIVENESS
TWO-PASS HEAT EXCHANGER
2.00 $/GALLON

	Legend
1	Ref Tech + Recup
2	Adv Aero
3	+ Cooling
4	+ Blade Matls
5	Adv Aero + Ceramics
6	+ Axial Stage
7	+ Ceramic Recup
8	+ (PT/Case)
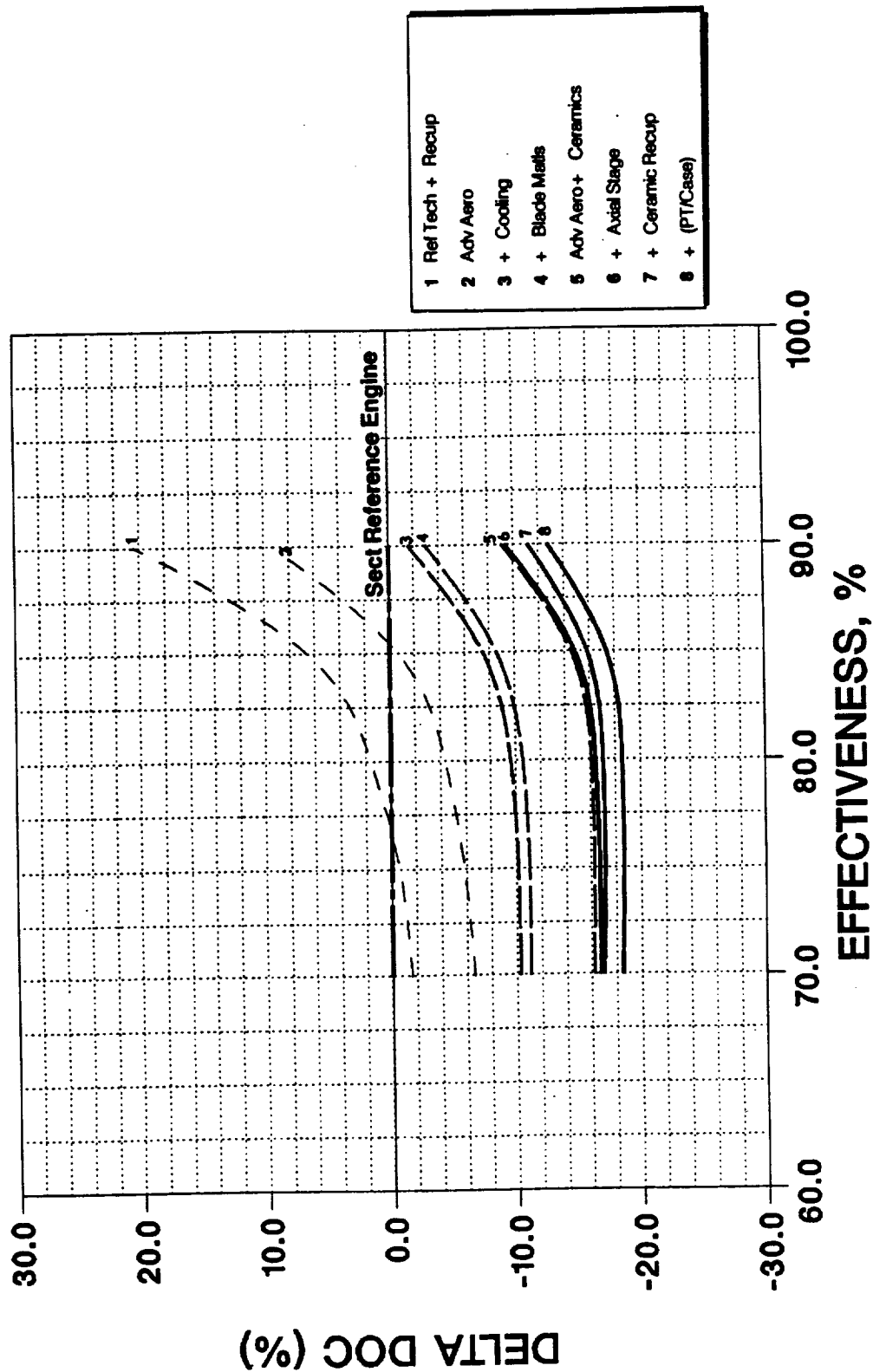
Figure 69. Aircraft ΔDOC, $2.00 Per Gallon Fuel Price

137

PD-2 PRELIMINARY DESIGN ENGINE
2-PASS ANNULAR RECUPERATOR
EFFECTIVENESS = 80%

$$\frac{Q}{Vol \times P} = 10^7 \text{ Btu/(hr} \times \text{ft}^3 \times \text{atm)}$$
$$= (3.67 \times 10^3 \text{ KJ/} (\text{hr} \times \text{m}^3 \times \text{Pa}))$$

TVR = 1.15

60.1 in. (1.53 m)

20.0 in. Dia. (0.51 m)

N_{GG} = 68,000 RPM

N_{PT} = 42,000 RPM

P_r = 1.7

P_r = 5.2

$M_{W_{t_i}}$ = 1.4

$M_{W_{t_i}}$ = 1.0

$\left[\dfrac{\Delta H}{U^2} \right]_H$ = 1.8

2.2

1.9

U_t = 2,160 Ft/s (658 m/s)
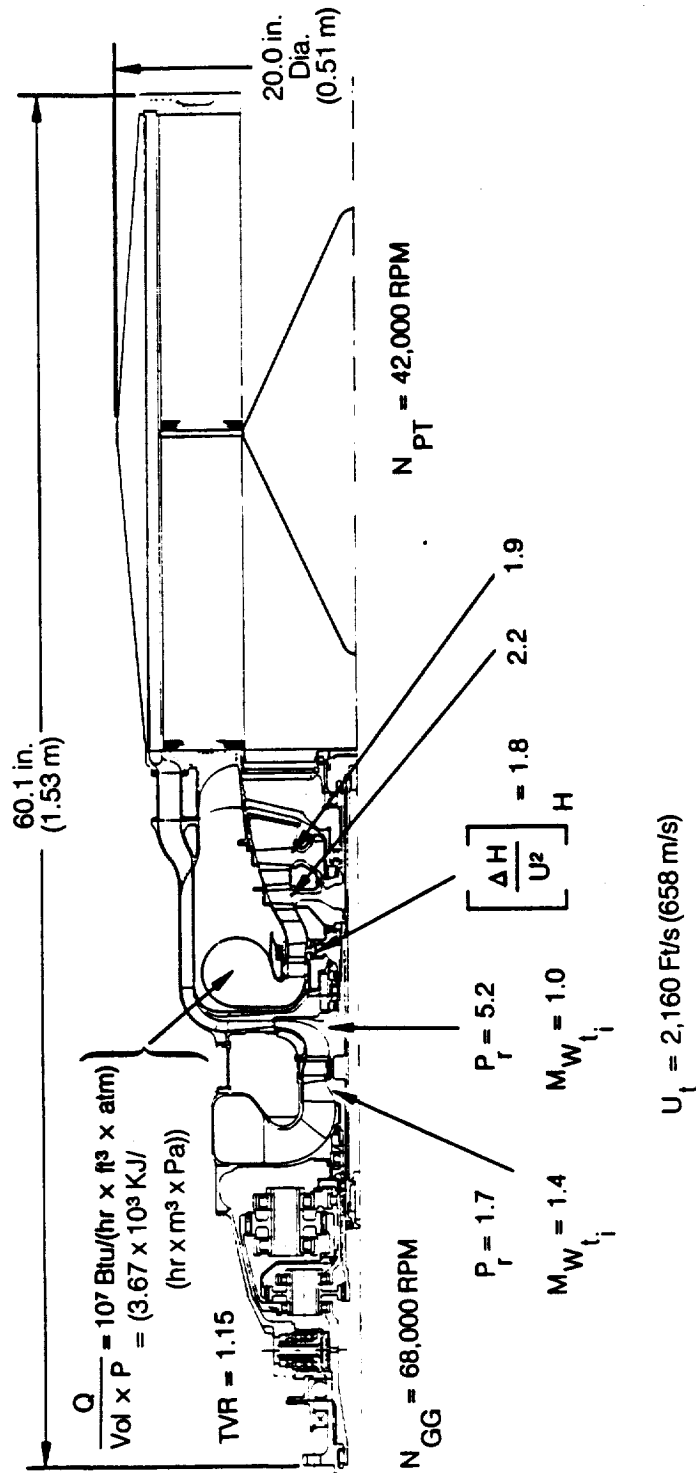
BT1245

Figure 70.   Preliminary Design Engine, PD-2

138

Figure 71. Technology Impact on Aircraft Fuel Burn
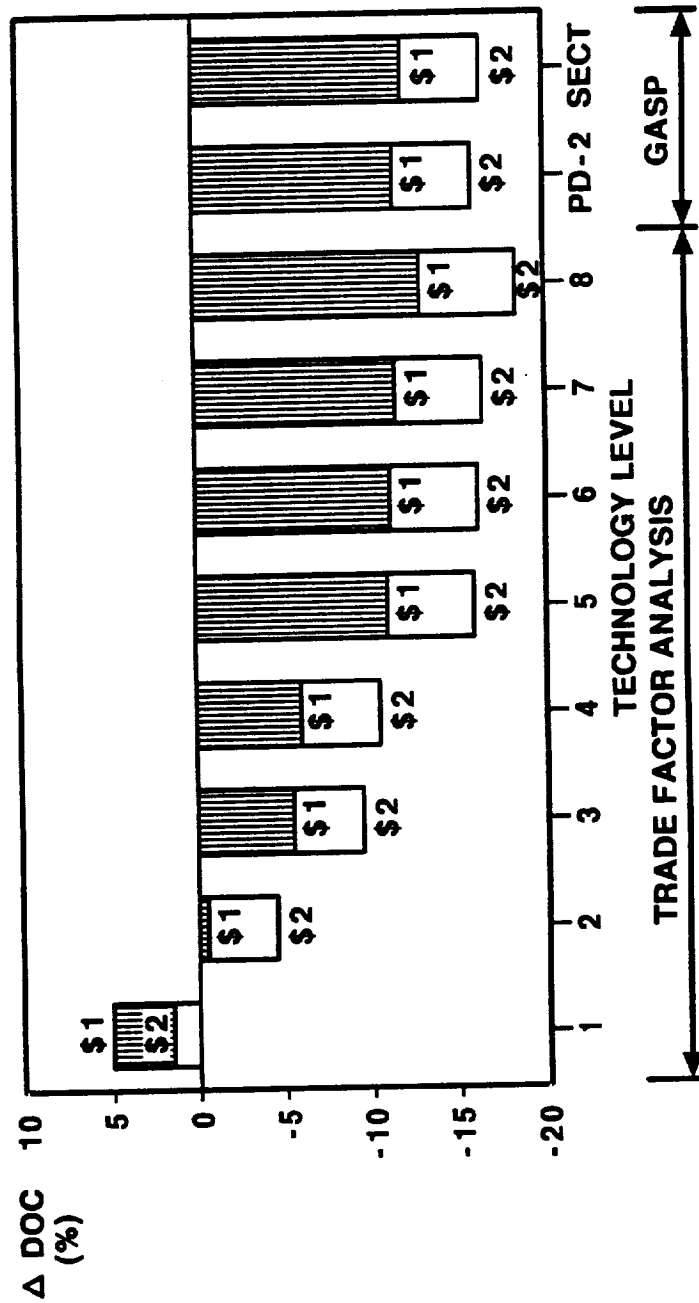
Figure 72. Technology Impact on Aircraft DOC

SECT REFERENCE AIRCRAFT

- 19 Passenger Pressurized

- Engines: Twin 950 hp (708 kw) Regenerative Turboprops

- Weight: 12,568 lb (5706 kg) TOGW
  11,454 lb (5200 kg) Zero-Fuel

- Wing Loading: 50.7 psf (2428 N/m²)
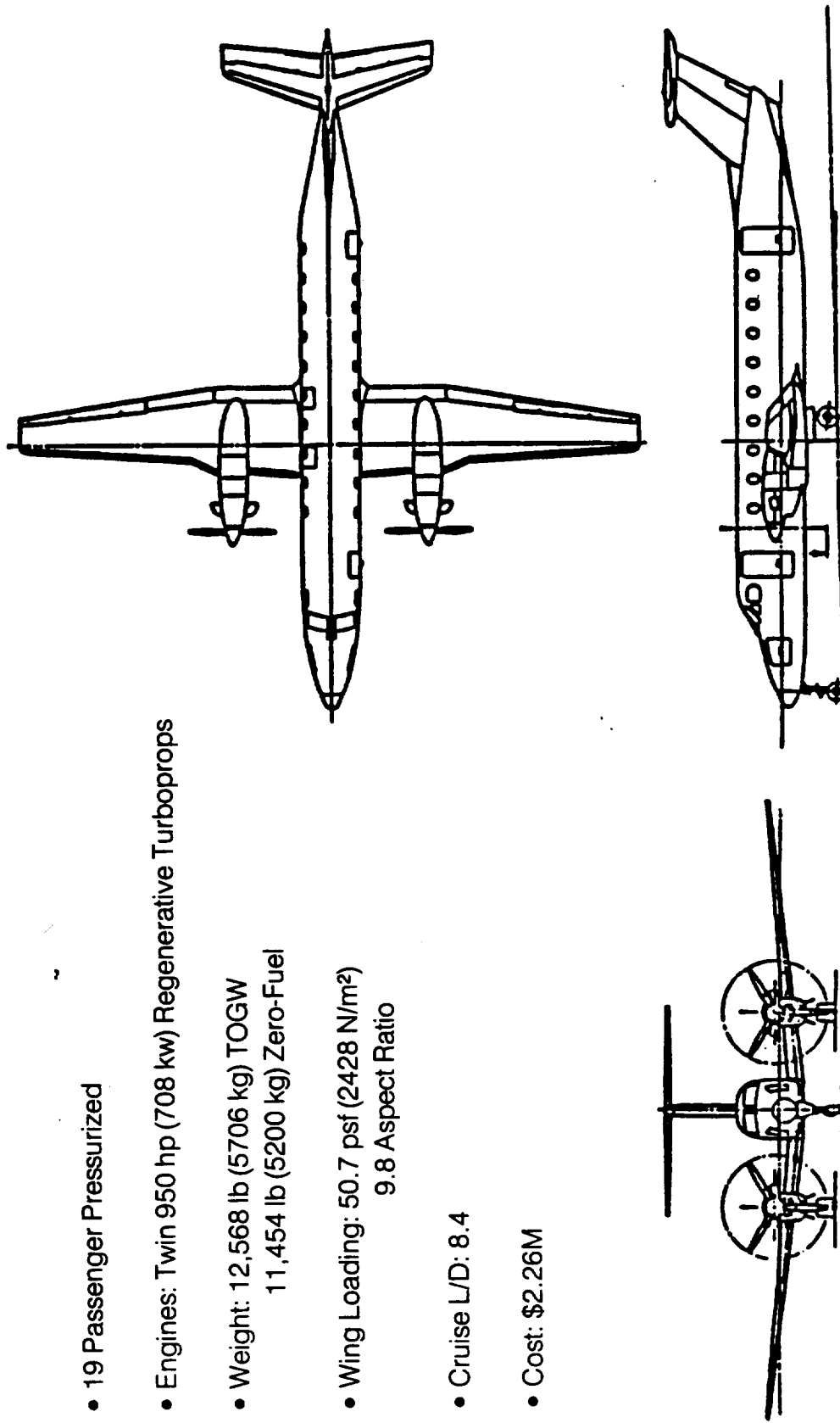 9.8 Aspect Ratio

- Cruise L/D: 8.4

- Cost: $2.26M

BT1273-2

Figure 73.   SECT Advanced Technology Aircraft

141
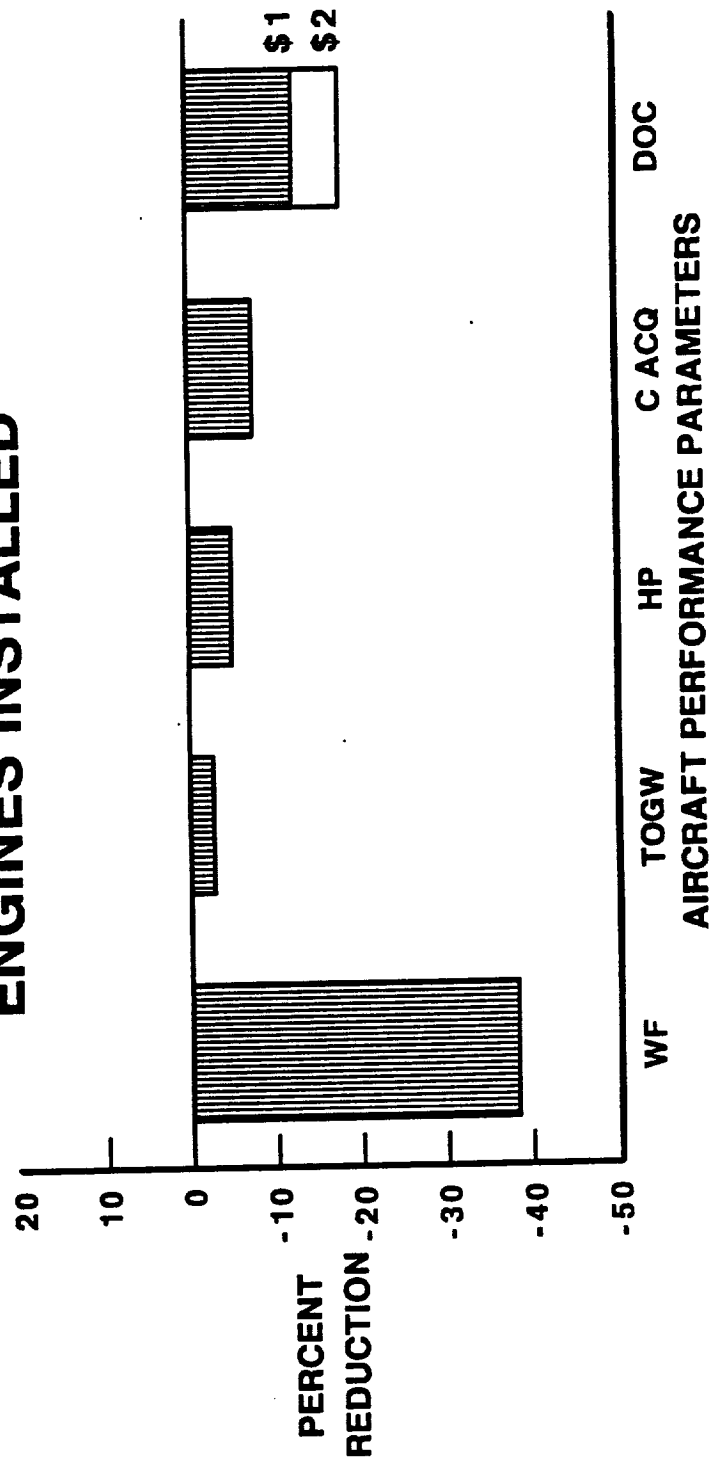
Figure 74. Advanced Technology Aircraft Performance Benefits

GASP SHORTHAUL METHOD
ECONOMIC MISSION
65% PAYLOAD
100 N.MI. (185 km) STAGE LENGTH

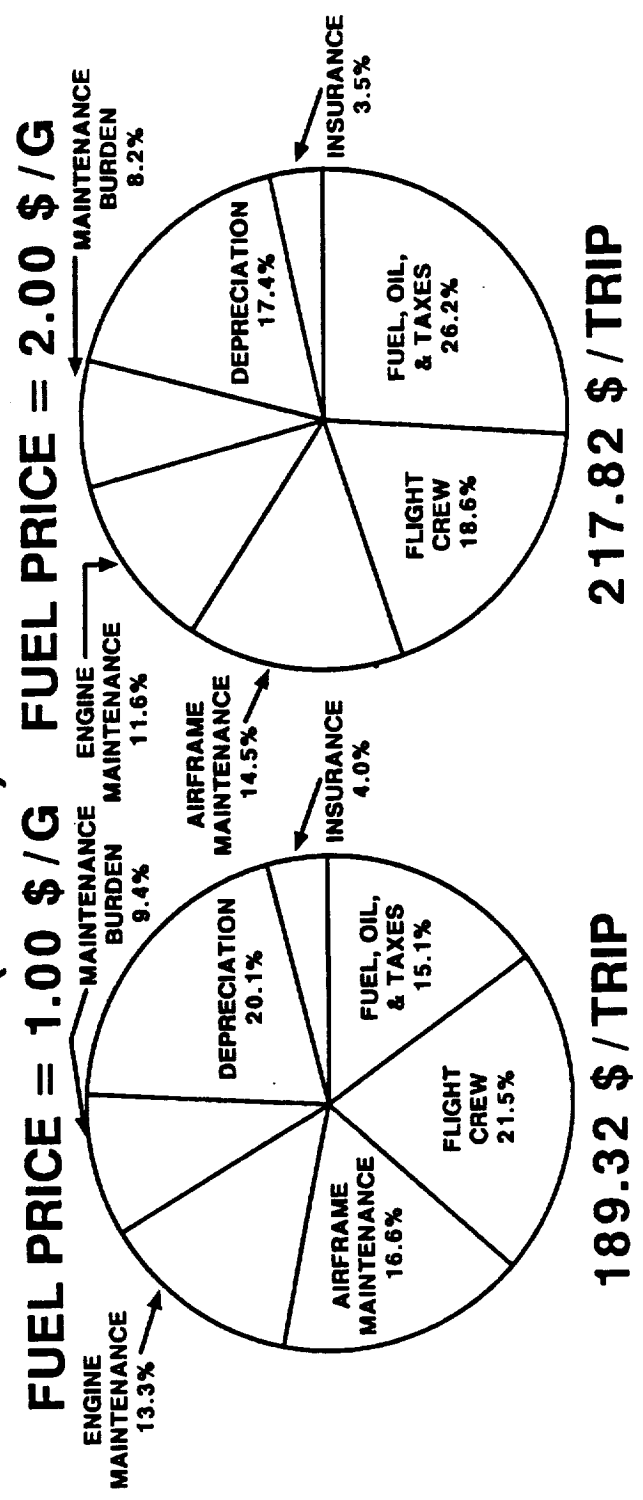FUEL PRICE = 1.00 $/G   FUEL PRICE = 2.00 $/G

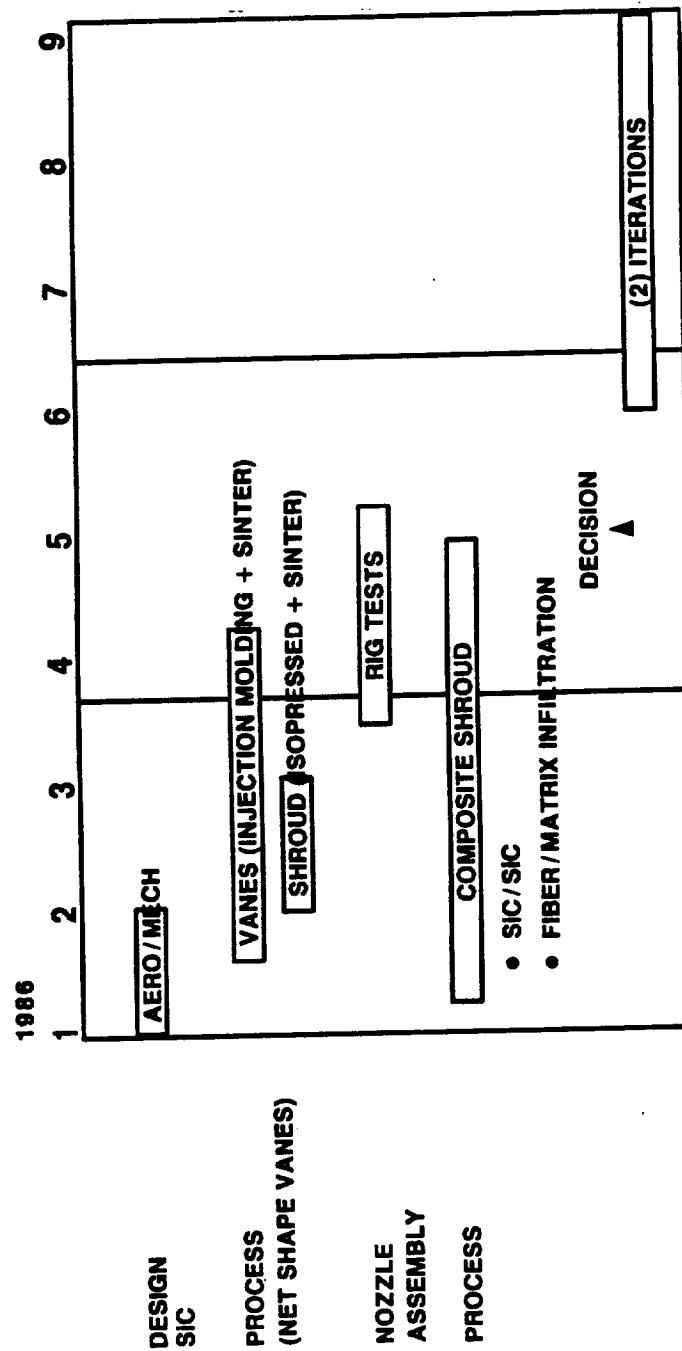189.32 $/TRIP

217.82 $/TRIP

Figure 75.   Advanced Technology Aircraft DOC Breakdown

143

Figure 76. Technology Schedule, Ceramic High Pressure Nozzle
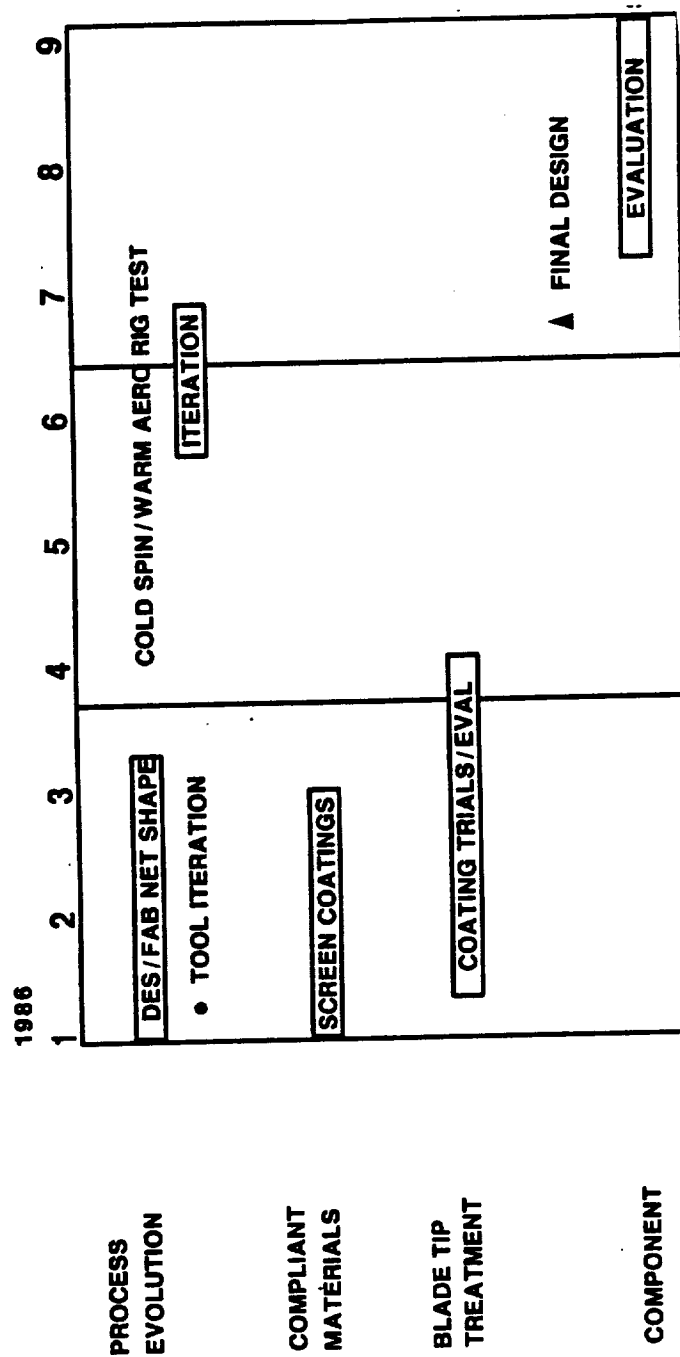
Figure 77. Technology Schedule, Ceramic High Pressure Turbine Blade

145
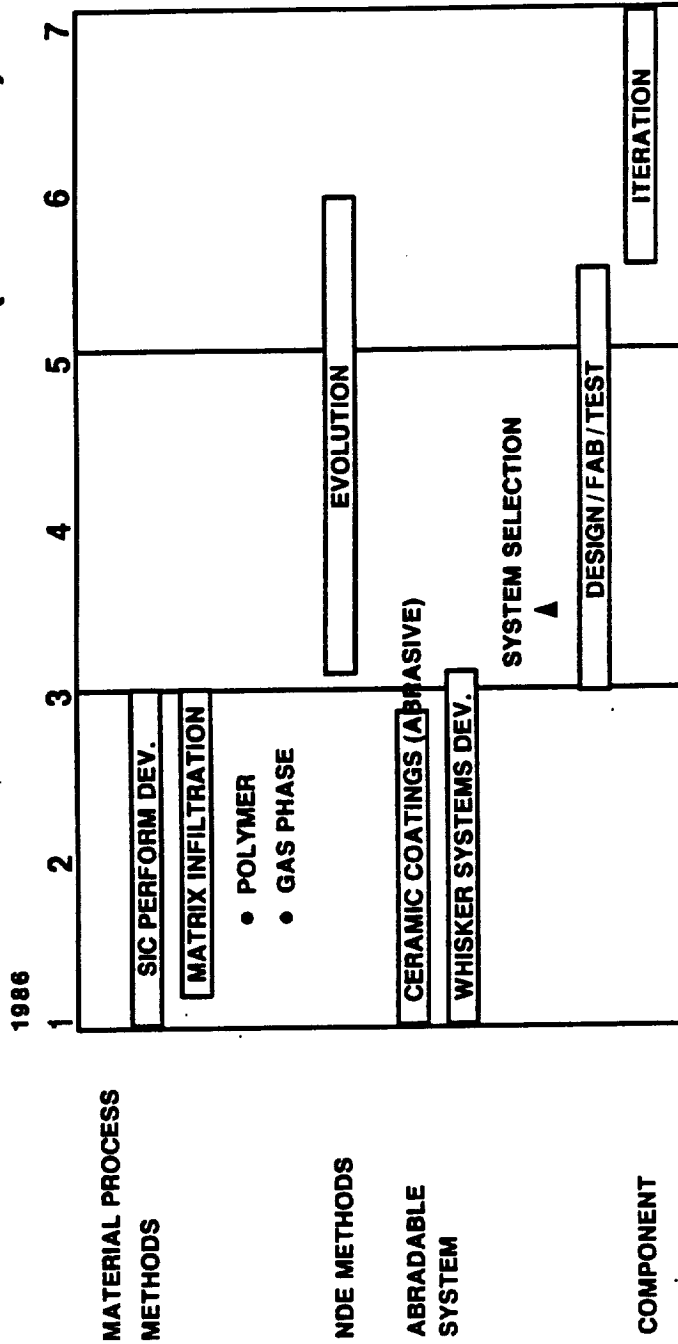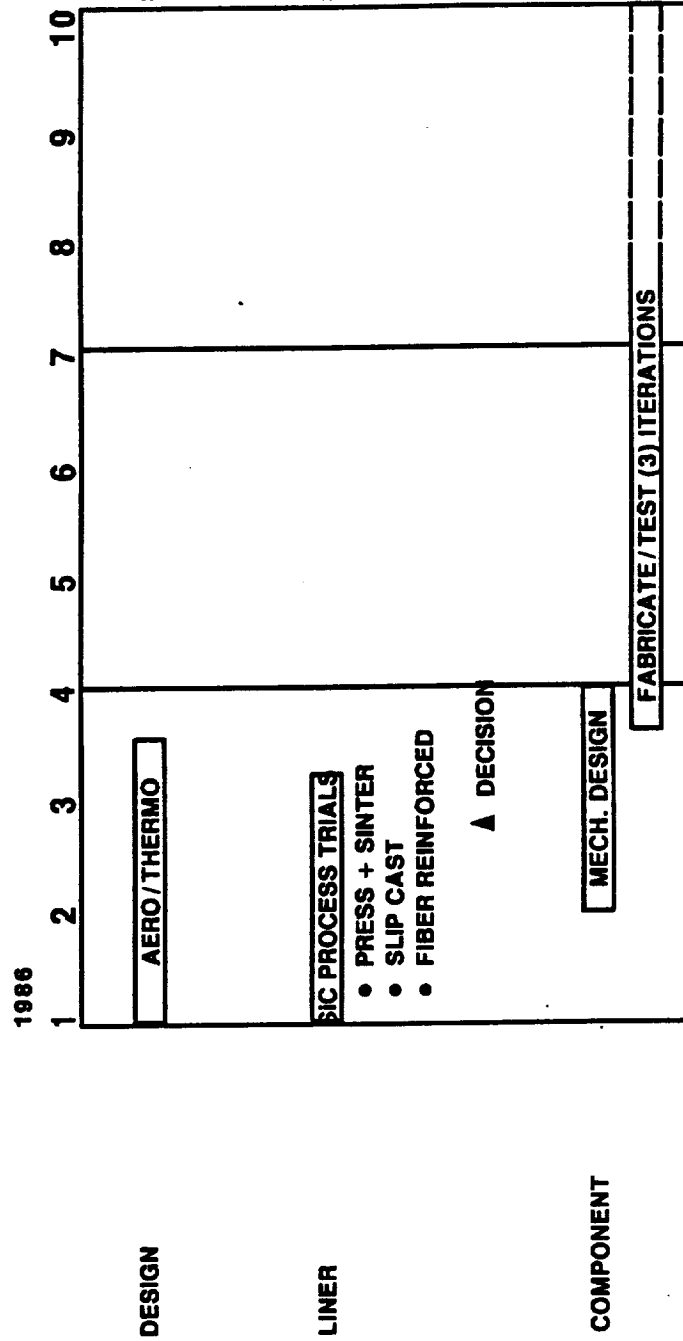
Figure 78. Technology Schedule, Ceramic Composite HP Turbine Tip Seal

146

Figure 79.   Technology Schedule, Ceramic Single Can Combustor
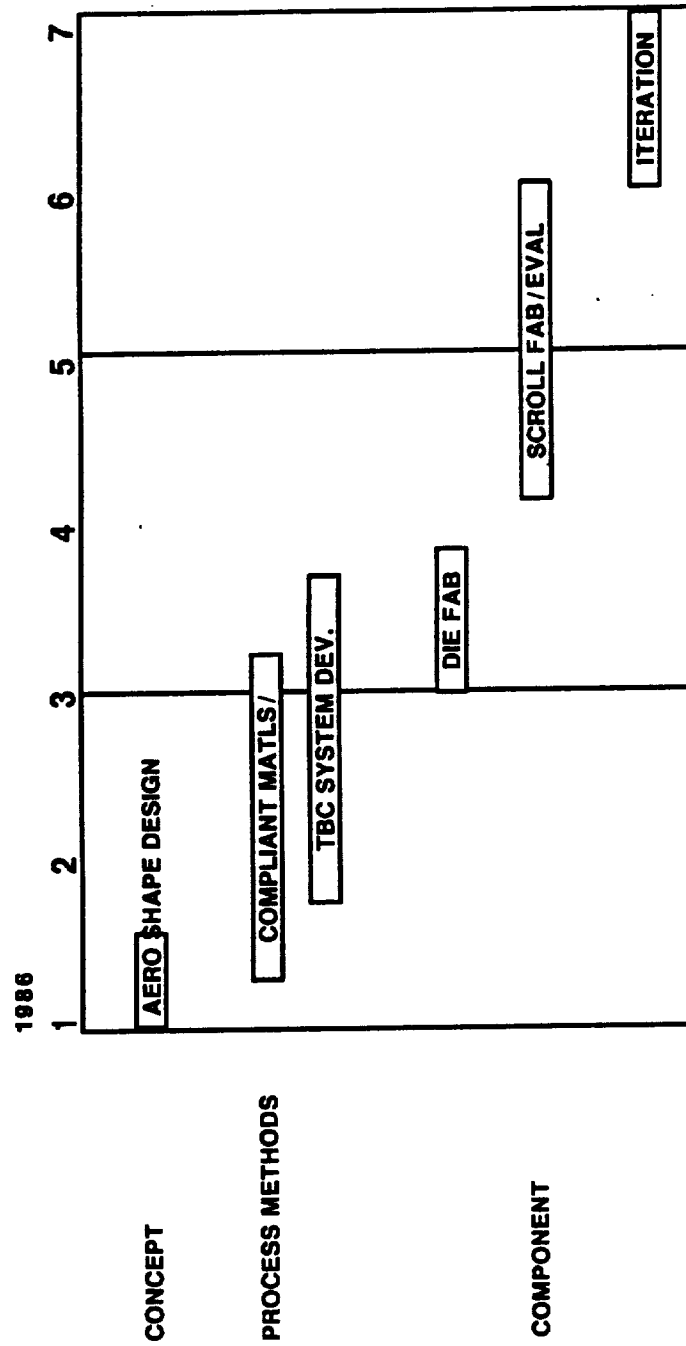
Figure 80. Technology Schedule, Combustor Scroll
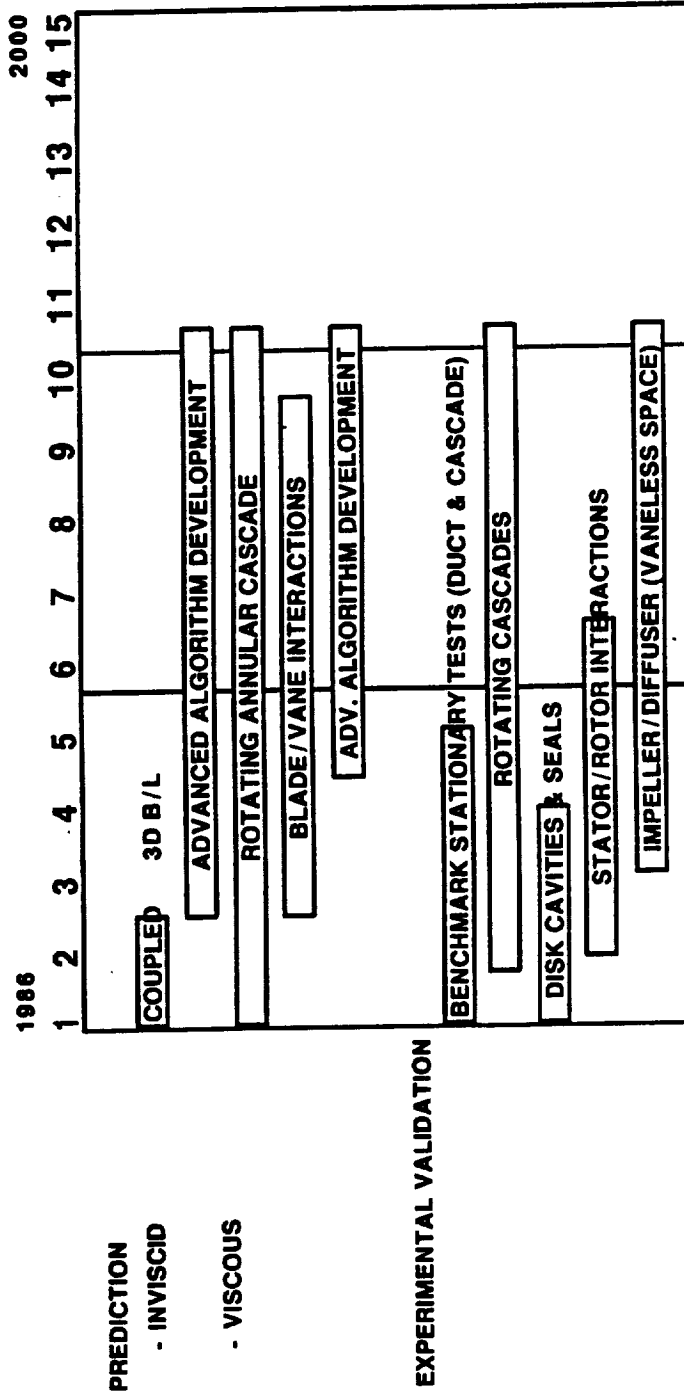
Figure 81. Technology Schedule, Flow Field Prediction

149
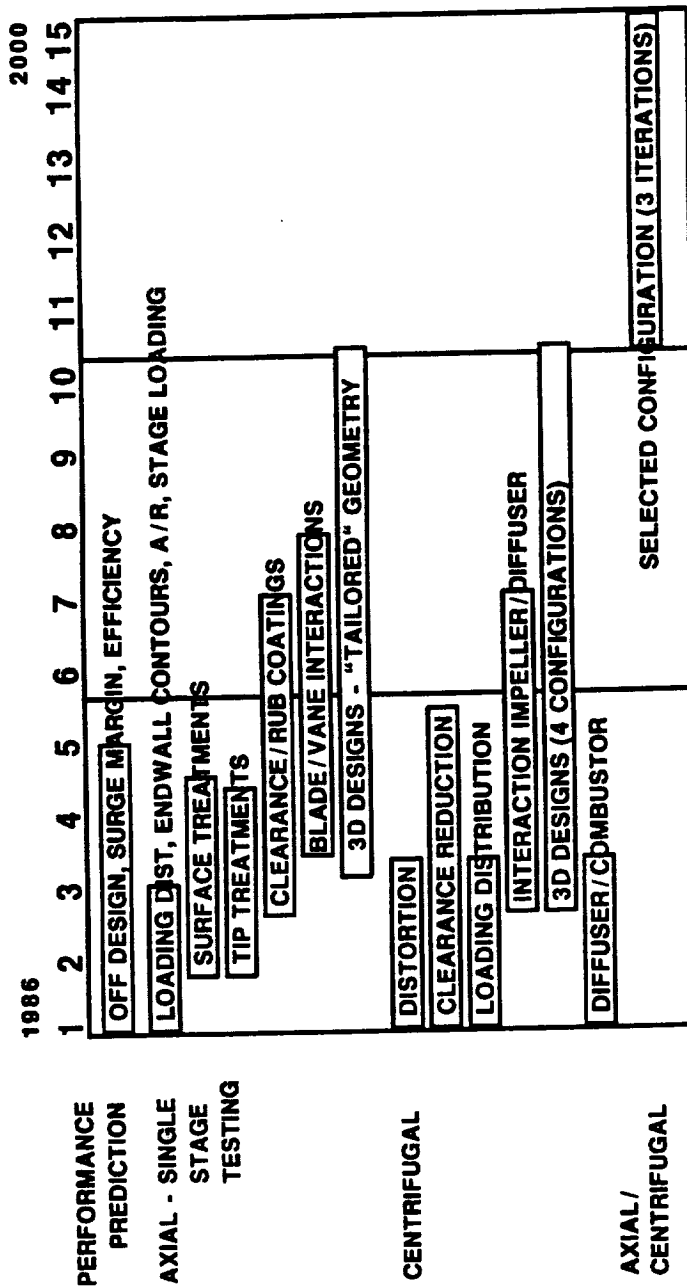
Figure 82.   Technology Schedule, Compressor Technology

150

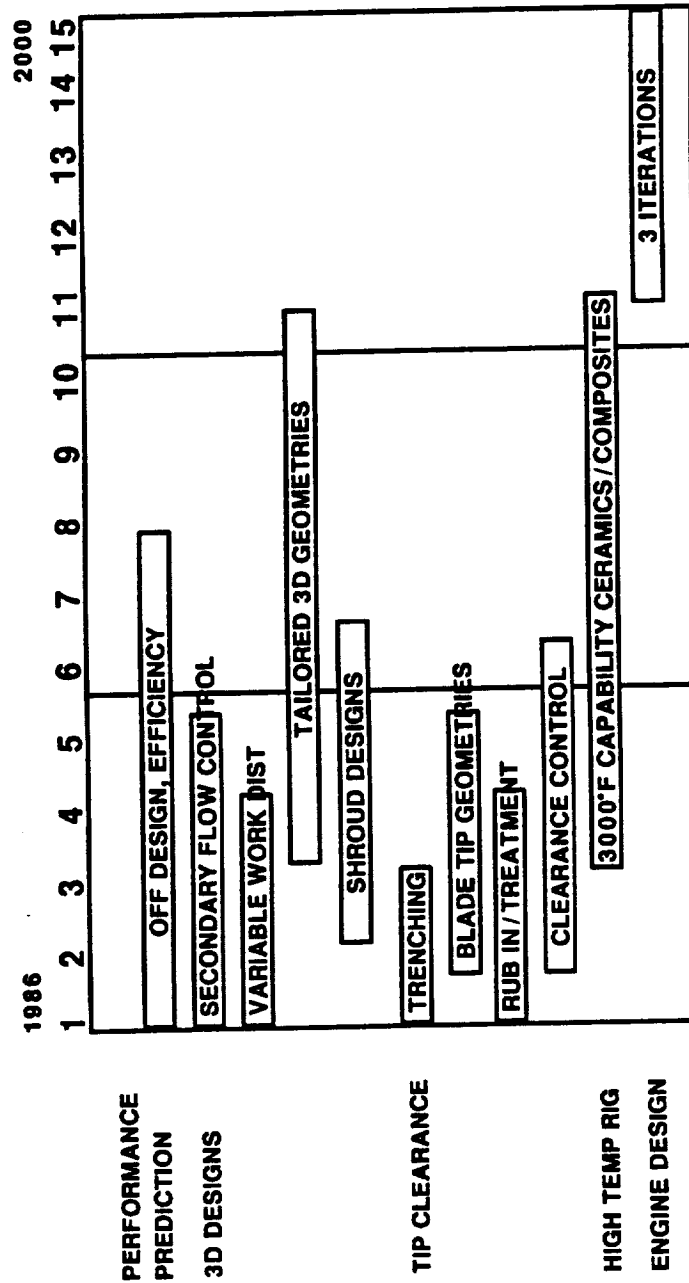Figure 83. Technology Schedule, Turbine Technology

151
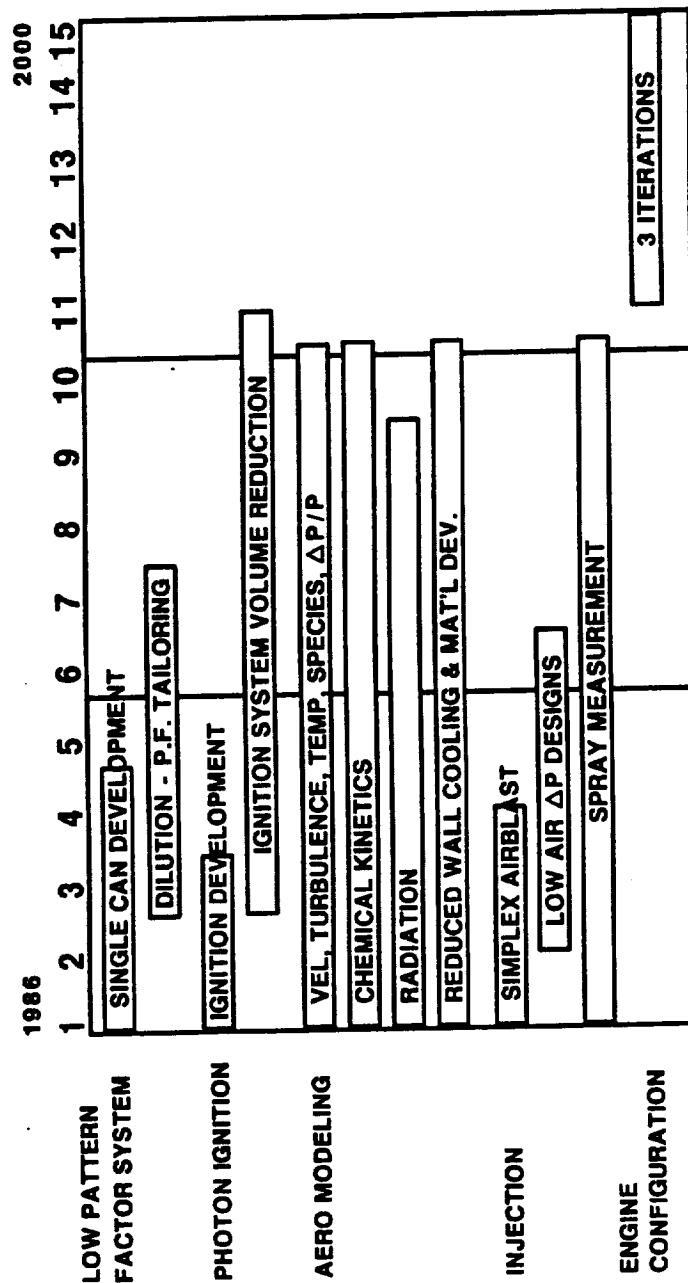
Figure 84.   Technology Schedule, Combustor Technology
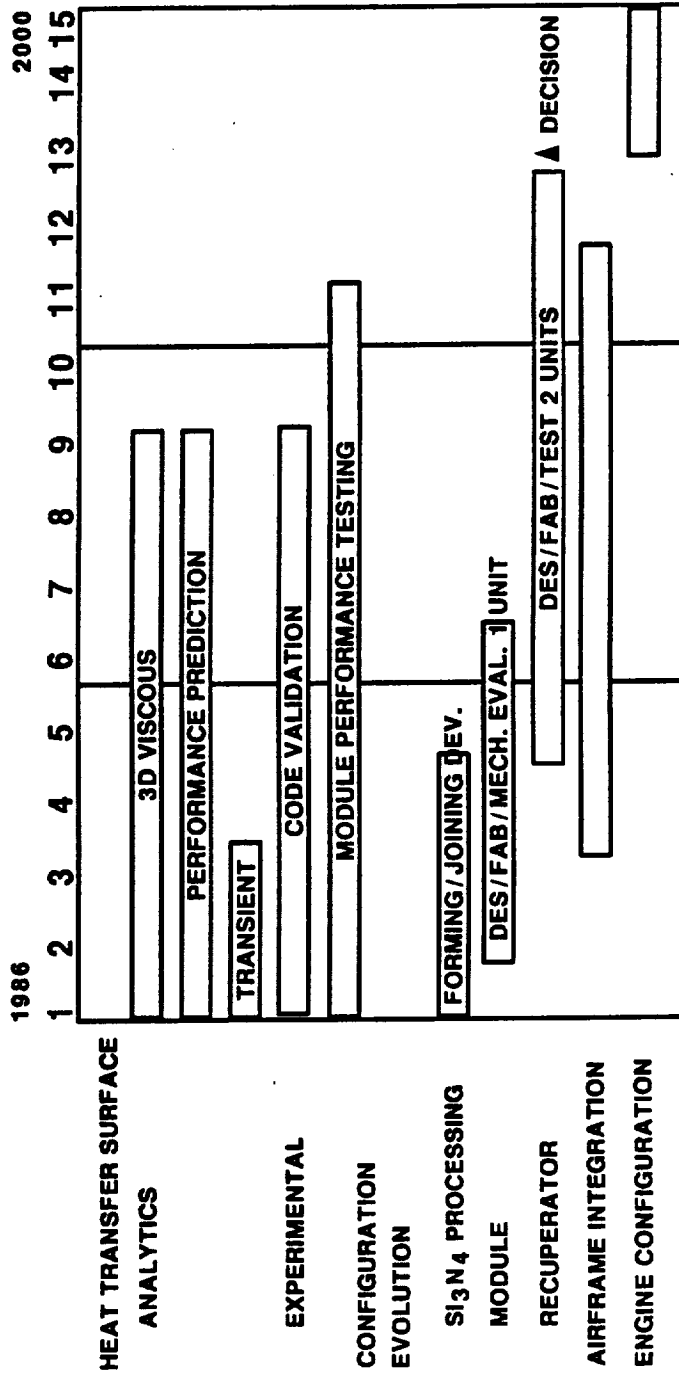
152

Figure 85.   Technology Schedule, Recuperator Aero/Thermo/Ceramics

DISTRIBUTION LIST

SECT STUDY REPORTS

NASA Lewis Research Center
21000 Brookpark Road
Cleveland, Ohio 44135

Attn:	Mail Stop
Library (2 copies)	60-3
Report Control Office	60-1
R. W. Graham	5-9
Major D. G. Kulchak	501-3
M. A. Beheim	3-9
N. T. Saunders	3-8
D. J. Poferl	3-8
D. C. Mikkelson	6-12
W. C. Strack	6-12
J. W. Gauntner	6-12
J. Eisenberg	6-12
A. J. Glassman	6-12
G. Knip	6-12
J. E. Haas	6-8
B. A. Miller	5-3
L. A. Povinelli	5-7
J. R. Wood	5-7
J. A. Ziemianski	86-1
R. C. Evans	77-6
P. T. Kerwin	77-6
T. N. Strom	77-6
P. G. Batterton	86-4
T. J. Biesiandy	86-4
G. A. Kraft	86-7
C. L. Ball	77-6
E. A. Willis	77-6
W. T. Wintucky	77-6
M. R. Vanco (5 copies)	77-6
R. W. Niedzwiecki	77-6
R. J. Roelke	77-6
F. A. Newman	77-6
R. J. Rollbuhler	77-6
J. S. Fordyce	3-5
H. R. Gray	49-1
R. L. Dreshfield	49-3
S. R. Levine	49-3
T. T. Serafini	49-3
D. E. Sokolowski	49-7
D. J. Gauntner	23-3
L. J. Kiraly	23-3
R. E. Kielb	23-3

U.S. Army Aviation Research and
  Technology Activity
Propulsion Directorate
NASA Lewis Research Center
Cleveland, OH 44135

Attn:	Mail Stop
J. Acurio	77-12
G. J. Weden (5 copies)	77-12
P. L. Meitner	77-12
G. A. Bobula	77-12
G. L. Klann	6-8
W. A. Acosta	77-6
G. J. Skoch	77-6
R. G. DeAnna	77-6

NASA Headquarters
Washington, D.C. 20546
Attn: RJ/Cecil Rosen
      RP/Robert Rosen
      RP/John Facey
      RP/Gordon Banerian

NASA Ames Research Center
Moffett Field, CA 94035
Attn: John Zuk, Mail Stop 237-11
      T. L. Galloway, Mail Stop 237-11

NASA Langley Research Center
Hampton, VA 23665
Attn: Robert W. Koenig, Mail Stop 249
      J. Stickle, Mail Stop 246A

Commander U.S. Army Aviation
  Systems Command
4300 Goodfellow Boulevard
St. Louis, MO 63120-1798
Attn: Mr. C. Crawford
      Mr. V. Edwards, DRSAV-EP

Headquarters
U.S. Army Aviation Research and
  Technology Activity (AVSCOM)
NASA Ames Research Center
Moffett Field, CA 94035-1099
Attn: Dr. J. R. Carlson
      Mr. W. Andre, SAVDL-AS

154

Aviation Applied Technology Directorate
U.S. Army Aviation Research and
  Technology Activity (AVSCOM)
Fort Eustis, VA 23604-5577
Attn: H. Morrow, SAVDL-ATL-ATP
       Mr. G. A. Elliott
       Mr. E. Johnson
       Mr. S. Morgan

U.S. Army Tank Automotive Command
28251 Van Dyke
Warren, MI 48397-5000
Attn: Mr. G. Cheklich
       Mr. C. Mason, AMSTA-RGRT
       Mr. E. Danielson

Commander Army Research Office
P.O. Box 12211
Research Park Triangle, NC 27709
Attn: Dr. R. Singleton

Naval Air Propulsion Center
P.O. Box 7176
Trenton, NJ 08628-0176
Attn: Mr. W. W. Wagner
       Mr. R. Valori, PE 34

Naval Weapons Center
Code 3246
China Lake, CA 93555
Attn: Mr. G. W. Thielman

Naval Air Systems Command
Washington, D.C. 20361
Attn: Commander J. L. Murphy III
       Mr. R. A. Grosselfinger, AIR-310 F

David Taylor Naval Ship R&D Center
Bethesda, MD 20084
Attn: Mr. M. Gallager, Code 1240

U.S. Marine Corps
Development and Education Command
LVT(X) Directorate, D16
Quantico, VA 22134
Attn: Carmen DiGiandomenico

Deputy Under Secretary of Defense
Research and Engineering
Research and Advanced Technology
The Pentagon
Washington, D.C. 20301
Attn: Dr. D. Dix, OUSDRE (MST)
       Mr. D. Gissendanner

Department of Army, SCSRDA
Room 3E429
The Pentagon
Washington, D.C. 20301
Attn: Mr. D. R. Artis
       Mr. R. Ballard

Defense Advanced Research Project
Agency
1400 Wilson Blvd.
Arlington, VA 22209
Attn: S. Sigman, Jr.
       R. Williams

Wright Patterson Air Force Base
Dayton, OH 45433
Attn: Mr. Erik W. Linder, AFWAL/POTA
       Mr. T. Gingrich
       Lt. J. Gagliardi
       Mr. E. A. Lake
       Mr. W. Troha, AFWAL/POTC

U.S. Department of Energy
Office of Transportation Systems
1000 Independence Avenue, S.W.
Washington, D.C. 20585
Attn: Richard T. Alpaugh, MS 5G-046

Naval Ship Systems Engineering Station
Philadelphia, PA 19112
Attn: Mr. L. Haryslak, Code 033D
       Mr. T. Bodman

U.S. Army Material Command
5001 Eisenhower Avenue
Alexandria, VA 22333
Attn: Mr. R. A. Mercure, AMCDE-SA

Allison Gas Turbine Division
General Motors Corporation
P.O. Box 420
Indianapolis, IN 46206-0420
Attn: P. C. Tramm
       H. C. Mongia, T14
       T. R. Larkin

AVCO Lycoming
550 South Main Street
Stratford, CT 06497
Attn: H. Moellmann
       L. Beatty
       H. Kaehler

General Electric
Aircraft Engine Business Group
P.O. Box 6301
Evandale, OH 45215-6301
Attn: L. H. Smith, K-70

General Electric
Aircraft Engine Business Group
1000 Western Avenue
Lynn, MA 01910
Attn: L. H. King
       R. Hirschkron

Garrett Turbine Engine Company
111 South 34th Street
P.O. Box 5217
Phoenix, AZ 85010
Attn: J. Howell
       J. R. Switzer
       M. L. Early

United Technologies Corporation
Pratt & Whitney
Engineering Division
400 Main Street
East Hartford, CT 06108
Attn: T. J. Gillespie, 162-23

United Technologies Corporation
Pratt & Whitney
Engineering Division
P.O. Box 2691
West Palm Beach, FL 33402
Attn: R. E. Davis
       J. Alcorta

Sundstrand Turbomach
P.O. Box 85757
4400 Ruffin Road
San Diego, CA 92138-5757
Attn: C. Rodgers

Teledyne CAE
Turbine Engines
1330 Laskey Road
P.O. Box 6971
Toledo, OH 43612
Attn: E. H. Benstein
       E. Razinsky
       B. Singh

Williams International
2280 West Maple Road
P.O. Box 200
Walled Lake, MI 48088
Attn: R. C. Pampreen
       D. A. Gries
       R. A. Horn, Jr.

Norton - TRW
Gottard Road
Northboro, MA 01532-1545
Attn: Dr. C. L. Quackenbush

Caterpillar Tractor Company
Defense Products Department, JB7
Peoria, IL 61629
Attn: Mr. G. G. Valbert

Beech Aircraft Corporation
9709 E. Central
Wichita, KS 67201
Attn: Mr. O. Scott
       Mr. C. McClure

Cessna Aircraft Corporation
P.O. Box 7704
Wichita, KS 67201
Attn: Mr. E. Kraus

Gulfstream Aerospace
P.O. Box 2206
Savannah, GA 31402
Attn: Mr. R. J. Stewart

Fairchild Aviation Company
International Airport
P.O. Box 32486
San Antonio, TX 78284
Attn: Mr. R. E. McKelvey

Bell Helicopter Textron
P.O. Box 482
Fort Worth, TX 76101
Attn: Mr. D. Karanian

Gates Learjet Corporation
P.O. Box 7707
Wichita, KS 67277
Attn: Mr. R. D. Neal

Boeing Vertol Company
Boeing Center
P.O. Box 16858
Philadelphia, PA 19142
Attn: D. R. Woodley

McDonald Douglas Helicopter Co.
Centinela Avenue and Teale Street
Building T 465
Culver City, CA 90230
Attn: D. Borgman

Piper Aircraft Corp.
P. O. Box 1328
Vero Beach, FL 32960
Attn: Max Bleck

Sikorsky Aircraft Division
United Technologies Corporation
N. Main Street
Stratford, CT 06602
Attn: H. Shohet

Boeing Military Airplane Co.
Research & Engineering
Wichita, KS 67210
Attn: Mr. Bert Welliver

Boeing Aerospace Company
Kent Space Center
P. O. Box 3999
Seattle, WA 98124-2499
Attn: Mr. L. Harding

Brunswick Corporation
Defense Division
3333 Harbor Blvd.
Costa Mesa, CA 92626
Attn: Mr. Richard L. Benton

General Dynamics Corporation
Convair Division
P. O. Box 85357
San Diego, CA 92138
Attn: Mr. Mark F. Dorian

Hughes Aircraft Co.
Missile Development
8433 Falbrook Avenue
Canoga Park, CA 91304
Attn: Mr. Larry Wong

Lockheed Missiles & Space Co.
Austin Division
2100 East St. Elmo Road
Austin, TX 78744
Attn: Mr. Michael Levin

Lockheed Georgia Co.
86 S. Cobb Drive
D72-16, Z399
Marietta, GA 30063
Attn: Mr. Rick Mattels

Martin Marietta Aerospace
P. O. Box 5837
Orlando, FL 32855
Attn: Mr. Victor Schilling, MP 275

McDonnel Douglas Astronautics Co.
Box 516
Bldg. 106, Level 2, Room 287
St. Louis, MO 63166
Attn: Mr. Thomas F. Schweickert

Northrop Corporation
Ventura Division
1515 Rancho Conejo Blvd.
P. O. Box 2500
Newbury Park, CA 91320
Attn: Mr. Marion Bottorff

Northrop Corporation
Hawthorne Division
One Northrop Avenue
Dept. 3810, Zone 82
Hawthorne, CA 90250
Attn: Mr. David McNally

Rockwell International Corp.
Missile Systems Division
Department 362
4405-A International Blvd.
Norcross, GA 30093
Attn: Mr. F. L. Goebel

Teledyne Ryan Aeronautical
2701 Harbor Drive
Box 80311
San Diego, CA 92138-9012
Attn: Mr. Vernon A. Corea

Hamilton Standard
Mail Stop 1-2-11
Windsor Locks, CT 06096
Attn: Mr. Fred Perkins

157